EFFECTS OF RESERVOIR RELEASES ON SLOPE STABILITY AND BANK EROSION

Soonkie Nam

Dissertation submitted to the Faculty of the
Virginia Polytechnic Institute and State University
in partial fulfillment of the requirements for the degree of

Doctor of Philosophy
in
Civil Engineering

Panayiotis Diplas, Co-Chairman, Marte S. Gutierrez, Co-Chairman
Thomas L. Brandon
John C. Little
Theresa M. Wynn

May 18, 2011
Blacksburg, VA

Keywords: slope stability, bank erosion, soil water characteristic curve (SWCC), unsaturated shear strength, multistage direct shear test, transient seepage, Roanoke River

Effects of Reservoir Releases on Slope Stability and Bank Erosion

Soonkie Nam

ABSTRACT

Reservoir release patterns are determined by a number of purposes, the most fundamental of which is to manage water resources for human use. Managing our water resources means not only controlling the water in reservoirs but also determining the optimum release rate taking into account factors such as reservoir stability, power generation, water supply for domestic, industrial, and agricultural uses, and the river ecosystem. However, riverbank stability has generally not been considered as a factor, even though release rates may have a significant effect on downstream riverbank stability. Riverbank retreat not only impacts land properties but also damages structures along the river such as roads, bridges and even buildings. Thus, reservoir releases need to also take into account the downstream riverbank stability and erosion issues.

The study presented here investigates the riverbank stability and erosion at five study sites representing straight as well as inside and outside channel meander bends located on the lower Roanoke River near Scotland Neck, North Carolina. Extensive laboratory and field experiments were performed to define the hydraulic and geotechnical properties of the riverbank soils at each site. Specifically, soil water characteristic curves were determined using six different techniques and the results compared to existing mathematical models. Hydraulic conductivity was estimated using both laboratory and in situ tests. Due to the wide range of experimentally obtained values, the values determined by each of the methods was used for transient seepage modeling and the modeling results

compared to the actual ground water table measured in the field. The results indicate that although the hydraulic conductivities determined by in situ tests were much larger than those typically reported for the soils by lab tests, numerical predictions of the ground water table using the in situ values provided a good fit for the measured ground water table elevation. Shear strengths of unsaturated soils were determined using multistage suction controlled direct shear tests. The test method was validated, and saturated and unsaturated shear strength parameters determined. These parameters, which were determined on the basis of results from both laboratory and field measurements, and the associated boundary conditions, which took into account representative flow rates and patterns including peaking, drawdown and step-down scenarios, were then utilized for transient seepage analyses and slope stability analyses performed using SLIDE, a software package developed by Rocscience. The analyses confirmed that the riverbanks are stable for all flow conditions, although the presence of lower permeability soils in some areas may create excess pore water pressures, especially during drawdown and step-down events, that result in the slope becoming unstable in those locations. These findings indicate that overall, the current reservoir release patterns do not cause adverse impacts on the downstream riverbanks, although a gradual drawdown after a prolonged high flow event during the wet season would reduce unfavorable conditions that threaten riverbank stability.

ACKNOWLEDGMENTS

I believe it is impossible to show my appreciations to all who have provided motivation, encouragement, and guidance, not only for research but also for surviving throughout this long journey.

First of all, I would like to express my deepest gratitude to my advisors, Dr. Panayiotis Diplas and Dr. Marte S. Gutierrez for their personal and professional support and guidance throughout this endeavor. Without their consistent advice and encouragement, I would not have been able to reach this moment. They have trained and guided me with endless efforts and time that I could never be able to pay back. They deserve my highest appreciation for their support and contribution to my professional development.

I also want to thank Dr. Thomas Brandon, Dr. John Little, and Dr. Theresa Wynn, for agreeing to serve on my committee and reviewing this manuscript. I am also grateful to Dr. Brandon, Dr. Wynn, Dr. Matthew Mauldon, Julie Burger, Dr. Ning Lu and Dr. Greg Hanson for providing laboratory and in situ test facilities and valuable advice. I would also like to express special thanks to Bob Graham, who was always willing to help the project with all the resources available.

This project was sponsored by Dominion, the U.S. Army Corps of Engineers and the other members of the Cooperative Management Team for Roanoke Rapids Hydropower Dam. The full license for the use of the numerical programs was granted by MIDAS Information Technology Co Ltd. and Rocscience Inc. These sponsorships are gratefully acknowledged. I also appreciate the Edna Bailey Sussman Foundation for their generous financial support.

I would also like to thank all my colleagues who participated in the field trips: John Petrie, David Liu, Derek Spurlock, Dr. Ozan Celik, Nikolaos Apsilidis, Hannah Cardwell, and R. Miles Ellenberg, for their laboratory and field work assistance, advice, and friendship. I will never forget the special friendship with John and Ozan, and their enthusiasm for research. I can't thank John Petrie enough for both the personal and professional activities he has provided. Without his collaboration, the field work could never have been accomplished in time. Two members of our group were unable to complete this study: Jeremy Herbstritt and Partahi "Mora" Lumbantoruan lost their lives in the tragedy on April 16, 2007. They are deeply missed.

I am grateful for the advice and support I have received from Dr. Sang-duk Lee and the IGUA families, who have provided all kinds of support. I would also like to thank Dr. Hojong Baik, Dr. Imsoo Lee, Dr. Youngjin Park, Dr. Hyun Shin, Dr. Younghan Jung, Dr. Myung Goo Jeong, Dr. Chul Park, Dr. Juneseok Lee, Kyusang Kim, Minchul Park, Junghan Kwak and all my other Korean friends in the CEE department. We have gone through some hard times together, but the support and encouragement of the group have sustained us all.

I would also like to express my appreciation of the endless love and support provided by Charlie and Judy Beazley, who have taken care of me, my wife, and all my other Korean friends as if we were members of their own family. Ever since I arrived in Blacksburg, their love and care has meant that I have never felt alone.

Above all, I would like to express my deepest appreciation to my family and to my wife, who have trusted and supported me with their love and sacrifices. No words can express how much I appreciate and love them. They are the most important reason that I live.

DEDICATION

To my wife,

Kyungeun Yoon,

To my family,

Dr. Youngkug Nam, Hyunsook Kwon,

Byungoh Yoon, Hyunja Sohn,

Soonyong Nam, Soohyun Shim, Soonkou Nam,

Charlie and Judy Beazley

Table of Contents

List of Figures

Chapter 1

Chapter 2

Chapter 3

Chapter 4

Chapter 5

List of Tables

CHAPTER 1. Introduction

1.1 Overview

Reservoirs offer a variety of advantages for human use. Although construction of large reservoirs has slowed down over recent decades, the demand for reservoirs that produce hydropower is expected to grow as this is a reliable, affordable, and sustainable clean energy source. Another important role of reservoirs is to manage water resources and, consequently, to prevent and reduce the damage caused by drought and floods. Managing water resources means not only maintaining the impounded water in reservoirs but also determining optimum release rates taking into account factors such as reservoir stability, power generation, water supply for domestic, industrial, and agricultural uses, and the river ecosystem. However, riverbank stability has generally not been considered in dam operation, even though release rates may have a significant effect on downstream riverbank stability.

To illustrate this point, consider the example of the dam controlling the flow of water in the lower Roanoke River, focus of this study. The discharge released from the Roanoke Rapids Dam is regulated by four operational modes, which are determined by the inflow rate to the reservoir and the special cases such as drought, flood, or fish spawning season; there is no specific regulation restricting discharge to protect downstream riverbank stability (Dominion, 2010). The flows regulated by the dam operation can be regarded as a simple steady state condition that can be generally assumed when downstream flow is expected to remain constant. However, when the water surface elevation (WSE) changes rapidly or frequently due to reservoir releases, the

riverbanks are directly affected by the WSE in terms of both slope stability and fluvial erosion.

Recently, some concern has arisen regarding reservoir operations due to the increased influence of global warming, which is accompanied by more prolonged and severe droughts, storms and hurricanes (Emanuel, 2005, Webster et al., 2005). There is a much higher likelihood that in response to these changes more instantaneous or prolonged reservoir releases may be required to maintain the safety of reservoirs and the downstream floodplain. These instantaneous releases may create rapid increase in the WSE that could reduce the stability of unsaturated slopes due to the loss of matric suction (Wong and Ho, 1997), and prolonged high flow may lead to overbank flow conditions.

The stability of riverbanks tends not to be taken into account for reservoir operations due to the relatively minor impact of a riverbank failure; a reservoir failure is likely to result in a disaster incurring fatalities and serious economic loss. However, unlike the other factors, discharge rates can be easily controlled without altering other factors. If the effects of reservoir release patterns on the downstream flow conditions and, consequently, riverbank stability are known, the operation of the reservoir can be managed to minimize the potential negative impacts on the river while at the same time supporting the other purposes of reservoir operations.

The unique contributions of this study are: i) riverbank stability analysis that takes into account actual reservoir operations and downstream conditions is performed, ii) unsaturated soil properties are considered for the transient seepage and slope stability analysis, and iii) the riverbank stability is predicted taking fluvial erosion into account, using actual erosion rates monitored by the U.S. Geological Survey (USGS).

1.2 Characteristics of riverbanks under the influence of dam operations

Transient seepage analysis

Although the fundamental concepts of slope stability analysis are similar for different structures such as levees, embankments, reservoirs, or excavated slopes, the riverbank is distinct due to the fact that the water surface elevation changes continuously. Riverbanks, especially those downstream from a dam, are exposed to frequent changes in the water surface elevation due to reservoir releases. Changes in the WSE also affect the phreatic surface and, thus, the pore water pressure distribution in the riverbanks. These changes may occur simultaneously and all affect the stability of a slope, indicating that transient seepage analysis is required to estimate the pore water pressure distribution for slope stability analysis.

Slope stability analysis taking into account the unsaturated shear strength

As riverbanks remain partially saturated except in the case of continuous and prolonged high flows, it is appropriate to analyze the riverbank stability by applying the concepts of unsaturated soil mechanics. The shear strength of unsaturated soils is presented in terms of independent stress state variables (Fredlund et al., 1978), and can take into account the increase of shear strength due to matric suction. This approach using unsaturated shear strength has been successfully adapted for riverbank stability analysis (Dapporto et al., 2001, Rinaldi and Casagli, 1999, Rinaldi et al., 2004).

Fluvial erosion

Bank erosion as a micro-scale failure is primarily affected by the river flow characteristics. Fluvial erosion alters the bank geometry and may ultimately affect the

riverbank stability. Erosion of the riverbank is frequently estimated using the effective stress equation (Hanson and Cook, 1997), and jet erosion test devices are often employed to determine the required parameters experimentally. However, although the consistency of the test results has been demonstrated on carefully prepared laboratory samples (Charonko, 2010) , the test results for natural riverbank soils have shown a wide range of values. These differences are typically thought to be due to the spatial and temporal variability of the soils as well as the complexity of inter-particle forces. In addition, it is difficult to estimate the shear stress applied on the riverbank by the flow experimentally or using numerical analysis. Erosion rates can be estimated directly by measuring how much erosion has occurred during a specific period of time. The U.S. Geological Survey (USGS) installed erosion pins along the lower Roanoke River, and the study sites for this study were selected to coincide with the USGS erosion pin locations in order to take advantage of the availability of this data.

1.3 Study sites information

This study was designed to assess the role of reservoir release patterns on downstream riverbank stability and erosion. Field data, laboratory tests, numerical modeling, and analytical modeling were used to gain insight into the processes involved in bank retreat. The field data used in this study was obtained for a study reach on the lower Roanoke River downstream of the Roanoke Rapids Dam, as shown in Figure 1. The Roanoke Rapids Hydropower dam is located at Roanoke Rapids, North Carolina, and Dominion is in charge of its operation.

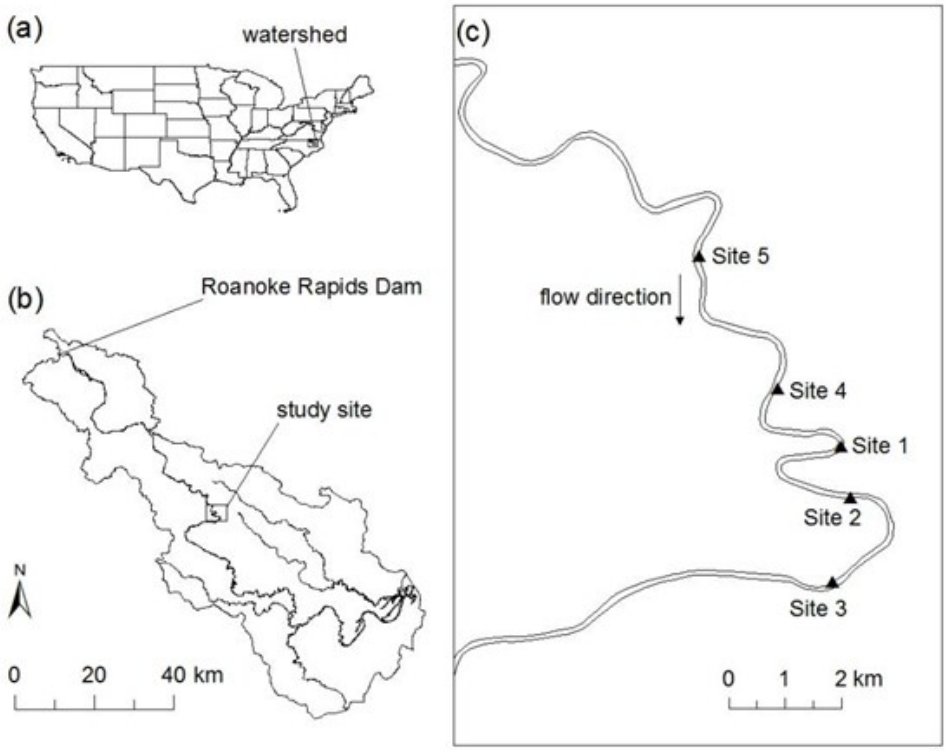

Figure 1 Location of study area. (a) the United States and the location of the lower Roanoke River watershed in N.C., (b) the Roanoke River watershed below the Roanoke Rapids Dam, and (c) the study sites on the lower Roanoke River.

As Figure 2 illustrates, the riverbanks in the study reach experience different types of bank retreat. The slopes tend to be steep and consist mainly of cohesive soils, and some local failures are observable. The surface of the bank slope usually remains dry and very firm, but easily turns slippery when wet. Different shapes of the riverbanks along the stretch of the river indicate the need to carefully select representative sites within the study reach. The five study sites shown in Figure 1 were selected for further investigation.

Figure 2 Severe erosion and bank failures near study sites in the lower Roanoke River, NC.

1.4 Research objectives

The study presented here investigated the effects of reservoir releases on bank stability and erosion on the lower Roanoke River. It focused primarily on the geotechnical aspects, including transient seepage analysis and slope stability analysis taking into account the concept of the shear strength of unsaturated soils. The ultimate goal of this study was to analyze riverbank stability exposed to representative hydropower dam operations including peaking and drawdown.

Brief summaries of the research objectives and tasks are as follows:

(1) Determine the representative flow scenarios

- Reservoir release data for 2005-2009 was analyzed and representative flow patterns were selected based on the basic operational modes as well as continuous peaking, drawdown, and step down scenarios.

(2) Investigate soil properties required for modeling using both laboratory and in situ tests

- Soil water characteristic curves were determined using six different techniques and the results compared to existing mathematical models.
- Hydraulic conductivity was estimated using laboratory and in situ tests, and then used for transient seepage modeling. The modeling results were compared to the actual ground water table measured in the field.
- A suction controllable direct shear test box was constructed and the multistage direct shear test technique was validated. The shear strengths of unsaturated soils were determined using multistage suction controlled direct shear tests.

(3) Determine the stability of riverbanks exposed to periodic changes in the WSE due to dam operations

- Laboratory and field measurements, applying associated boundary conditions that took into account representative flow rates and patterns including peaking, drawdown and step-down scenarios, were utilized for transient seepage analyses and slope stability analyses performed using the SLIDE software package.
- Perform transient seepage and slope stability analyses

1.5 Organization of the dissertation

The dissertation consists of six chapters, including four main chapters submitted or about to be submitted to journals. Chapter 1 has introduced the research, providing an overview and discussing the study objectives. This is followed by Chapter 2, "Comparison of testing techniques and models for establishing the soil water characteristic curves (SWCC) of riverbank soils", which has already been published in *Engineering Geology*. Chapter 3, "Multistage direct shear test for unsaturated shear strength of riverbank soils", has been reviewed and is to be resubmitted to *Engineering Geology*. Chapter 4, "Laboratory and in-situ determination of hydraulic conductivity and the implications for transient seepage analysis", is being prepared for submission to the *Journal of Hydraulics*. Chapter 5, "Effect of reservoir releases on riverbank stability", will also be submitted to a journal. Chapter 6 summarizes the research findings and integrated conclusions of this study. Following Chapter 6, supplemental data and analyses of riverbank erosion including a manuscript "Effects of spatial variability on the estimation of erosion rates for cohesive riverbanks" presented in the peer reviewed conference "River Flow 2010", are provided in the Appendix. All the chapters prepared for publication are co-authored with Dr. Diplas, Dr. Gutierrez, and John Petrie, a Ph.D. candidate whose research focuses on the hydraulic aspects of the study. However, all the work presented in this dissertation has been planned, executed, and analyzed primarily by myself as the first author.

1.6 References

[1] Charonko, C. M. (2010). "Evaluation of an in situ measurement technique for streambank critical shear stress and soil erodibility " Master of Science, Virginia Polytechnic Institute and State University, Blacksburg.

[2] Dapporto, S., Rinaldi, M., and Casagli, N. (2001). "Failure mechanisms and pore water pressure conditions: Analysis of a riverbank along the Arno River (Central Italy)." *Engineering Geology*, 61(4), 221-242.

[3] Dominion (2010). "Description of operational modes." <http://www.dom.com/about/stations/hydro/operational-modes.jsp>. (Sep 29, 2010).

[4] Emanuel, K. (2005). "Increasing destructiveness of tropical cyclones over the past 30 years." *Nature*, 436(7051), 686-688.

[5] Fredlund, D. G., Morgenstern, N. R., and Widger, R. A. (1978). "Shear strength of unsaturated soils." *Canadian Geotechnical Journal*, 15(3), 313-321.

[6] Hanson, G. J., and Cook, K. R. (1997). "Development of excess shear stress parameters for circular jet testing." *Proc., 1997 ASAE Annual International Meeting*, ASAE, 97-2227.

[7] Rinaldi, M., and Casagli, N. (1999). "Stability of streambanks formed in partially saturated soils and effects of negative pore water pressures: the Sieve River (Italy)." *Geomorphology*, 26(4), 253-277.

[8] Rinaldi, M., Casagli, N., Dapporto, S., and Gargini, A. (2004). "Monitoring and modelling of pore water pressure changes and riverbank stability during flow events." *Earth Surface Processes and Landforms*, 29(2), 237-254.

[9] Webster, P. J., Holland, G. J., Curry, J. A., and Chang, H.-R. (2005). "Changes in tropical cyclone number, duration, and intensity in a warming environment." *Science*, 309(5742), 1844-1846.

[10] Wong, H. N., and Ho, K. K. S. (1997). "The 23 July 1994 landslide at Kwun Lung Lau, Hong Kong." *Canadian Geotechnical Journal*, 34(6), 825-840.

CHAPTER 2. Comparison of Testing Techniques and Models for Establishing the SWCC of Riverbank Soils[1]

ABSTRACT

The soil water characteristic curve (SWCC), also known as soil water retention curve (SWRC), describes the relationship between water content and soil suction in unsaturated soils. Water content and suction affect the permeability, shear strength, volume change and deformability of unsaturated soils. This paper presents results of the laboratory determination of the SWCC for soil samples obtained from the riverbank of the Lower Roanoke River in North Carolina. Six different testing methods were used to establish the SWCC including the filter paper, dewpoint potentiameter, vapor equilibrium, pressure plate, Tempe cell and osmotic methods. It is concluded that each suction measurement technique provides different measurable ranges of suction values, and the combined results from the different tests provide continuous SWCCs. Three widely available models were also shown to adequately fit the experimental SWCC data, particularly for matric suction values under 1,500 kPa. These results will be valuable to practitioners in deciding which methods to use to establish the SWCC, and which empirical relationship to use for modeling the SWCC of riverbank soils.

Keywords: soil suction; soil water characteristic curve; unsaturated soils; riverbank; laboratory investigation, experimental techniques

---

[1] This manuscript was published in *Engineering Geology*, and is co-authored by **Soonkie Nam,** Marte Gutierrez, Panayiotis Diplas, John Petrie, Alexandria Wayllace, Ning Lu, and Juan Jorge Muñoz

2.1 Introduction

The soil water characteristic curve (SWCC) defines the relationship between water content and suction in unsaturated soils. Soil suction and water content are important parameters that control many geotechnical properties of unsaturated soils including permeability, volume change, deformability and shear strength (Barbour, 1998). Due to its importance, several test methods have been developed to establish the SWCC in Soil Science and Geotechnical Engineering. At the same time, several models have been developed to analytically describe the SWCC. The most well-known and widely used model is that of van Genuchten (1980) and its several modifications and extensions.

From a practical perspective, methods for establishing the SWCC should be simple, easy to perform, inexpensive, quick and reliable. Since soil suction can vary tremendously depending on the soil type, with a theoretical maximum value of up to 10^6 kPa, several test methods have been developed to establish the SWCC (Lu and Likos, 2004). The different methods have different ranges of applicability, and only the use of electrical resistance and capacitance sensors appears to be capable of determining the full range of potential suction values. Test procedures vary in terms of complexity, accuracy, repeatability, and more importantly, cost and required duration of testing. Most methods require much longer testing periods compared to other soil tests. Thus, it is essential to select the most appropriate methods to establish the SWCC.

There have been numerous studies on the different laboratory testing techniques to establish the SWCC. At the same time, newer techniques and testing equipment are continuously being developed and introduced. It is not possible to evaluate all the

different available techniques and procedures, and, thus, this paper focuses on some of the most commonly used methods. There have also been a few studies that were specifically performed to compare the different methods. For instance, Agus and Schanz (2007) compared four methods (noncontact filter paper method, psychrometer technique, relative humidity (RH) sensor, and chilled-mirror hygrometer technique) in determining the suction of a bentonite-sand mixture. Patrick et al. (2007) compared chilled-mirror and filter paper measurements of total soil suction. Most of the available studies show comparable suction data from the different test procedures provided the tests are conducted under careful and controlled conditions.

While studies have been performed to evaluate and compare different testing methods, these studies appear to have used single soil types and a subset of the currently available techniques. Typically, granular soils ranging from sands to silts, or artificial soil mixtures are used to study the performance of testing procedures. Relatively fewer data are available for natural clayey soils. This is primarily due to the relative difficulty of establishing the SWCC for clayey materials in comparison to granular soils. This paper deals with the SWCC of natural riverbank soils and the applicability of different commonly used SWCC testing methods for typical materials found in riverbanks, which range from sandy and silty to clayey soils. Changes in water content and suction affect the shear strength of the riverbank soils and seepage in riverbanks due to changes in river water level and rainfall. The seepage forces and the variation in soil shear strength due to changing soil suction affect soil erosion and bank stability, and are critical parameters controlling the stability of riverbanks. The mechanisms responsible for riverbank erosion and instability and the development of methodologies for studying them have received

wide attention recently (e.g., Dapporto et al., 2003, Piegay et al., 2005, Rinaldi et al., 2004, Simon et al., 2002). All these studies point to the importance of unsaturated soil behavior in the understanding of riverbank erosion and instability.

In summary, the objectives of the research described in this paper are to: 1) compare the results of six widely used laboratory methods of establishing the desorption SWCC for natural riverbank soils, 2) compare the validity of the most widely used SWCC models against the experimental data, and 3) provide SWCC data for typical natural riverbank soils. The study used undisturbed and disturbed soil samples obtained from the riverbank of the Lower Roanoke River near Scotland Neck, North Carolina. The desorption SWCCs were established using the filter paper, dewpoint potentiameter, vapor equilibrium, pressure plate, Tempe cell and osmotic methods. The results were then modeled using SWCC equations proposed by van Genuchten (1980), Fredlund and Xing (1994), and Houston et al. (2006).

2.2 Background

2.2.1 Soil suction

Water in soil is represented by both the amount of water present and by its energy state. The energy is typically assumed to be in the form of kinetic and potential energies. Generally, kinetic energy due to water flow in soil is neglected in geotechnical engineering due to slow fluid velocities. Thus, potential energy is the primary component that determines the water condition in soil. As shown below, the potential energy is the algebraic sum of the component potentials: matric potential, osmotic potential, pressure potential, and gravitational potential (Campbell, 1988, Or and Wraith, 1999).

$$\psi_T = \psi_M + \psi_O + \psi_P + \psi_Z \quad (1)$$

where ψ_T =total potential, ψ_M =matric potential, ψ_O =osmotic potential, ψ_P =pressure potential, and ψ_Z =gravitational potential.

Matric potential is often the largest component of the total potential in unsaturated soils, resulting from combined effects of capillarity and adsorptive forces within the soil matrix. The capillarity effect can be explained by surface tension forces at the air–water-soil interface and the adsorptive forces arise mainly from electrical and van der Waals force fields. Osmotic potential is due to the solutes in soil water, and pressure potential is the hydrostatic pressure exerted by water above a point. Gravitational potential is determined by the elevation of a point relative to a reference point. Typically in unsaturated soils, pressure potential is zero, and gravitational potential is also assumed zero as it is a relative value from an arbitrary reference level (Or and Wraith, 1999). Thus, the total potential primarily consists of two components, matric potential and osmotic potential. The term "suction" is also widely used instead of "potential." The individual components are generally expressed in terms of pressure and given by the equation below.

$$\psi_T = \psi_M + \psi_O \quad (2)$$

Based on the thermodynamic relationship between the total suction ψ_T (in kPa) and the partial pressure of the pore water vapor, the total suction can be written as follows (Fredlund and Rahardjo, 1993, Miller and Nelson, 1993):

$$\psi_T = -\frac{RT}{\nu_{0\omega}\omega_\nu}\ln\left(\frac{u_\nu}{u_{0\omega}}\right) \quad (3)$$

where R=universal gas constant (J/(mol·K)), T=absolute temperature (°K), $\nu_{0\omega}$=specific volume of water (m^3/kg), which is the inverse of the density of water, ω_ν=molecular mass of water vapor (g/mol), u_ν=partial pressure of pore-water vapor (kPa), and $u_{\nu 0}$ =saturation pressure of water vapor (kPa). The ratio $u_\nu / u_{0\omega}$ is equal to the relative humidity (RH). For constant temperature at T=20°C, Eq. (3) becomes a simple logarithmic equation with relative humidity as shown in Eq. (4):

$$\psi_T = -135{,}055 \ln(RH) \tag{4}$$

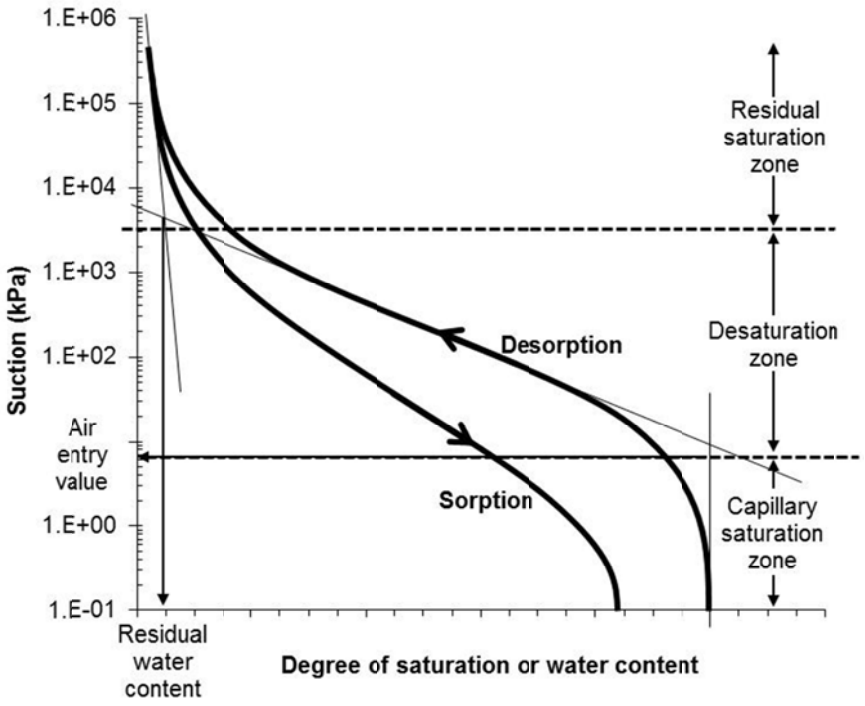

Figure 1 Typical elements of soil water characteristic curves (modified from Sillers et al. (2001)).

Figure 1 shows the main elements of a typical SWCC obtained from a continuous curve fit through experimental data points. The horizontal axis can be expressed as gravimetric water content w, volumetric water content θ, degree of saturation S, or

normalized water content Θ_n. The gravimetric water content is the ratio of the mass of water to mass of soil, and the volumetric water content is the ratio of the volume of water to the total volume. One measure can be converted to the others using the soil void ratio and specific gravity. The normalized water content is the ratio of the difference of a water content and residual water content to the difference of saturated and residual water contents, and can be in either gravimetric or volumetric form.

There is a hysteresis in the SWCC due to the non-coincidence of the sorption and desorption curves. Basic quantities required to establish the SWCC include: 1) the residual volumetric water content θ_r, 2) the saturation volumetric water content θ_s, and 3) the air entry value ψ_a. The residual water content θ_r is the water content where a large suction change is required to remove additional water or the amount of water for which continuity of the liquid phase is lost. The air entry value ψ_a is the matric suction where air starts to enter the largest pores in the soil (Fredlund and Xing, 1994). Typically, soils with finer particles have higher air entry value and saturation water content. Depending on the magnitude of suction, there are three zones of the SWCC corresponding to: 1) the capillary suction zone for suction less than the air entry pressure, 2) the desaturation zone for suction above air entry pressure and water content below residual value, and 3) the residual saturation zone for water contents above residual value.

The complete SWCC consists of sorption and desorption curves (Figure 1). In general, soil samples from the field are in between sorption and desorption conditions. When the samples are saturated for laboratory tests, the samples follow the sorption curve until it is fully saturated. After a test starts, water content changes are measured as air

pressure increases, and the relationship is plotted as the desorption curve. Most laboratory tests for the SWCC measure the desorption curve, including the results reported here. However, it should be noted that the magnitude of soil suction at the same water content may differ as much as 10 to 1,000 kPa between sorption and desorption (Fredlund, 2002).

A variety of experimental methods are available to determine the SWCC. A tensiometer is a classic and widely used method for field measurements of soil suction, but typically measures suction up to 100 kPa due to cavitation (Lu and Likos, 2004). Recently high capacity tensiometers have been developed to enable suction measurements above 100 kPa (Delage et al., 2008, Ridley and Burland, 1993, Toker, 1999). However, these high capacity tensiometers are still mostly used in research and not yet widely used in routine SWCC determination. The axis translation technique is a commonly used laboratory method with a typical suction range of 0 to 1,500 kPa. Controlling and measuring relative humidity and temperature can provide total suction information for any value of soil suction. Osmotic suction needs to be considered in arid and near-shore areas where soluble salt content is expected to be high. Depending on the suction type and range of suction values, the proper tests should be carefully selected.

2.2.2 Models for soil water characteristic curves (SWCC)

Along with the development of experimental methods to determine the SWCC, numerous models have been proposed for fitting analytical functions through experimental results. Many of these models are derived from the pore-size distribution through micromechanical relationships between effective pore size and soil suction (Sillers et al., 2001). One of the most frequently used models was proposed by van

Genuchten (1980). The model is based on the same basic relationships for predicting hydraulic conductivity of unsaturated soil proposed by Mualem (1976):

$$S = \frac{1}{\left[1 + \left(\frac{\psi}{a}\right)^{n}\right]^{m}} \tag{5}$$

where S = degree of saturation, ψ = soil suction, and a, n and m = curve-fitting parameters. Van Genuchten derived the equation as a particular case of the original equations of Mualem (1976) and Burdine (1953), assuming m=(1-1/n) and m=(1-2/n). For curve fitting purposes, a simpler two-parameter equation can be derived, although the three parameter models provides more flexibility than the two parameter model (Sillers et al., 2001).

Fredlund and Xing (1994) also proposed a similar three-parameter equation, which requires fewer iterations for convergence of the curve fitting parameters than the van Genuchten model (Sillers, 1997). The equation is given as:

$$S = \frac{1}{\ln\left[e + \left(\psi / a\right)^{n}\right]^{m}} \tag{6}$$

Fredlund and Xing (1994) presumed from previous experimental results that the maximum soil suction reaches 10^6 kPa at zero water content. It is also thermodynamically supported from Eq. (4) that the suction value approaches 10^6 kPa if the relative humidity is as low as 0.01% (Leong and Rahardjo, 1997). The result is the following modified equation with a correction function factor applied to Eq. (6):

$$S = C(\psi)\frac{1}{\left[\ln\left[e+\left(\psi/a\right)^{n}\right]\right]^{m}} \tag{7}$$

where $C(\psi)$ is a correction factor equal to:

$$C(\psi) = 1 - \frac{\ln\left(1+\psi/\psi_r\right)}{\ln\left(1+10^6/\psi_r\right)} \tag{8}$$

and ψ_r=suction corresponding to the residual water content.

The last model considered in this study was proposed by Houston et al. (2006). This model extends the original equation of Fredlund and Xing (1994) by using fitting parameters for both plastic and non-plastic soils based only on particle gradation and soil plasticity. The SWCC equation is the same as Eq. (7). For non-plastic soils, empirical relations are provided to determine the model parameters *a*, *m* and *n* from D_{10}, D_{20}, D_{30}, D_{60} and D_{90}, where $D_{\%}$ is the soil particle diameter in mm related to the percentage of soil passing the corresponding sieve size. For plastic soils, the model parameters *a*, *m* and *n* can be obtained empirically from the weighed plasticity index *wPI*, the plasticity index *PI* and P_{200}=percent passing the #200 (75μm) sieve (expressed as decimal). Details of the equations to determine the model parameters from soil index properties are available in Houston et al. (2006) and are not repeated here.

In all the four models, the parameter *a* is a suction value related to the inflection point on the SWCC, which is also related to the air entry value. The parameter *n* affects the slope of the SWCC in the desaturation zone, and the parameter *m* is related to the asymmetry of the curve about the inflection point (Sillers et al., 2001). Further details are

available in Sillers et al. (2001), and Leong and Rahardjo (1997), and each provides examples of the influence of the parameters in each model.

2.3 Experiments

2.3.1 Soil samples and properties

Soil samples were obtained from the riverbank of the Lower Roanoke River near Scotland Neck, North Carolina in the eastern United States. The site where the soil samples were obtained has undergone extensive levels of riverbank erosion and failure (Hupp et al., 2009). Figure 2 shows the extent of riverbank erosion and failure at a typical site along this river. The photograph clearly shows that the riverbank is actively undergoing failure close to the toe. The site shown in the Figure 2 is one of the locations where undisturbed soil samples were obtained using Shelby tubes. Disturbed soil samples were also collected and tested for grain size distribution, Atterberg limits, and specific gravity, and classified by the United Soil Classification System (USCS). A representative soil profile of the riverbank along the river consists of silty sand SM (0-0.6 m), low plasticity clay CL (0.6-2.5 m), high plasticity silt MH (2.5-3.8 m), and low plasticity clay CL (3.8-4.5 m). The soil samples obtained were mostly silt and clay except those taken from near the surface on the top of the bank which were mainly silty sand. Representative grain size distribution curves and the Atterberg limits of soil samples are shown in Figures 3 and 4, respectively. Table 1 summarizes the properties of the soil samples used in the study.

Figure 2 A segment of the riverbank along the Lower Roanoke River in North Carolina that has undergone extensive erosion and bank instability. Soil samples from this site were used in the present study.

Table 1 Properties of the riverbank soil samples used in the study.

Location	USCS Soil Type	Soil composition (%)			LL	PI	Specific Gravity	Number of samples
		Sand	Silt	Clay				
0 - 0.6 m	SM	68-71	20-24	8-9	NP		2.69	2
0.6 - 2.5 m	CL	4-24	28-58	30-48	39-52	16-20	2.72	7
2.5 - 3.8 m	MH	5-14	41-48	42-50	50-57	18-24	2.73	6
3.8 - 4.5m	CL	4-18	50-66	23-43	37-43	15-20	2.72	6

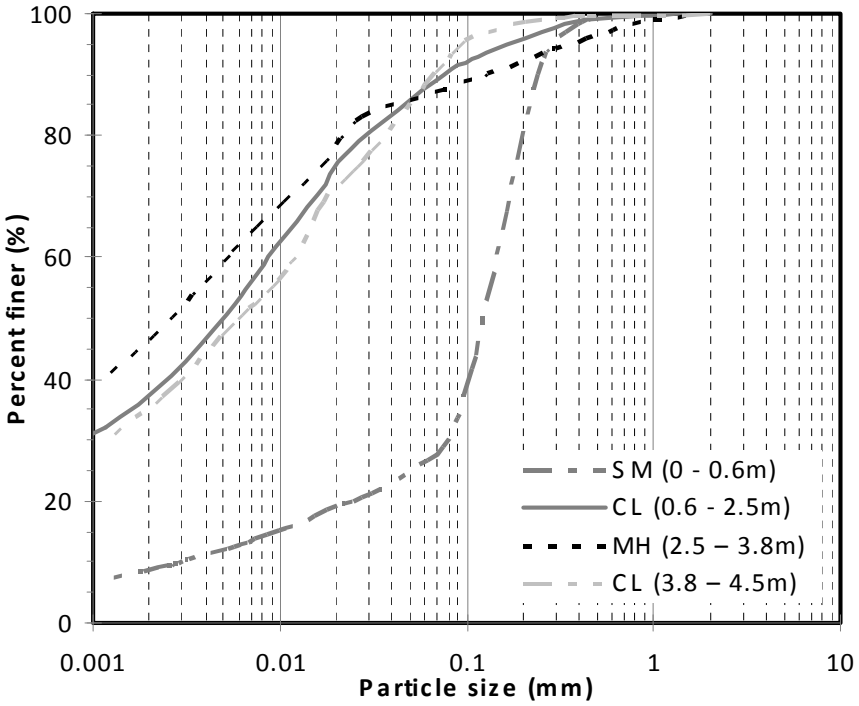

Figure 3 Representative grain size distributions of the tested soil samples.

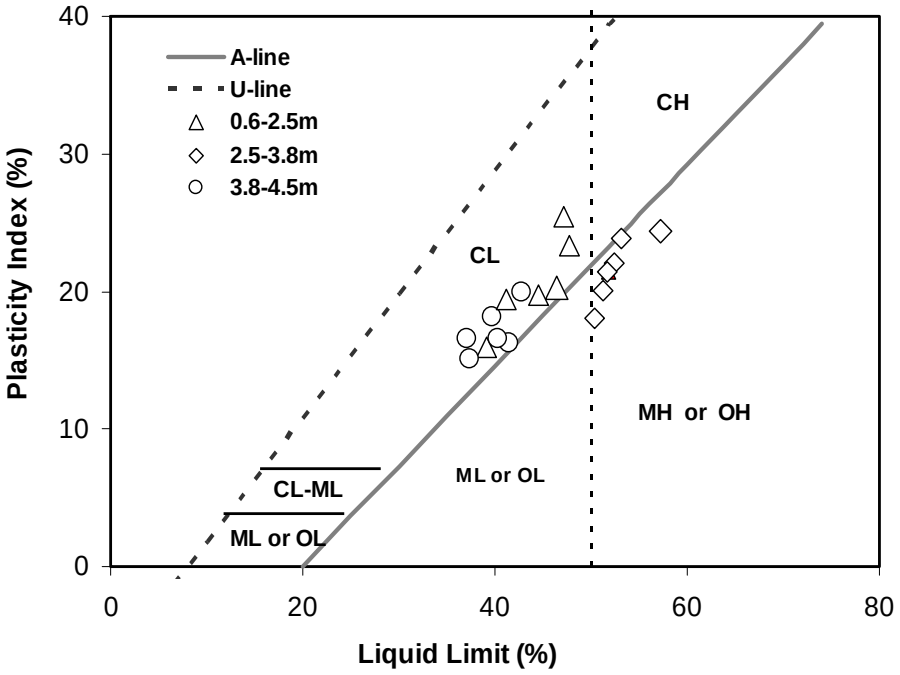

Figure 4 PI vs. LL values of the tested soil samples in the plasticity chart.

2.3.2 Testing methods

Soil suction can be obtained either by direct or indirect methods. The direct method measures the negative pore water pressure due to suction directly, whereas the indirect method requires the measurement of other parameters such as relative humidity, resistivity, conductivity or water content and then relates the results to the suction through calibration (Agus and Schanz, 2007, Ridley and Wray, 1995). The direct method typically requires good contact between the suction sensor and the soil, and measures only matric suction. The indirect method can measure both total and matric suctions, and requires isothermal equilibrium between the sensor, soil and the vapor space around the sample (Agus and Schanz, 2005, Ridley et al., 2003). Direct methods include tensiometers and the axis translations technique. Examples of the indirect methods are filter paper technique, thermal conductivity sensor technique, chilled-mirror hygrometer technique, and use of capacitance sensors that measure water content.

2.3.3 Filter paper method

Due to its simple testing setup, procedures and data analysis, the filter paper method has been widely used to evaluate soil suction. The filter paper method uses a filter paper to reach vapor equilibrium with the soil. Typically, one filter paper is in contact with the soil sample and another is placed at a small distance above the sample. Water from the soil sample migrates to the filter paper in contact with the soil by capillary flow due to imbalance in matric suction. Water is transferred to the filter paper above the sample by vapor transfer, measuring total suction. The most commonly used filter papers are the Whatman No. 42, and the Schleicher and Schuell No. 589 papers,

both of which have known ASTM calibration curves (ASTM D 5298, 2003). A minimum of seven days is required to reach equilibrium.

One of the major drawbacks of the filter paper method is that one test is required to generate one data point in the SWCC, which means that a lot of time and effort are required to construct the entire SWCC. Also, when a soil sample is dry, with a suction value typically higher than 500 kPa, it becomes very difficult to establish good contact between the soil and the filter paper which causes errors (Bulut et al., 2001, Bulut and Wray, 2005, Leong et al., 2002). The current study followed testing procedures from the ASTM standard D5298 and calibration curves for the Whatman No. 42 filter paper. Both measurements for the total and matric suction of the undisturbed soil samples were performed. The differences between the total and matric suction values are compared below with the osmotic suctions estimated by the electrical conductivity measurement.

2.3.4 Axis translation technique (Pressure plate method and Tempe cell method)

The pressure plate test and Tempe cell test are based on the axis translation technique, which directly controls matric suction by increasing air pressure while maintaining pore water pressure equal to atmospheric pressure. It prevents cavitation in the water, but still can create higher matric suction conditions. Typically, this technique uses high air entry (HAE) ceramic discs, and a matric suction of up to 1,500 kPa can be generated. It has been widely adapted in conjunction with conventional soil testing equipment since the HAE ceramic disc can easily substitute for the porous stone in the equipment as long as pressurized conditions are maintained.

The HAE ceramic disc is placed in the pressure chamber. The bottom of the HAE ceramic disc is sealed with rubber and connected to the outside, which provides atmospheric pressure for pore water. A pressure chamber can handle several soil samples simultaneously. Water contents are measured after each test, and new soil samples are saturated and used for different pressures. The limitation of the applicable suction depends on the maximum bubbling pressure of the HAE ceramic disc, and it can be increased by using special cellulose membranes instead of the HAE ceramic disc.

The Tempe cell is typically smaller than the pressure plate apparatus and one soil sample is placed in one cell. Although one Tempe cell can hold one soil sample per test, testing can typically be performed continuously from lower to higher matric suction by measuring the water expelled from the sample. The change in water draining from the soil sample is recorded. When the sample reaches equilibrium, the test proceeds to the next pressure level continuously. Once the air pressure reaches the maximum, the final water content of the soil sample is measured and used for back calculation of water content for each matric suction measurement.

The soil samples for the tests were extruded from Shelby tubes. The samples for the pressure plate test were prepared by using copper retaining rings similar to the one used for direct shear tests but smaller. The samples with the copper rings were placed on the HAE ceramic disc in the pressure plate test chamber. The soil samples for the Tempe cell test were also prepared with an acrylic retaining ring and pushed into the retaining cells. The pressure plate tests were performed under matric suction between 10 and 1,500 kPa and the Tempe cell tests were limited to between 10 and 300 kPa, due to the strength

of the acrylic retaining ring. Stress state changes during the sampling, saturating, and testing were assumed to be negligible.

2.3.5 Dewpoint potentiameter method

Axis translation is limited by the applicable suction due to the bubbling pressure of the HAE ceramic disc. The typical limit of the method is 1,500 kPa, and suction above this value must be measured using another method. As shown in Eq. (3), total suction can be derived from relative humidity thermodynamically. Although the relative humidity method is very sensitive to temperature changes, representing a major drawback, it is still preferable because of its simplicity and relatively short testing duration. The dewpoint potentiameter, also known as a chilled-mirror hygrometer, measures dewpoint and temperature very accurately in a closed space above the soil sample. The sealed chamber has a mirror and condensation detector with precise temperature control. At equilibrium, the relative humidity of the air in the chamber is the same as the relative humidity of the soil sample. When the first condensation appears on the mirror, the vapor pressure is measured and total suction can be calculated (Decagon Devices Inc., 2003, Leong et al., 2002, Patrick et al., 2007, Petry and Jiang, 2003, Thakur et al., 2006).

The WP4-T dewpoint potentiameter manufactured by Decagon Device Inc. was used in this research. It has an internal temperature control function to minimize the effects of changes in temperature. However, the temperature of the soil samples must be maintained close to that of the equipment to minimize the fluctuation of readings. The typical accuracy of the equipment is ±0.1 MPa for suction from 0 to 10 MPa, and ±1% for values from 10 to 300 MPa. However, due to the accuracy of the equipment and the rapid suction increase with decreasing relative humidity at low suctions, a significant

increase in data scatter data can be observed below about 1,000 kPa (Lu and Likos, 2004). Thus, the typical operational range for dewpoint potentiameter seems to be above 1,000 kPa. Recent research demonstrated successful use of the equipment for total suction measurement when compared with other suction measurement methods, and recommended factors to be considered during testing (Bulut and Leong, 2008, Decagon Devices Inc., 2003, Petry and Jiang, 2003, Shah et al., 2006, Sreedeep and Singh, 2006a, Sreedeep and Singh, 2006b, Thakur et al., 2005, Thakur et al., 2006, Thakur et al., 2007).

The WP4-T dewpoint potentiameter was calibrated with 0.5 M KCl standard solution before the tests, and the testing procedures provided in the WP4-T manual and ASTM D6836 were followed. A single undisturbed soil sample was prepared and placed into a sample container, and the initial water content of the soil sample was measured. The container was covered and sealed with a cap and left for 24 hours in a constant temperature environment to achieve water vapor equilibrium. Then the sample was placed in the equipment for measurement. Several readings were taken to confirm equilibrium in the chamber. Once the suction was recorded, the sample weight was measured and left with the cover opened. When a certain weight change was observed, the sample container was covered and left for equilibrium. After one hour, the sample was then placed into the equipment for another measurement. This procedure was repeated several times. After the final reading, the final water content was measured and the water contents for each step were back calculated with the measured weight changes. As temperature affects relative humidity, it is important to maintain a constant temperature and wait for equilibrium to reduce errors.

2.3.6 Vapor equilibrium and osmotic techniques

The vapor equilibrium technique uses a chemical solution, and constant total suction conditions can be created in a closed space. The osmotic potential of the chemical solution forces the closed space and soil samples to reach equilibrium. Typically there are two different types of chemical solutions for the constant suction environment: saturated salt solutions and unsaturated acid solutions. The advantage of using the saturated salt solutions is the consistency of the concentration of the osmotic solution during the equilibrium period. However, the controlled suction is influenced by the specific salt type, and the purity of the chemicals and water (Blatz et al., 2008). The typical range of the suction is also limited to as low as 0 to 10 MPa. The unsaturated acid solutions can create and control much higher suctions. However, unlike the saturated salt solutions, water exchanges which cause changes in osmotic solution concentrations occur during equilibrium. The test does not require any special equipment and is very easy to set up. However, long periods of equilibrium time and strict temperature control are required (Blatz et al., 2008).

Unlike the vapor equilibrium method, water transfer in the osmotic technique is created by the process of osmosis. Since the water transfer takes place in the liquid phase and ion transfer is also allowed through the semi-permeable membrane, the osmotic technique controls the matric suction of a soil (Blatz et al., 2008). The soil samples are placed inside a semi-permeable membrane, then the soil sample and membrane are submerged in a polyethyleneglycol (PEG) solution, which is a polymeric substance made up of large sized molecules (Delage and Cui, 2008). The benefits of using the osmotic technique are that it is simple, safe, and inexpensive, since no air pressure is required.

Similar to the vapor equilibrium technique, the suction is generated under null stress. However, good contact is also required between the sample and the membrane, and an equilibrium period is required. The fragility of the membrane is also a consideration in the osmotic technique (Blatz et al., 2008).

The vapor equilibrium test and osmotic technique test were performed using undisturbed soil samples of the CL soil from 3.8-4.5 m at Ecole Nationale des Ponts et Chaussées. Each soil sample was kept in a closed, temperature controlled space under different suctions for 13 days to reach equilibrium. Each suction level was controlled by the concentration of the PEG and water solution. A magnetic stirrer is used to mix the solution to ensure uniform solution concentration. To calculate the porosity of each sample at each step, the weight of the sample was measured to three decimal places and the volume was measured from the dimensions of the cylindrical sample using a caliper.

2.3.7 Osmotic suction measurements

When total suction is measured, matric suction can be calculated by subtracting osmotic suction from the total suction. As the osmotic suction in soils is due to the presence of soluble salt in the pore water, quantifying the amount of soluble salt is required. Ions of the soluble salts carry electric current, which is measured in terms of electrical conductivity (*EC*). The *EC* is measured from the soil water, which requires extraction of the soluble salt using dilution or saturation, leaching, centrifuging, gas extraction or mechanical squeezing (Iyer, 1990). One of the common methods in soil science is to use dilution or saturation of soil with water. Air dried soil is mixed with a certain amount of de-ionized water, and the soil water is extracted by filtering with a low vacuum.

Two equations are used to convert the osmotic suction from the *EC* of the saturated soil paste. The first equation is from the US Salinity Laboratory (1954) and uses the units of atm for ψ_0 and mS/cm for *EC*:

$$\psi_0 = 0.36EC \tag{9}$$

The second equation is from Romero et al. (1999), cited in Peroni and Tarantino (2003), and uses the units of kPa for ψ_0 and μS/cm for *EC:*

$$\psi_0 = 0.0240EC^{1.065} \tag{10}$$

In the tests, the soil samples were prepared as a saturated paste, and the pore water of the soil samples was extracted by vacuum suction method using a Buchner funnel. The *EC* was measured with a Cole-Parmer Instrument Co. conductivity meter 1481-60. Results using both Eqs. (9) and (10) indicate minimal values of osmotic suction.

2.4 Test results and discussions

The results of the experiments described above are compared by soil type and test method. In addition, the experimental results were compared with the different SWCC models presented above. Figure 5 presents the matric suctions measured by the axis translation technique using disturbed and undisturbed soil samples. As the porosities of the disturbed samples were not available, the results were compared using gravimetric water content. For the SM and CL soils, suction values for disturbed samples are consistently much lower than those for undisturbed soil samples. The experimental results shown in Figure 5 for disturbed and undisturbed samples strongly suggest that suction is dependent on the soil structure. However, at lower suction values the soil

suction is less sensitive to the structure of soil as observed by Romero et al. (1999). For the silty sand (SM) soil, the water content of the undisturbed soil was higher than that of the disturbed soil when the applied suction was the same, which makes the measured suction points move laterally depending on the degree of soil disturbance. For silt and clay, the results for the disturbed soils show a linear increase of matric suction with water content with a logarithmic *y*-axis, whereas those of the undisturbed soils show a bilinear or steeper increase in suction as the water content decreases. The higher water content of the disturbed soil samples at lower matric suction also indicates that loosened and disturbed soils have more pores filled with water. The disturbed soils lost water as matric suction increased. This also indicates that disturbed soil has a lower air entry value than the undisturbed soil samples.

The SWCC of each soil type and testing method are presented in Figure 6. As expected, silt and clay have much higher air entry values and suction than the sandy soil. In turn, the CL soils show higher values of suction than the MH soil. For the CL soil at 0.6-2.5 m, and the MH soil, the matric suction values appear to be slightly lower than the total suction. Although the results from the six different tests do not show perfect agreement for different suctions and degree of saturation, the results appear to be comparable and the scatter in the results appears to be within the range expected from the sample variability. The calibrated van Genuchten's models for the SWCC are also shown and appear to provide good fit with the experimental results, which also supports the validity of the different tests results. Table 2 summarizes the best-fit van Genuchten model parameters for each soil type.

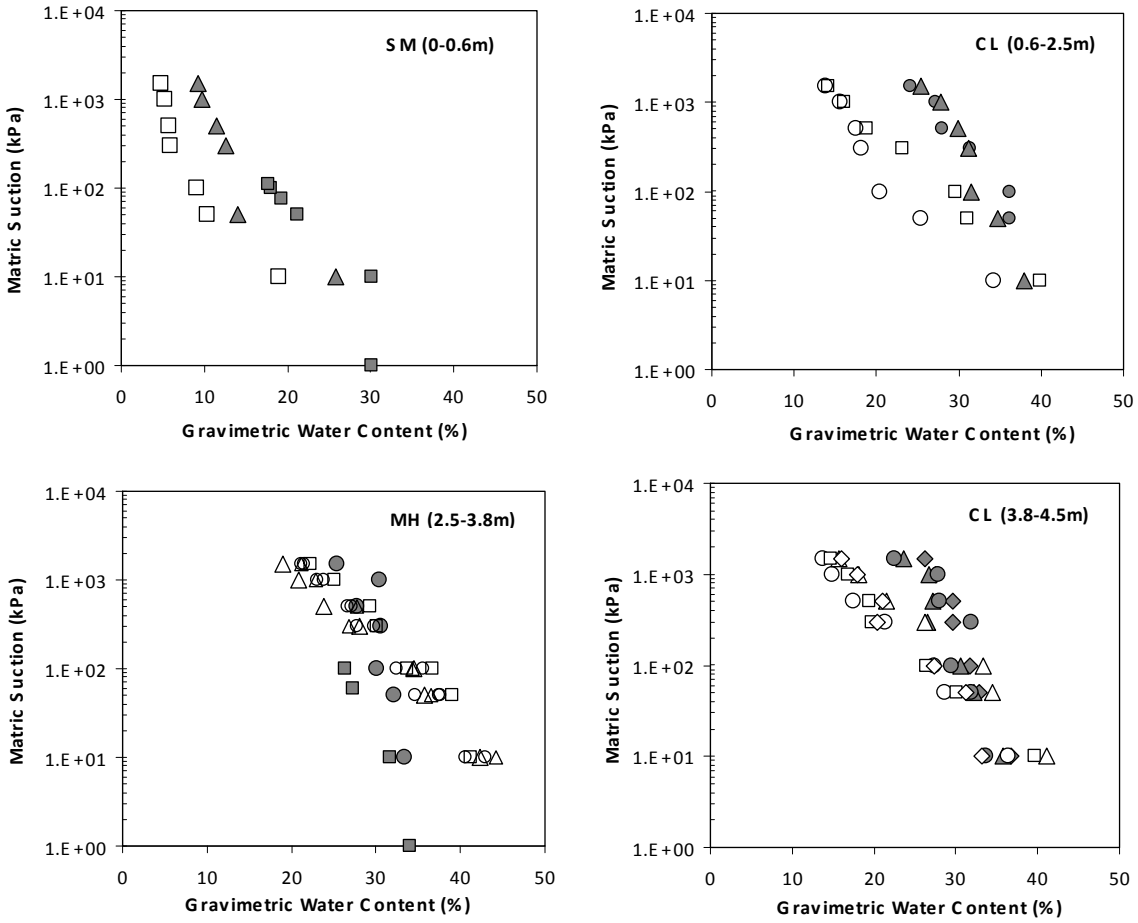

Figure 5 SWCCs from the axis translation technique for disturbed samples (open symbols) and undisturbed samples (solid symbols).

Typically, the direct methods can measure suction up to 1,500 kPa, although in many cases the total suction may need to be measured above that. In this study, the axis translation technique provided results up to 1,500 kPa, and the osmotic technique gave suction values of up to 2,150 kPa. The total suction above 1,500 kPa was measured using the dewpoint potentiameter and the vapor equilibrium methods. It is shown in Figure 6 that both osmotic and axis translation methods produced very similar results, although the suctions from the dewpoint potentiameter and axis translation technique were slightly lower than the osmotic and vapor pressure techniques. This seems to be due to the volume change measurement during the tests. Although the volume change is an

important factor in suction calculations, the porosity of the samples in the axis translation technique was not recorded during testing, and assumed to be constant and equal to the initial porosity, whereas the porosity in the vapor and osmotic techniques was monitored and found to decrease during the equilibrium period especially at higher suction. As the *y*-axis of the SWCC uses a logarithmic scale, the actual suction differences by not accounting for volume changes may not be small enough to be negligible. However, considering possible errors from the test procedures and equipment, and from natural sample variability and quality, the results appear to be in comparable ranges.

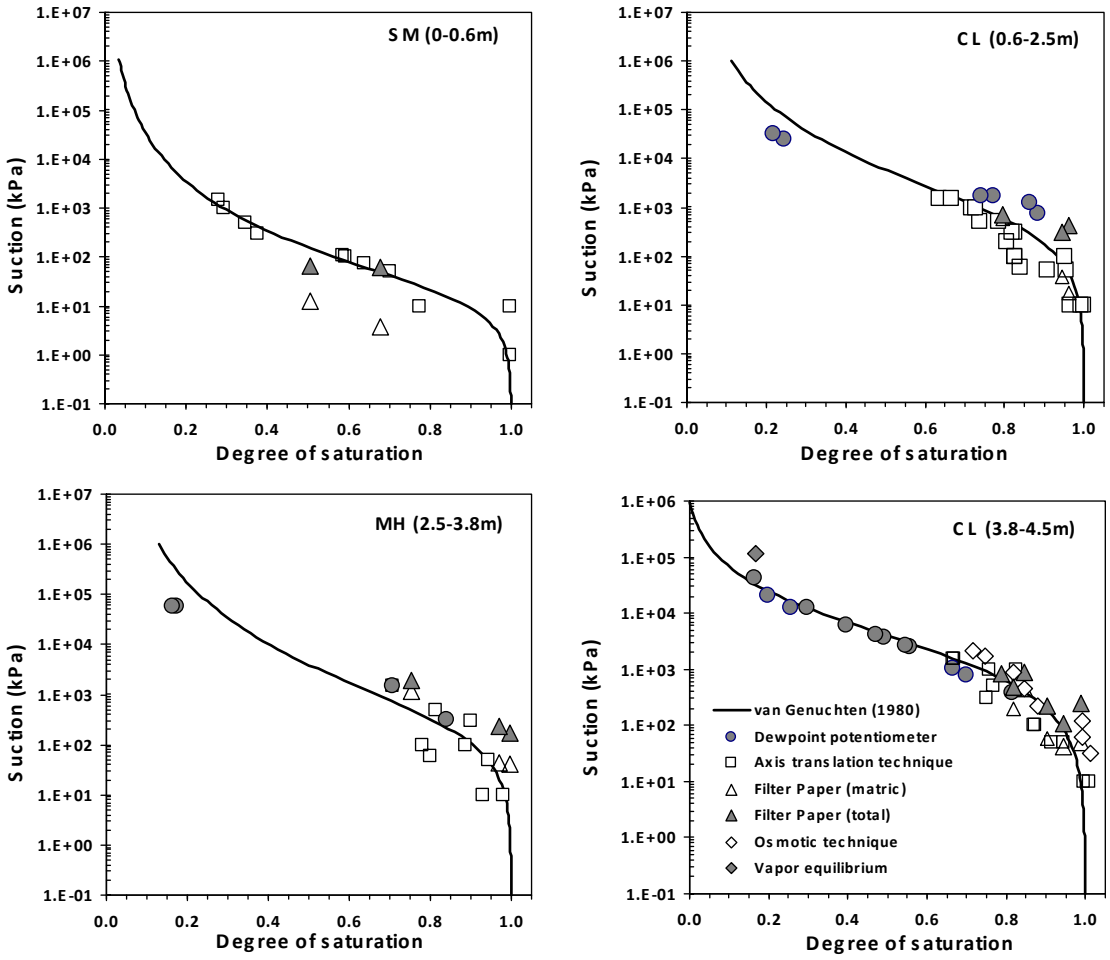

Figure 6 SWCCs for undisturbed soil samples from different testing methods. Open symbols are for matric suction, and solid symbols are for total suction.

Table 2 Model parameters and best-fit R^2 values according to model type for all soil types (the units used are kPa for S and a, and water content is in decimal numbers).

Model	Parameters			
	SM (0-0.6 m)	CL (0.6-2.5 m)	MH (2.5-3.8 m)	CL (3.8-4.5 m)
van Genuchten (1980)	a=17.2, m=0.27, n=1.12, R^2=0.93	a=3439.1, m=0.79, n=0.65, R^2=0.86	a=1978.4, m=0.57, n=0.85, R^2=0.97	a=3684.3, m=0.95, n=0.74, R^2=0.95
Fredlund & Xing (1994)	a=29.4, m=1.00, n=0.94, R^2=0.93	a=2663.8, m=1.80, n=0.65, R^2=0.86	a=2332.6, m=1.63, n=0.82, R^2=0.97	a=3112.7, m=2.22, n=0.75, R^2=0.95
Fredlund & Xing (1994) with correction	a=22.1, m=0.81, n=1.04, ψ_r=10^5, R^2=0.93	a=3375.7, m=1.90, n=0.60, ψ_r=10^5, R^2=0.87	a=2393.8, m=1.55, n=0.76, ψ_r=10^5, R^2=0.98	a=3709.5, m=2.40, n=0.72, ψ_r=10^5, R^2=0.95
Houston et al. (2006)	D_{10}=0.003, D_{20}=0.023, D_{30}=0.08, D_{60}=0.13, D_{90}=0.23 a=9.1, m=2.78, n=0.39, R^2=0.75	PI=19.7%, % passing 200=0.90, wPI=17.7%, ψ_r=500, a=126.9 m=0.57, n=0.09, R^2=0.75	PI=21.6%, % passing 200=0.88, wPI=19.0%, ψ_r=500, a=129.1, m=0.56, n=0.08, R^2=0.91	PI=16.6%, % passing 200=0.92, wPI=15.2%, ψ_r=500, a=121.9, m=0.60, n=0.13, R^2=0.83

The filter paper method may not be practical in constructing the SWCC due to long equilibrium periods, as well as the size and number of the sample required. However, it has the benefit that the total and matric suctions can be measured at the same time in a single test. The filter paper results show that the method provides good data for the SWCC construction. The results are also relatively consistent with the other total suction data. Even though the data for the silty sand soil seems to be far from the predicted curve, the actual difference between the total and matric suctions is smaller than for other soils due to the logarithmic scale. However, the osmotic suctions calculated by subtracting the matric suctions from total suctions obtained from the filter paper tests do not agree to those estimated from the EC measurement. The EC measurement

estimated that the osmotic suctions are only 5 to 10 kPa, whereas the osmotic suction calculated from the filter paper results varied from 60 to 380 kPa. No significant reasons were found, but one possible reason is that the *EC* was measured using the water extracted from the saturated paste, which has a water content much higher than the natural water content. Krahn and Fredlund (1972) measured the osmotic suctions of a low and a high plasticity clays by the *EC* measurement using the squeezing technique, and found that the measured osmotic suctions from the squeezing technique closely agree with suction values calculated from the total and matric suctions measured by a psychrometer and axis translation technique, respectively, whereas the suctions measured from the saturated paste differed significantly. *EC* measurements for osmotic suction performed at the natural water content are expected to be larger than the measured values using the saturated paste. Another reason could be the measurement sensitivity associated with filter paper method. As the method requires a weight measurement resolution of 0.0001 g, any factor that can affect the balance or the weight of filter paper can cause error. Using inappropriate calibration curves for the filter paper method could also be a source of the differences.

Figure 7 shows the results of all soils for suction values above and below 1,500 kPa. Both results show no significant differences between each soil type except for the silty sand, and the range of data can again be due to sample variability. The similarity in the SWCC's of the CL (from 0.6 to 2.5 m), MH and CL (from 3.8 to 4.5 m) soils can be due to the similarity in the grain size distribution curves and the Atterberg limits of the different soils.

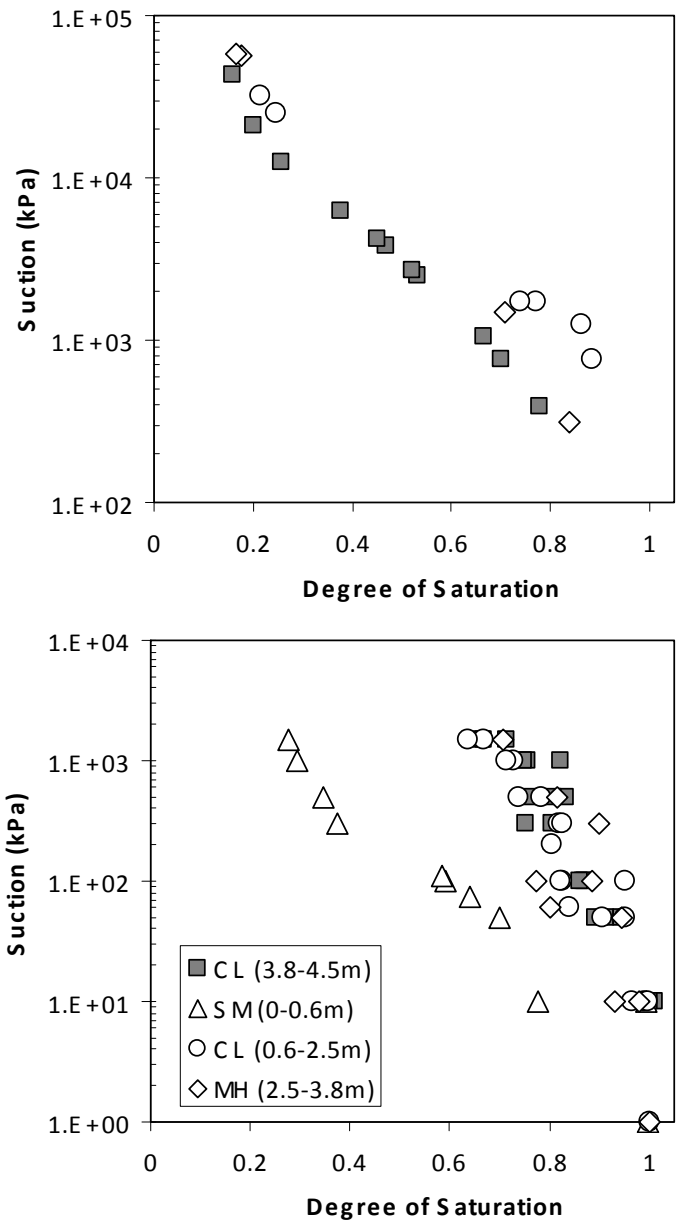

Figure 7 SWCCs for different soils at suction values above and below 1,500 kPa.

The models with fitting parameters proposed by van Genuchten (1980), and Fredlund and Xing (1994) with and without a correction factor, and the modified model from Houston et al. (2006) are compared with experimental data in Figure 8 for the four soil types. Both the van Genuchten, and Fredlund and Xing models use three parameters

(i.e., a, n, and m). The Houston et al. model uses the same parameters but determines them not by data fitting but by correlations using plasticity index, gradation information, and water content. Table 2 presents the parameters and R^2 values for the four models for all four soil types. The parameters for the van Genuchten, and Fredlund and Xing (1994) (with and without correction) models were obtained by nonlinear regression, while the parameters for the Houston et al. model were taken directly from the results of the soil index tests. The van Genuchten, and the uncorrected and corrected Fredlund and Xing models are fitted adequately over the entire range of available experimental data. The van Genuchten, and Fredlund and Xing models predict almost identical SWCCs, and differences can only be observed at high suction values. For the SM soil, the uncorrected Fredlund and Xing model significantly deviates from the other models for saturation values less than 20%. The differences between the three models are less significant for the other three soil types.

The model of Houston et al. gives reasonable results for matric suction values below 1,500 kPa, and generally deviates from the experimental data for suction values above 1,500 kPa. In general, the Houston et al. model provide worse fit of the experimental than the other three models as can be seen in Figure 8 and the R^2 values from Table 2. For the SM soil type, the Houston et al. model yield lower suction values than the three models for suction values above 1,500 kPa. For the other three soil types, the Houston et al. model shows linear relationship between the logarithm of suction and water content, and higher suction values than the data from the experiments and the other three models, for suction values above 1,500 kPa. The original family of desorption curves from Houston et al. have very mild curvatures, with no significant inflections after

the air entry value, when the *wPI*<5. Perera et al. (2005) state that the SWCCs in the Houston et al. were constructed using pressure plate tests, which are limited to suction values under 1,500 kPa. This may explain the relatively reduced performance of the Houston et al. model for suction values over 1,500 kPa. Nevertheless, the Houston et al. model for establishing the SWCC appears to be suitable for the lower suction range, and it has the convenience of requiring parameters that are easy to determine to establish the SWCC.

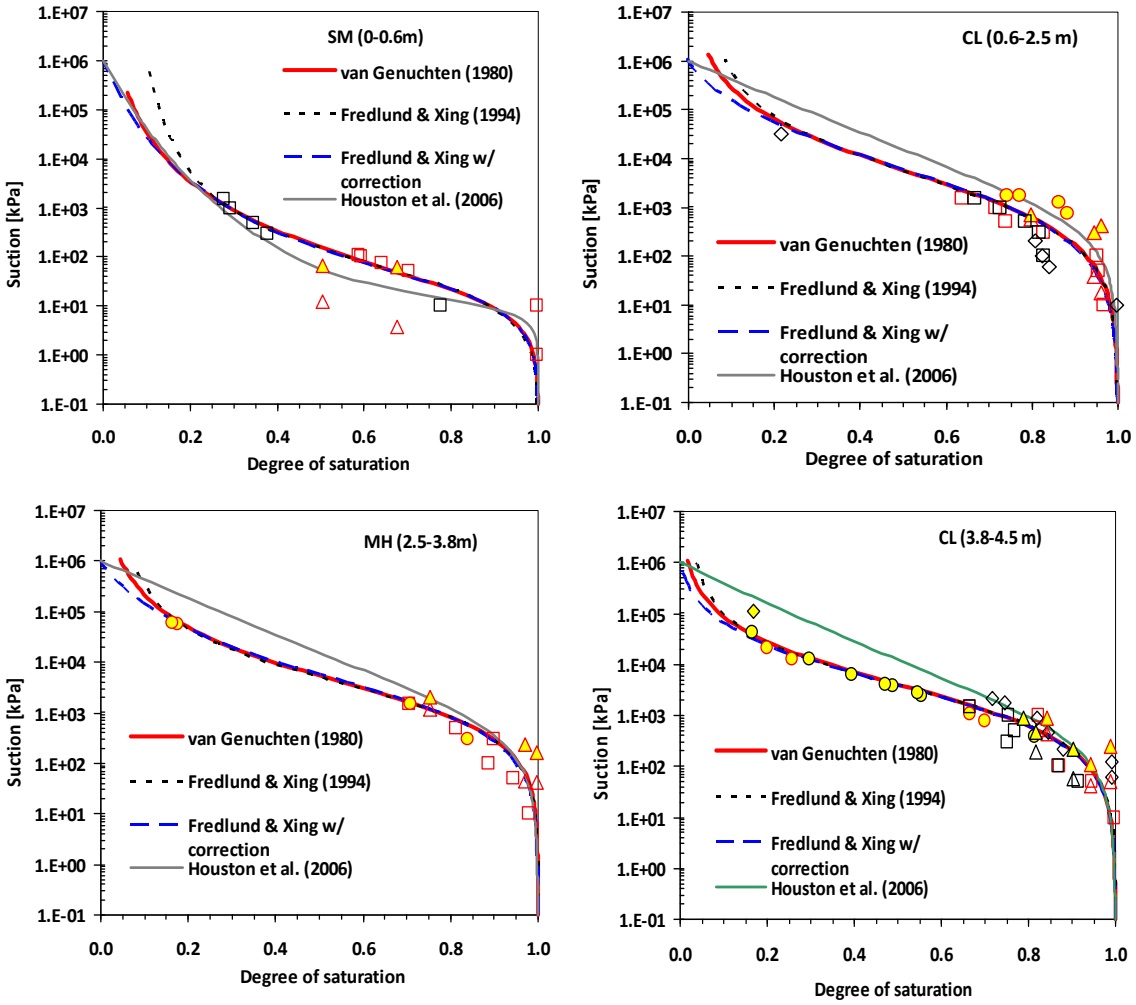

Figure 8 Comparisons of SWCC models against experimental data for all soil types and test procedures.

2.5 Conclusions

The desorption branch of the SWCCs of natural soils from the riverbank of the Lower Roanoke River in North Carolina were established using six different methods. The tested soil samples represent a typical soil profile along the riverbank of the Lower Roanoke River in North Carolina, and consisted of silty sand, low plasticity clay, high plasticity silt, and another layer of low plasticity clay. For total suction measurement, the dewpoint potentiameter, filter paper, and vapor equilibrium methods were used. For direct matric suction measurement, the pressure plate, Tempe cell, and the osmotic methods were used. The osmotic suction was indirectly estimated by measuring electrical conductivity of the pore water, and was found to be negligible for the tested soil samples. Except for silty sand, the differences in SWCCs between the soil samples were not significant due to the similar physical properties of the soils (i.e., grain size distribution and Atterberg limits). The results indicate that the six different measuring techniques used in the study provide comparable results. The differences in results from the different test methods appear to be less significant than the expected scatter from soil sample variability.

The filter paper test is the only test that could provide both matric and total suction at the same time. It is simple and low cost testing method, and does not require special equipment. However, it is sensitive to small differences in weight, and there are still controversies related to the calibration method and the length of the required equilibrium period. The dewpoint potentiameter also provides a wide range of suction measurement, but it yields larger variation for low suction values. Vapor pressure and osmotic techniques generally require long equilibrium periods, but they are relatively

easier and safer to use for high suctions. Axis translation technique is one of the most common methods and the procedure is simple. However, it requires long equilibrium period and is applicable only to narrow range of suction values.

It is recommended that separate techniques be employed for determining total and matric suction. The dewpoint potentiameter method is recommended for total suction measurement. The method is simple and required the shortest time among the six tests that were evaluated. The suction is measured continuously with a single soil sample and the results can be monitored instantaneously. For matric suction, either the axis translation technique or osmotic technique is recommended. The axis translation technique has been widely used, has proven accurate and reliable, and the required equipment is readily available. However, when the equipment is not accessible, the osmotic technique could be an alternative, which can be easily setup and performed. The most favorable attribute of the osmotic technique is that it can generate higher suction than the axis translation technique. It is also safe as it does not require high air pressure. If none of these methods are available, the filter paper technique is still an option.

The experimental data were compared to the mathematical models proposed by van Genuchten (1980), Fredlund and Xing (1994), and Houston et al. (2006). The comparison confirmed that the Fredlund and Xing, and van Genuchten models, which are both based on pore-size distribution functions and use three fitting parameters, provide almost identical results, except at very high suction values, and yield good fits with the experimental data. The model by Houston et al., using parameters based only on particle gradation and soil plasticity, showed good agreement only for suction below 1,500 kPa. At suction values higher than 1,500 kPa, the Houston et al. model deviated significantly

from experimental data and showed a linear change in the logarithmic value of suction as function of water saturation. Model parameters for the four different tested soils types, and the SWCC models were presented, which can be used as representative parameters for the riverbank soils in the study.

2.6 References

[1] Agus, S. S., and Schanz, T. (2005). "Comparison of four methods for measuring total suction." *Vadose Zone Journal*, 4(4), 1087-1095.

[2] Agus, S. S., and Schanz, T. (2007). "Errors in total suction measurements." *Experimental Unsaturated Soil Mechanics*, 59-70.

[3] ASTM D 5298 (2003). "Standard Test Method for Measurement of Soil Potential (Suction) Using Filter Paper." *ASTM International*.

[4] Barbour, S. L. (1998). "Nineteenth Canadian geotechnical colloquium: the soil-water characteristic curve: a historical perspective." *Canadian Geotechnical Journal*, 35(5), 873-894.

[5] Blatz, J. A., Cui, Y.-J., and Oldecop, L. (2008). "Vapour equilibrium and osmotic technique for suction control." *Geotechnical and Geological Engineering*, 26(6), 661-673.

[6] Bulut, R., and Leong, E. (2008). "Indirect measurement of suction." *Geotechnical and Geological Engineering*, 26(6), 633-644.

[7] Bulut, R., Lytton, R. L., and Wray, W. K. (2001). "Soil suction measurements by filter paper." American Society of Civil Engineers, Houston, TX, United States, 243-261.

[8] Bulut, R., and Wray, W. K. (2005). "Free energy of water-suction-in filter papers." *Geotechnical Testing Journal*, 28(4), 355-364.

[9] Burdine, N. T. (1953). "Relative permeability calculations from pore size distribution data." *Journal of Petroleum Technology*, 5(3), 71-78.

[10] Campbell, G. S. (1988). "Soil water potential measurement: An overview." *Irrigation Science*, 9(4), 265-273.

[11] Dapporto, S., Rinaldi, M., Casagli, N., and Vannocci, P. (2003). "Mechanisms of riverbank failure along the Arno River, Central Italy." *Earth Surface Processes and Landforms*, 28(12), 1303-1323.

[12] Decagon Devices Inc. (2003). "WP4 dewpoint potentiameter operator's manual version 4."Pullman, WA, USA.

[13] Delage, P., and Cui, Y. J. (2008). "An evaluation of the osmotic method of controlling suction." *Geomechanics and Geoengineering*, 3(1), 1-11.

[14] Delage, P., Romero, E., and Tarantino, A. (2008). "Recent developments in the techniques of controlling and measuring suction in unsaturated soils." *Proc., The 1st European Conference on Unsaturated Soils, Unsaturated Soils. Advanced in Geo-Engineering*, Taylor & Francis Group, London, 33-52.

[15] Fredlund, D. G. (2002). "Use of soil-water characteristic curves. in the implementation of unsaturated soil mechanics." *The Third International Conference of Unsaturated Soils*, J. F. T. Juca, T. M. P. de Campos, and F. A. M. Marinho, eds., A.A. Balkema Publishers, Recife, Brazil, 887-902.

[16] Fredlund, D. G., and Rahardjo, H. (1993). *Soil mechanics for unsaturated soils*, Wiley, New York :.

[17] Fredlund, D. G., and Xing, A. (1994). "Equations for the soil-water characteristic curve." *Canadian Geotechnical Journal*, 31(4), 521-532.

[18] Houston, W. N., Dye, H. B., Zapata, C. E., Perera, Y. Y., and Harraz, A. (2006). "Determination of SWCC using one point suction measurement and standard curves." *Proceedings of the Fourth International Conference on Unsaturated Soils*, American Society of Civil Engineers, Reston, VA 20191-4400, United States, Carefree, AZ, United States, 1482-1493.

[19] Iyer, B. (1990). "Pore water extraction-Comparison of saturation extract and high-pressure squeezing." Publ by ASTM, Philadelphia, PA, USA, St. Louis, MO, USA, 159-170.

[20] Krahn, J., and Fredlund, D. G. (1972). "On total, matric and osmotic suction." *Soil Science*, 114(5), 339-348.

[21] Leong, E. C., He, L., and Rahardjo, H. (2002). "Factors affecting the filter paper method for total and matric suction measurements." *Geotechnical Testing Journal*, 25(3), 322-333.

[22] Leong, E. C., and Rahardjo, H. (1997). "Review of soil-water characteristic curve equations." *Journal of Geotechnical and Geoenvironmental Engineering*, 123(12), 1106-1117.

[23] Lu, N., and Likos, W. J. (2004). *Unsaturated soil mechanics*, J. Wiley, Hoboken, N.J. USA.

[24] Miller, D. J., and Nelson, J. D. (1993). "Osmotic suction as a valid stress state variable in unsaturated soil mechanics." *Proc., Unsaturated Soils*, ASCE, New York, NY, USA, 64-76.

[25] Mualem, Y. (1976). "A new model for predicting the hydraulic conductivity of unsaturated porous media." *Water Resources Research*, 12(3), 513-522.

[26] Or, D., and Wraith, J. M. (1999). "Soil water content and water potential relationships." *Handbook of soil science*, M. E. Sumner, ed., CRC Press, Boca Raton, FL, A53-A85.

[27] Patrick, P., Olsen, H., and Higgins, J. (2007). "Comparison of chilled-mirror measurements and filter paper estimates of total soil suction." *Geotechnical Testing Journal*, 30(5), 1-8.

[28] Perera, Y. Y., Zapata, C. E., Houston, W. N., and Houston, S. L. (2005). "Prediction of the soil-water characteristic curve based on grain-size-distribution and index properties." *the Geo-Frontiers 2005 Congress*, C. W. Schwartz, E. Tutumluer, and L. Tashman, eds., ASCE, Reston, VA, United States, Austin, TX, United States, 49-60.

[29] Peroni, N., and Tarantino, A. (2003). "Measurement of osmotic suction using the squeezing technique." *From Experimental Evidence towards Numerical Modeling of Unsaturated Soils*, T. Schanz, ed., Springer, Weimar, Germany, 159-168.

[30] Petry, T. M., and Jiang, C. P. (2003). "Evaluation and utilization of the WP4 dewpoint potentiameter phase I and II." Center for Infrastructure Engineering Studies, University of Missouri-Rolla, United States, 34.

[31] Piegay, H., Darby, S. E., Mosselman, E., and Surian, N. (2005). "A review of techniques available for delimiting the erodible river corridor: a sustainable approach to managing bank erosion." *River Research and Applications*, 21, 773-789.

[32] Ridley, A. M., and Burland, J. B. (1993). "A new instrument for the measurement of soil moisture suction." *Géotechnique*, 43(2), 321-324.

[33] Ridley, A. M., Dineen, K., Burland, J. B., and Vaughan, P. R. (2003). "Soil matrix suction: Some examples of its measurement and application in geotechnical engineering." *Geotechnique*, 53(2), 241-253.

[34] Ridley, A. M., and Wray, W. K. (1995). "Suction measurement: A review of current theory and practices." *Proc., Proceedings of the first international conference on Unsaturated Soils*, Balkema, 1293-1322.

[35] Rinaldi, M., Casagli, N., Dapporto, S., and Gargini, A. (2004). "Monitoring and modelling of pore water pressure changes and riverbank stability during flow events." *Earth Surface Processes and Landforms*, 29(2), 237-254.

[36] Romero, E., Gens, A., and Lloret, A. (1999). "Water permeability, water retention and microstructure of unsaturated compacted Boom clay." *Engineering Geology*, 54(1-2), 117-127.

[37] Shah, P. H., Sreedeep, S., and Singh, D. N. (2006). "Evaluation of methodologies used for establishing soil-water characteristic curve." *Journal of ASTM International*, 3(6).

[38] Sillers, W. S. (1997). "The mathematical representation of the soil-water characteristic curve." M.Sc, University of Saskatchewan, Saskatoon, Canada.

[39] Sillers, W. S., Fredlund, D. G., and Zakerzadeh, N. (2001). "Mathematical attributes of some soil-water characteristic curve models." *Geotechnical and Geological Engineering*, 19(3-4), 243-283.

[40] Simon, A., Thomas, R. E., Curini, A., and Shields Jr, F. D. (2002). "Case study: Channel stability of the Missouri River, eastern Montana." *Journal of Hydraulic Engineering*, 128(10), 880-890.

[41] Sreedeep, S., and Singh, D. N. (2006a). "Methodology for determination of osmotic suction of soils." *Geotechnical and Geological Engineering*, 24(5), 1469-1479.

[42] Sreedeep, S., and Singh, D. N. (2006b). "Nonlinear curve-fitting procedures for developing soil-water characteristic curves." *Geotechnical Testing Journal*, 29(5), 409-418.

[43] Thakur, V. K. S., Sreedeep, S., and Singh, D. N. (2005). "Parameters affecting soil-water characteristics curves of fine-grained soils." *Journal of Geotechnical and Geoenvironmental Engineering*, 131(4), 521-524.

[44] Thakur, V. K. S., Sreedeep, S., and Singh, D. N. (2006). "Laboratory investigations on extremely high suction measurements for fine-grained soils." *Geotechnical and Geological Engineering*, 24(3), 565-578.

[45] Thakur, V. K. S., Sreedeep, S., and Singh, D. N. (2007). "Evaluation of various pedo-transfer functions for developing soil-water characteristic curve of a silty soil." *Geotechnical Testing Journal*, 30(1), 25-30.

[46] Toker, N. K. (1999). "Improvements and reliability of MIT tensiometers and studies on soil moisture characteristic curves." MS, MIT, Boston, MA.

[47] United States Salinity Laboratory (1954). "Diagnosis and improvement of saline and alkali soils. Agricultural Handbook No. 60." *Agriculture handbook*, L. A. Richards, ed., United States Department of Agriculture, Washington, 160.

[48] van Genuchten, M. T. (1980). "A closed-form equation for predicting the hydraulic conductivity of unsaturated soils." *Soil Science Society of America Journal*, 44(5), 892-898.

CHAPTER 3. Laboratory and In-situ Determination of Hydraulic Conductivity and the Implications for Transient Seepage Analysis[1]

ABSTRACT

This paper critically compares the use of laboratory tests against in-situ tests combined with numerical seepage modeling to determine the hydraulic conductivity of natural soil deposits. Laboratory determination of hydraulic conductivity used the constant head permeability and oedometer tests on undisturbed Shelby tube and block soil samples. The auger hole method and Guelph permeameter tests were performed in the field. To examine the validity of the various test results, the groundwater table elevations for different hydraulic conductivity values were predicted using finite element seepage modeling and compared with field measurements of the groundwater table. Hydraulic conductivity values obtained by the auger hole method provided better predictions of the location of the groundwater table for a continuous drawdown of water surface elevation, indicating that hydraulic conductivity determined from in-situ tests represents actual conditions in the field better than those performed in a laboratory setting. The differences between the laboratory and in-situ hydraulic conductivity values can be attributed to factors such as sample disturbance, soil anisotropy, fissures and cracks, and soil structure, in addition to the conceptual differences in test methods and sample size as reported by previous researchers.

Keywords: In-situ permeability test, Guelph permeameter, auger hole test, transient seepage analysis

---

[1] This manuscript has been prepared for submission to a journal, and is co-authored by **Soonkie Nam**, Marte S. Gutierrez, Panayiotis Diplas, and John Petrie

3.1 Introduction

Understanding and predicting the movement or seepage of water in soils is a vital part of geotechnical engineering. One of the major factors governing the movement of water through the soil is gravity. Seepage, which is generally slow and assumed to be laminar, is described by Darcy's law which states that the velocity of a flowing liquid (v) through a porous medium is directly proportional to the pressure gradient causing the flow, and is the product of the hydraulic gradient (i) and the hydraulic conductivity (k). Hydraulic conductivity k, which is also commonly and erroneously referred to as permeability in soil mechanics, is the most fundamental parameter used to predict the flow of water through soils. Thus, an accurate determination of k is vital for predicting water seepage in soils for engineering applications.

Hydraulic conductivity can be determined using either indirect or direct methods. Indirect methods are based on the use of empirical equations that take into account soil properties such as particle size distribution or void ratio. Most indirect methods are based on the fundamental theory of flow through porous media modeled as a system of circular cross sectional tubes of different diameters (Vukovic and Soro, 1992) and thus generally perform better with granular soils than cohesive soils. As a result, application of indirect methods is generally limited to sandy soils. In contrast, direct methods are based on laboratory tests with undisturbed samples or re-constituted samples and in-situ tests, and flow conditions that are closer to field conditions are used. Laboratory tests are performed under controlled test conditions such as constant cross sectional areas, hydraulic gradients or flow rates. The ability to impose a desirable set of conditions constitutes the main advantage of laboratory testing. However, using small test samples

in a one dimensional flow condition limits how representative this approach can be of actual field conditions. On the other hand, in-situ tests have the advantage of representing the complexity of field conditions more accurately than laboratory tests. The sample disturbances that are likely during sampling and transportation are avoided by using in-situ tests. The differences observed between laboratory and in-situ hydraulic conductivity, k_L and k_F, respectively, are frequently unpredictable and the hydraulic conductivity values often differ by several orders of magnitude. Most often, k_F is reported to be larger than k_L including a case where the in-situ value was up to 46,000 times larger than the laboratory value (Weber, 1968); however, some researchers have reported conductivity in the lab k_L to be larger (Bouma and Woesten, 1979, Goodall and Quigley, 1977). These results cannot be interpreted to reach a general conclusion because flow characteristics, particularly in cohesive soils, can vary significantly depending on a number of factors. Therefore, determination of hydraulic conductivity not only requires the meticulous execution of tests but also proper determination of experimental methods that consider the variability of field conditions.

To analyze groundwater flow, it is often necessary to perform multiple determinations of hydraulic conductivity using different methods. If hydraulic conductivity shows a wide range of variation, it is critical that the most representative value is selected, and thus utilizing the information from other sources is recommended in order to increase reliability. Field monitoring of the groundwater table (GWT) is one of the most commonly used methods, along with transient seepage analysis if available. The results of modeling for various values of hydraulic conductivity and the GWT measured at different locations can be compared to determine a more reliable value.

The main objective of the study presented in this paper is to critically evaluate hydraulic conductivity data obtained from laboratory tests and in-situ tests combined with transient seepage computer modeling for natural soil deposits obtained from the riverbank of the lower Roanoke River, North Carolina, U.S.A. The hydraulic conductivity values from the different methods are compared and the potential causes for the differences are reviewed and discussed.

3.2 Site description and materials

3.2.1 Study sites

The five study sites used for soil sampling, groundwater monitoring wells, and transient seepage analysis were located on the lower Roanoke River near Scotland Neck, North Carolina, U.S.A. The lower Roanoke River flows through the northern Coastal Plain, where the surface soil consists of Quaternary alluvium, with Miocene and Upper Cretaceous sedimentary materials underlying the alluvium soil layer (Brown et al., 1972, Hupp et al., 2009). Unconsolidated fine sands, silts and clays are the primary materials, but there are also clayey Miocene deposits in places (Hupp et al., 2009, Weems and Lewis, 2007, Weems et al., 2009).

Three major reservoirs, Kerr Lake, Lake Gaston, and Roanoke Rapids Lake, were created after the construction of the John H. Kerr Dam, Gaston Dam, and Roanoke Rapids Dam respectively. The Roanoke Rapids Dam (RRD) is located about 72 km upstream from the sampling sites, as shown in Figure 1. Depending on the time of year and prevailing hydrologic conditions, the dam typically operates in one of four operational modes: normal, flood control, fish spawning, and drought flow (Dominion,

2010). It is worth mentioning that 88% of the Roanoke River basin area, including all three major reservoirs, are located above the RRD (Roanoke River Basin Interest Subcommittee, 2009, U.S. Army Corps of Engineers Wilmington District, 2010) and that no significant tributaries join the river between RRD and the study sites. Therefore, water surface elevations (WSE) near the study sites are primarily controlled by the discharge from the Roanoke Rapids Dam and are little affected by the local climate. Consequently, downstream WSE can be estimated based on the dam operational mode, supplemented by actual data provided by USGS gage stations near the dam and study sites.

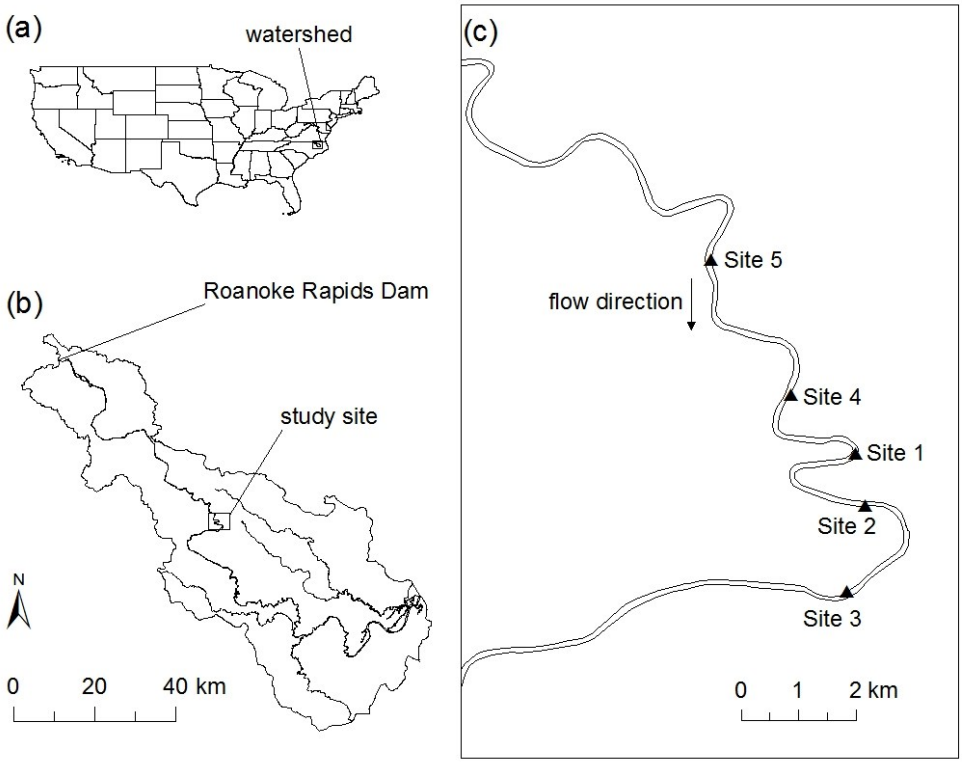

Figure 1 Location of study area. (a) the United States and the location of the lower Roanoke River watershed in N.C., (b) the Roanoke River watershed below the Roanoke Rapids Dam, and (c) the study sites on the lower Roanoke River.

3.2.2 Soil samples and properties

Soil samples were collected from 10 cm diameter holes drilled vertically up to 3 m from the top and slope surfaces of the riverbank by hand auger, and analyzed for water content, void ratio, grain size distribution, specific gravity and Atterberg limits. The top surface soil layer of the riverbank at the study sites consists of sandy soil, classified as silty sand (SM) by the Unified Soil Classification System (USCS). The top sandy soil layer is less than 0.5 m deep, and roots and decomposed debris were observed in the samples. The layers below the top of the bank consisted of thick layers of cohesive soils, with the lower clayey layer containing lenses of gray Myocene clay. Although the cohesive soils were classified as either CL, ML or MH, their visual characteristics and physical properties such as composition of sand, silt, and clay, and liquid and plastic limits, were very similar, as can be seen in Figure 2. Their soil properties are listed in Table 1. The depth of the cohesive soil layers was measured to be up to 6 m from the bank top and was assumed to extend down to 10 m, underlain by an impervious soil layer.

When an exposed surface of the cohesive soil layers was submerged, it became very sticky and slippery, a feature typical of clay soils. However, once the surface dried, superficial cracks developed and the soil became hard and brittle. Although no distinct soil layers were observable in the riverbank, chunks of soil easily fell off when it was dry, which indicates pre-developed small scale structured layers. As shown in Figure 3, the silt and clay soils in the field are not as homogeneous as marine clays but contain pores, cracks, and aggregates that may lead to the development of characteristics of randomly structured soil when the soils dry out.

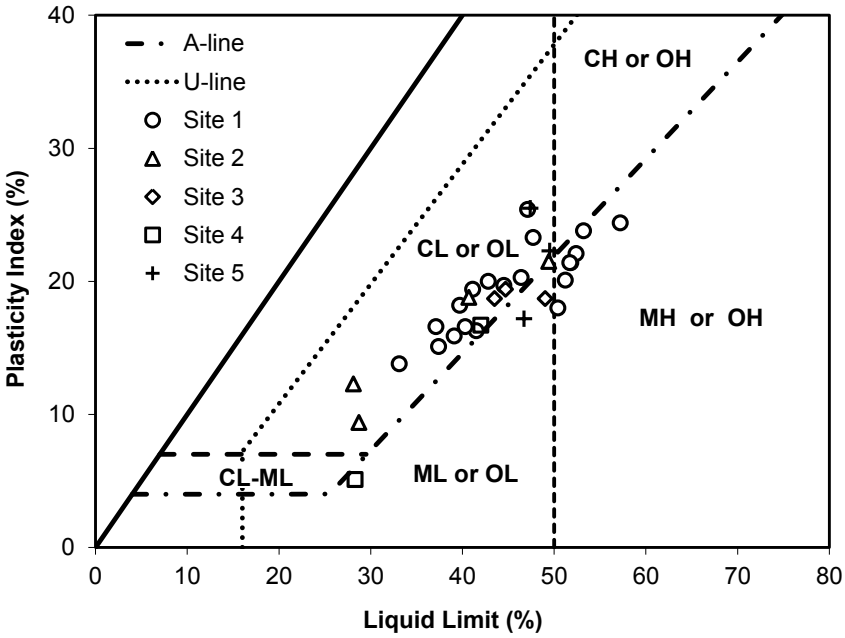

Figure 2 Soil properties of the soils from the test sites.

Table 1 Physical properties of the soils from the riverbanks of the lower Roanoke River.

USCS Soil Type	Soil Properties				
	Liquid Limit LL (%)	Plasticity Index I_P (%)	Sand content (%)	Silt content (%)	Clay content (%)
SM	N.P		69.5	22.0	8.5
CL	41.6	18.3	16.9	50.1	33.0
MH	52.7	21.6	9.2	44.6	46.2
ML	41.2	13.7	25.4	48.2	26.4

(a) Surface condition of CL soil in the field

(b) Small scale structured layer on a dried sample

Figure 3 Evidence of structured soils.

3.3 Determination of hydraulic conductivity

The flow of water through soil is described by Darcy's law, which states that the rate of flow Q is proportional to the soil cross sectional area A (unit: L^2), and head difference $\Delta h = (h_1 - h_2)$ (unit: L), but inversely proportional to the length of flow ΔL, resulting in the well-known Darcy's equation:

$$Q = kiA \tag{1}$$

where Q = flow rate (unit: L^3/T), k = hydraulic conductivity (unit: L/T), and i = hydraulic gradient ($\Delta h / \Delta L$). Darcy's law is valid only under laminar flow conditions, which generally holds true for the movement of water in soils.

3.3.1 Constant head permeability test

The most commonly used laboratory methods are constant head permeability (CHP) and falling head permeability (FHP) tests. In general the CHP test is better suited to granular soils and the FHP test to fine grained soils, as the latter allows smaller flows to be easily measured. However, the CHP test can also be applied to finer soils using a Mariotte bottle or by superimposing a constant pressure in which the testing time is reduced by increasing the flow rate (Olson and Daniel, 1981). This must be done cautiously, however, because high pressure can initiate fractures in the soil samples and incorrect values of hydraulic conductivity can result.

In this study, CHP tests with a constant air pressure were conducted using Tempe cells. The diameter of the cell was 5 cm, and the thickness of each sample was about 1 cm. An initial pressure of below 5 kPa was applied to drain water in the system, and then

a higher pressure was applied and maintained until the drainage rate reached equilibrium. The hydraulic conductivity was determined using the equation:

$$k = \frac{Qh}{PA} \tag{2}$$

where, Q = flow rate, h = sample thickness, P = applied pressure, and A = cross sectional area of soil sample. To check for the development of fractures during the test, the pressure was increased in stages, and the results compared to confirm the hydraulic conductivity remained constant.

3.3.2 Oedometer test

The oedometer test is the most widely used test for one-dimensional consolidation. As explained in the ASTM standard (ASTM D 2435, 2004), a constant vertical load is applied to the sample and a time-deformation curve plotted. After a series of oedometer tests, steadily increasing the constant load for each test, primary consolidation under each loading is determined. The results are plotted in a void ratio e vs. $\log(p')$curve, where p' is the effective vertical stress. Terzaghi (1943) proposed an equation that can be used to determine hydraulic conductivity from the oedometer test. The hydraulic conductivity for each load increment can be calculated from the equation:

$$k = c_v m_v \gamma_w \tag{3}$$

where k = hydraulic conductivity, c_v = coefficient of consolidation, m_v = coefficient of volume change, and γ_w = unit weight of water. The coefficient of volume change m_v is determined from the slope of the e vs. $\log(p')$ curve. The consolidation test provides

hydraulic conductivity values *k* as function of the void ratio *e,* which can be used to establish empirical *e* vs. *k* relationships for the tested soil samples.

3.3.3 Auger hole method

Due to some of the drawbacks of laboratory tests, such as sample disturbance and the inability to precisely reproduce field conditions, additional tests that more accurately represent field conditions are often preferred. The auger hole method is a quick and simple test that can be easily performed in the field when the water table is shallow, and does not required sophisticated equipment. It was proposed by Diserens (1934) and later improved by many researchers (van Beers, 1983). Additional benefits of the test are: i) the soil profile can be identified during the test, ii) disturbed and undisturbed soil samples can be collected while drilling the holes, and iii) several tests can easily be done at the same time.

The auger hole (AH) method requires a monitoring well to be drilled that extends below the groundwater table. Once the observation well is completed and the water table inside the well reaches equilibrium, the test starts by removing the water in the hole. Fresh water then seeps into the hole, rising until it returns to the original level, and the time required to reach the equilibrium is measured. As shown in Figure 4, the main parameters required when conducting an auger hole test are the hole dimensions (diameter, depth), the location of the water table in the hole, and the location of the impermeable layer below the hole. The results of an auger hole test can be easily interpreted using plots developed by Boumans (1953) or by applying an equation first proposed by Ernst (1950). Although the graphical method is known to be more accurate, the equation is preferable when the plots are not readily available or for specific field

conditions (van Beers, 1983). The following equation applies to homogeneous soil with an impermeable layer existing 0.5*H* or more below the bottom of the auger hole (Ernst, 1950).

$$k = \frac{4000}{\left(\frac{H}{r} + 20\right)\left(2 - \frac{y}{H}\right)} \frac{r}{y} \frac{\Delta y}{\Delta t} \tag{4}$$

where k = hydraulic conductivity (m/day) , H = depth of the hole below the groundwater table, and the other variables are as shown in Figure 4.

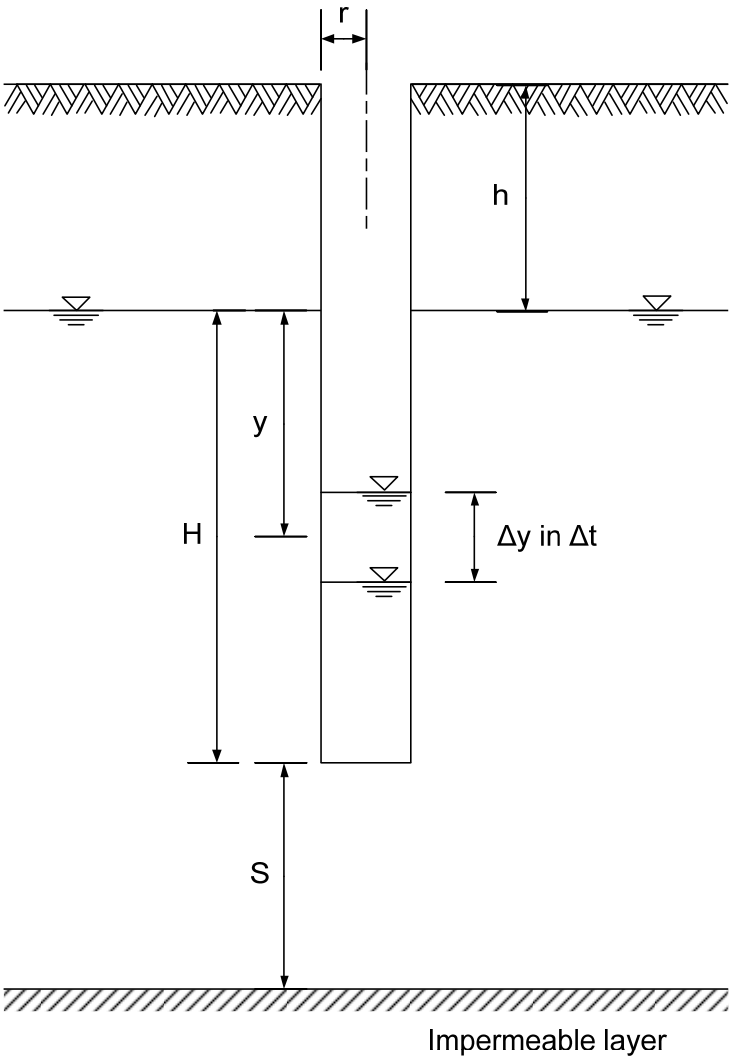

Figure 4 Schematic of the auger hole method.

A total of 14 AH tests were performed at three different riverbank locations. The depth of each auger hole varied from 0.6 m to 1.2 m, and the volume of water withdrawn from each hole was also different due to the prevailing field conditions.

3.3.4 Guelph permeameter

The Guelph permeameter (GP) method is an in-situ constant head test that measures the saturated hydraulic conductivity of unsaturated soils using a Mariotte siphon reservoir. Here, the rate at which water flows out of a cylindrical well above the groundwater table is measured assuming that the soils around the well are homogeneous and saturated during the test. However, due to the saturation process that occurs in soils above the GWT, GP measurements are known to be smaller than the actual saturated hydraulic conductivity because of the entrapped air in the soils. In addition, factors such as the initial water content of the soils and the smearing and compaction of well walls are also known to significantly affect the results (Bagarello and Provenzano, 1996). Thus, each hole in this study was finished with a well preparation brush to remove any smear layer. Five GP tests were performed at three different riverbank locations.

Interpretation of the test results can be made with either one or two point measurements (Soilmoisture Equipment Corp., 2006). Although two point measurements provide a better estimate of α^*, the ratio of saturated hydraulic conductivity k to matric flux potential ϕ_m, measurements of one steady flow rate with a single ponded head, in which the hydraulic conductivity can be obtained using Eq. (4), is known to be sufficient for a good estimation of hydraulic conductivity (Elrick et al., 1989).

$$k = \frac{CQ}{\left(2\pi H^2 + \pi H^2 C + \frac{2\pi H}{\alpha *}\right)} \quad (5)$$

where Q = steady intake rate of water, H = well height, a = well radius, C = dimensionless shape factor dependent on H/a, and $\alpha *$ = ratio of k to ϕ_m.

Further information on the advantages and disadvantages of the GP method and apparatus can be found in the literature (e.g. Bagarello, 1997, Dorsey et al., 1990, Elrick et al., 1984, Gallichand et al., 1990, Reynolds and Elrick, 1985, Salverda and Dane, 1993, Soilmoisture Equipment Corp., 2006).

3.4 Groundwater table monitoring

The location of the phreatic surface as an initial boundary condition is an important input parameter that may significantly affect the modeling results in transient seepage analysis. On the other hand, it is also one of the output results from seepage analysis that can be most conveniently compared to the observed GWT location in the field. Especially when the WSE changes considerably with time, the predicted modeling results are strongly dependent on the values used for the hydraulic conductivity of the soils. Thus, field observations of the GWT can be used to validate the hydraulic conductivity and, consequently, the modeling results.

A groundwater table monitoring well was drilled on a riverbank using a hand auger to a depth of 3.2 m to measure continuous changes in the GWT in response to the WSE, as shown in Figure 5. One GWT sensor was installed at the bottom of the monitoring well and another pressure sensor in the river so changes in the WSE and the corresponding GWT were monitored simultaneously at Site 1.

The GWT sensors were built based on the sensor design originally developed by Dedrick et al. (2000) and upgraded by Riley et al. (2006). A GWT sensor consists of a differential pressure sensor and a logger with a 12-bit microcontroller and a non-volatile 16K EEPROM. The pressure sensor measures differential pressures between atmospheric and water pressures. The logger digitizes the analog voltage from the sensor and stores the data in the EEPROM. The measurement period is determined by the battery life. Lithium batteries were used so the sensor was capable of operating continuously for several months. The resolution of the data logger is generally determined by the capacity of the sensor and microcontroller (Riley et al., 2006). Here, the maximum measureable depth of water and theoretical resolution of the sensor were 10 m and 2.57 mm, respectively.

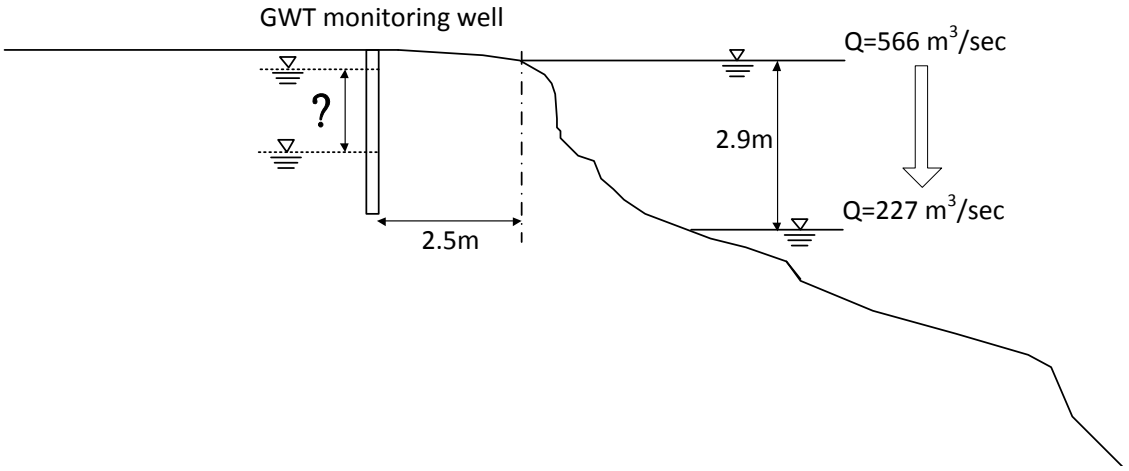

Figure 5 Schematic of the groundwater table observation hole at the field study site with an example drawdown event.

3.5 Transient seepage analysis

The main objective of the transient seepage analysis was to compare the locations of the phreatic surface predicted by the seepage analysis model using different hydraulic

conductivities with the actual groundwater levels measured in the monitoring holes. By comparing the modeling results and measured data, the hydraulic conductivity values that produced the simulated results closest to those observed could be determined. However, unlike a steady state seepage model, a transient seepage analysis requires additional parameters that account for unsaturated soil conditions, in particular the hydraulic conductivity function, which shows the relationship between hydraulic conductivity and the volumetric water content of the soil or soil suction. Determining this relationship also involves some level of uncertainty and is generally cumbersome due to the nature of the experimental procedures needed to deal with unsaturated soils.

As an alternative technique, the hydraulic conductivity function can be estimated from the saturated hydraulic conductivity and soil water characteristic curve (SWCC). Several methods have been suggested for this estimation, among which the methods proposed by Green and Corey (1971), van Genuchten (1980), and Fredlund et al. (1994) are the most widely known.

3.6 Governing equation

Darcy's law can be applied to the flow of water through unsaturated soils (Richards, 1931). Thus, the governing differential equation for the flow in unsaturated soils is also derived from Darcy's law for saturated soils, and can be defined as follows (Lam et al., 1987):

$$\frac{\partial}{\partial x}\left(k_x \frac{\partial h}{\partial x}\right) + \frac{\partial}{\partial y}\left(k_y \frac{\partial h}{\partial y}\right) + \frac{\partial}{\partial z}\left(k_z \frac{\partial h}{\partial z}\right) + Q = \frac{\partial \theta_w}{\partial t} \qquad (6)$$

where, h = total hydraulic head, k_x, k_y and k_z = hydraulic conductivity in x, y, and z directions respectively, Q = external boundary flux, and θ_w = volumetric water content.

Equation (6) describes the conservation of fluid mass in soils and states that the sum of the rates of flow changes in the *x*, *y* and *z* directions, and the external boundary flux are equal to the rate of change of volumetric water content per unit time (Ng and Shi, 1998).

Assuming that the total stress is constant and the air phase is continuous in the unsaturated soils, the change of volumetric water content can be simplified as below (Lam et al., 1987):

$$\partial\theta_w = m_w \partial u_w \tag{7}$$

where, u_w = pore water pressure, and m_w = slope of the SWCC.

The governing equation for two dimensional flows is then expressed as follows:

$$\frac{\partial}{\partial x}\left(k_x \frac{\partial h}{\partial x}\right) + \frac{\partial}{\partial y}\left(k_y \frac{\partial h}{\partial y}\right) + Q = m_w \gamma_w \frac{\partial h}{\partial t} \tag{8}$$

3.7 Modeling parameters

Green and Corey (1971) introduced an equation similar to that given by Kunze et al. (1968), which estimates hydraulic conductivity for different levels of water content or degrees of saturation using the Soil Water Characteristic Curve (SWCC).

$$k(\theta_w)_i = \frac{k_s}{k_{sc}} \frac{30\gamma^2}{\rho g \eta} \frac{\varepsilon^p}{n^2} \sum_{j=1}^{m} \left[(2j+1-2i)h_j^{-2}\right] \tag{9}$$

where $i = 1,2,\cdots,m$, $k(\theta)_i$ is the calculated hydraulic conductivity for a specified water content or pressure (cm/min), θ_w is the volumetric water content (cm^3/cm^3), k_s/k_{sc} is a matching factor consisting of the ratio of the measured k to the calculated k, γ is the surface tension of water (dynes/cm), ε is porosity, p is a parameter that accounts for the interactions of pores, ρ is the density of water (g/cm^3), g is the gravitational constant (cm/s^2), η is the viscosity of water ($g/cm\ s^{-1}$), n is the total number of pore classes between zero and 100% saturation, h_i is the pressure or suction head, and i is the water content at the wet end of the sample.

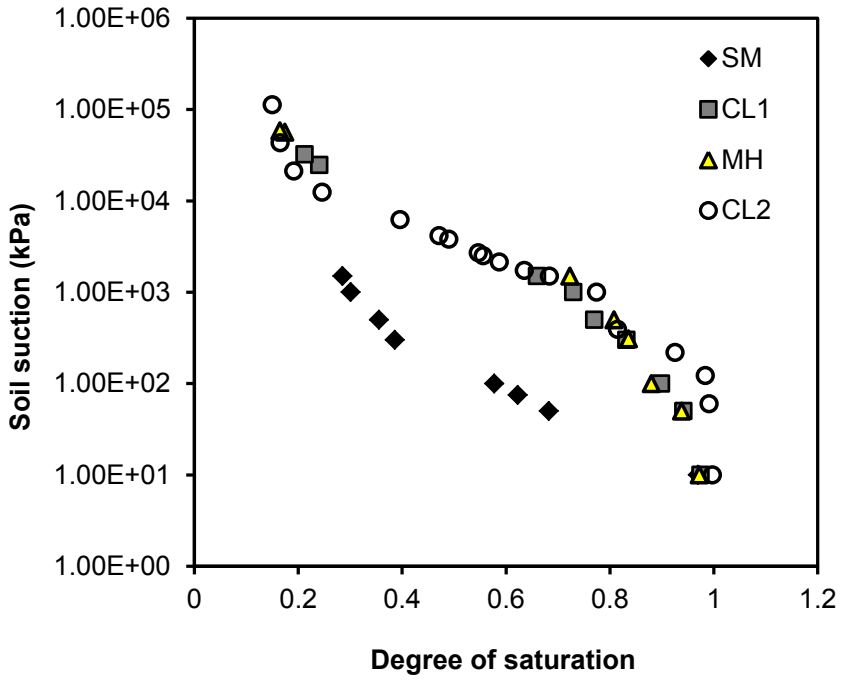

Figure 6 Soil water characteristic data for modeling.

The SWCC was determined using a combination of Tempe cell tests, pressure plate tests, filter paper tests, and a chilled mirror hygrometer. The results are presented as a group of data points that construct a continuous SWCC for each soil (Figure 6). Further

details of how the SWCCs for the soil deposits in the lower Roanoke River were obtained are described in Nam et al. (2010).

The transient seepage analysis was performed using the finite element program MIDAS GTS developed by MIDAS IT Co. Ltd. (MIDAS Information Technology, 2010). Average values of the additional modeling parameters used for the analysis are provided in Table 2.

Table 2 Soil properties for transient seepage analysis.

Depth (m)	USCS Soil Type	k_{Auger} (m/s)	k_{Guelph} (m/s)	k_{Lab} (m/s)	Volumetric Water Content (%)
0.0-0.6	SM	1.84E-04	1.44E-05	5.09E-07	46.1
0.6-2.5	CL	2.64E-05	2.08E-07	7.32E-10	50.3
2.5-3.8	MH	1.35E-05	1.69E-08	4.99E-09	48.3
3.8-10.0	CL	2.58E-05	2.86E-08	1.26E-09	47.8
10.0-	Impervious hard soil	1.26E-08	1.26E-10	1.26E-10	26

3.8 Riverbank geometry and soil profile

Riverbank geometry was determined by ground-based light detection and ranging (LiDAR) above the river elevation, and acoustic Doppler current profiler (ADCP) measurements below the river elevation. The soil profile was determined by visual observation and in-situ tests in the field, as well as laboratory tests using soil samples obtained from vertical holes drilled up to 6 m deep at different locations along the riverbank at each site. As previously mentioned, the riverbanks primarily consisted of silt

and clay. Soil layers deeper than 6 m from the bank top could not be visually identified even during low flow seasons, so the thickness of the lowest cohesive soil layer below 6 m was assumed based on previous reports in the literature (Weems and Lewis, 2007, Weems et al., 2009). The vertical soil profile of the riverbanks was simplified to 3-5 soil layers including the assumed bottom impervious layer for the purpose of modeling. Soil samples were obtained from several sites to provide average values for the required input parameters for the seepage modeling, namely *k*, SWCC, and water content at saturation, and the transient seepage analysis was performed for a riverbank at a meander bend due to the availability of the measured GWT data.

Figure 7 shows the cross section geometry of the riverbank used for the seepage modeling. The width and height of the model are 90 m and 30 m, respectively, following the ratio suggested by Desai (1975), and the meshes were generated with 8 node quadrilateral elements. Changes in the WSE were simulated with a boundary function such that head changes with time on the right of the figure, with the left edge assumed to be the constant head boundary condition farthest from the riverbank.

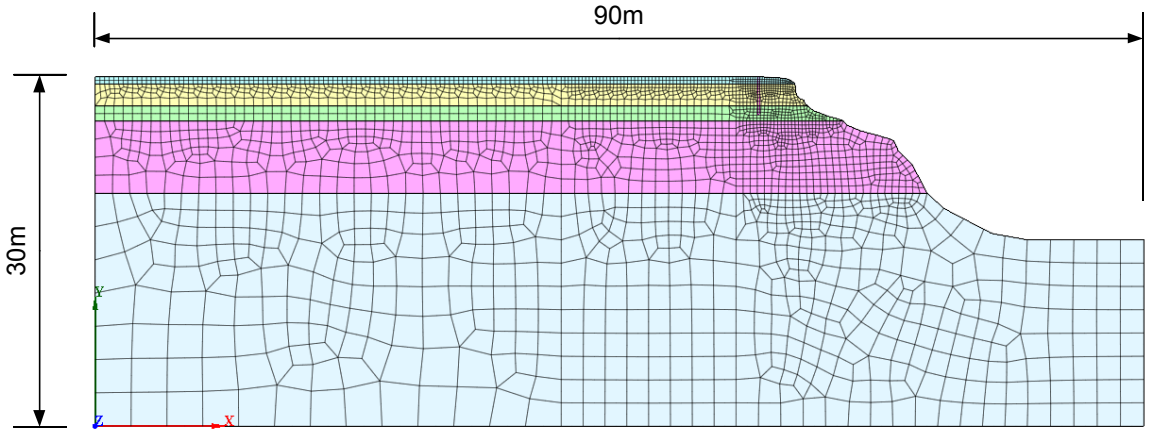

Figure 7 Bank geometry and numerical mesh for the transient seepage analysis.

To determine the initial location of the GWT, long term GWT observation data from the closest GWT monitoring station (station no. F22B7, latitude 36.24° N, longitude 77.19° W) operated by the North Carolina Department of Environmental and Natural Resources (NC DENR) Division of Water Resources (DWR) in Roxobel, NC was analyzed, as shown in Figure 8. This GWT monitoring station is located approximately 14 km from the study reach, and thus, the changes in the GWT shown in Figure 8 are not expected to be the results of instantaneous responses to changes in dam discharge or WSE changes. When the GWT log overlapped the daily average WSE near the site during the same period, it indicated that both the local groundwater and river elevations fluctuate regularly on a seasonal basis. Based on this observation, the initial location of the GWT was determined.

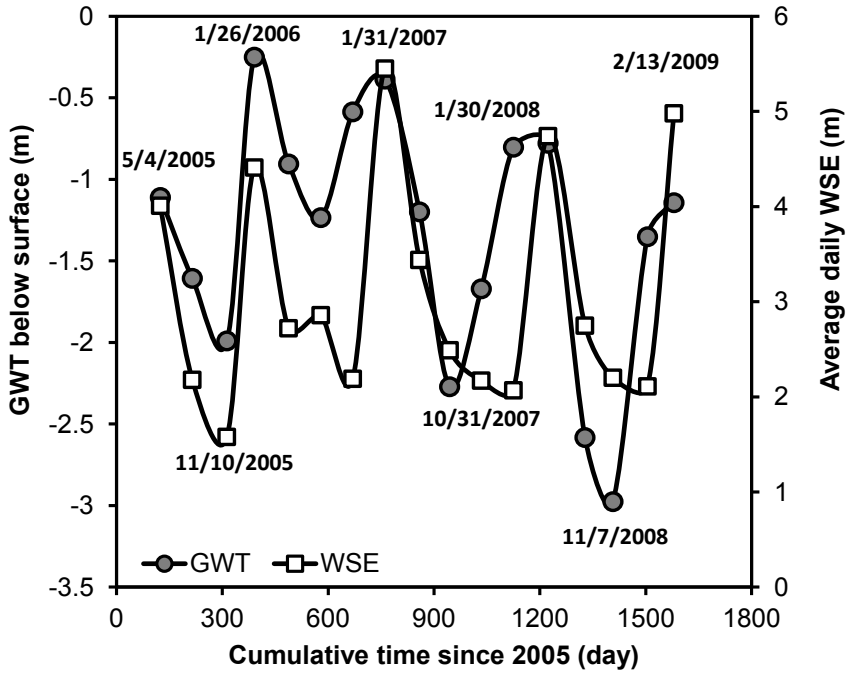

Figure 8 Variation of groundwater table and water surface elevation between 2005 and 2009 as monitored by the NC DENR DWR GWT station in Roxobel, NC.

3.9 Results and discussion

3.9.1 Comparison of hydraulic conductivities

Hydraulic conductivity of the saturated soils k at four different riverbank sites was estimated using 35 laboratory or in-situ tests. The estimated hydraulic conductivity is presented in Figure 9 and reveals wide variations depending on the soil type, test method used, and measuring location. As Figure 9 shows, the hydraulic conductivity of the saturated clay soil k_{CL} varied from 10^{-9} m/s to 10^{-5} m/s. The other two silty soils, ML and MH, showed similar ranges between 10^{-8} m/s and 10^{-5} m/s. These wide ranges for the hydraulic conductivity of each soil can be attributed to the different test methods used and natural variations in the soils. However, the differences in the hydraulic conductivity between soil types are much smaller than those between test methods. Similar trends were observed for the different sampling locations and test methods. Thus, the soil types and sampling locations seem to be relatively insignificant factors in the saturated hydraulic conductivity k estimation for the conditions encountered on the lower Roanoke River.

The auger hole method (AH) resulted in the highest hydraulic conductivity values of close to 10^{-5} m/s, followed by the Guelph permeameter test (GP) with values of around 10^{-7} m/s. The two laboratory methods, the constant head permeability test (CHP) and consolidation test (CON) yielded much lower values of around 10^{-9} m/s. The two laboratory methods yielded similar values, whereas the differences between the two in-situ methods were considerable. As k varies with void ratios in consolidation tests as shown in Figures 10 and 12, the k values for the consolidation tests in Figure 9 were

determined for the void ratios corresponding to 100 kPa of vertical effective stress for CL soils deeper than 4 m and 50 kPa of vertical effective stress for all other soils which are located within 4 m of the top of the bank. The *e* vs. *k* relationship will be discussed in more detail later.

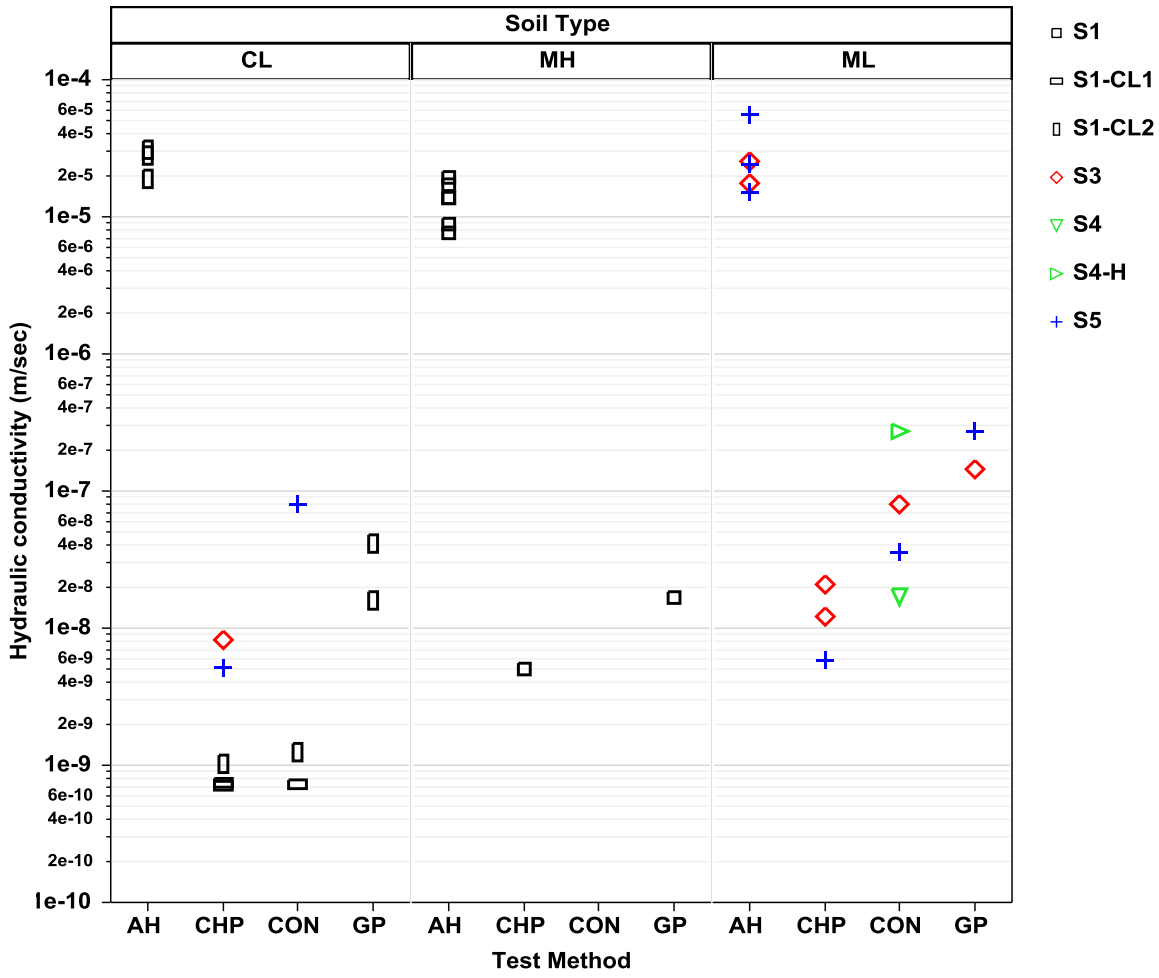

Figure 9 Hydraulic conductivity measured by different methods.

Consolidation tests were performed for both the horizontal and vertical hydraulic conductivity using soil samples that were trimmed perpendicular and parallel to the bedding plane. The results revealed that the horizontal *k* was about 10 times larger than the vertical *k* (Figure 10). Although there was only one set of tests performed to examine

the anisotropic characteristic of hydraulic conductivity, the finding that horizontal *k* was the larger of the two is consistent with other reports for alluvial soils (i.e. Chen, 2004, Phonate et al., 2001). The higher horizontal permeability compared to vertical permeability can be attributed to the presence of bedding plane cracks and anisotropic depositional structure in the soil samples.

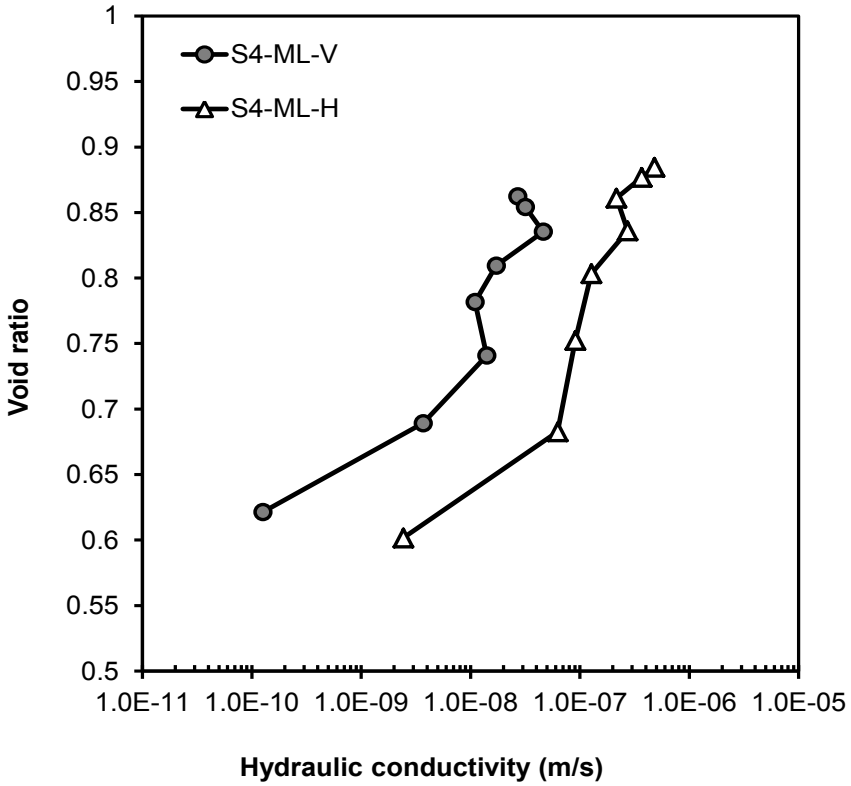

Figure 10 Influence of anisotropy and sampling method (V=vertical hydraulic conductivity and H=horizontal hydraulic conductivity).

3.9.2 Seepage analysis with different hydraulic conductivities

The laboratory and in-situ experimental methods used to determine the *k*-values produced a very wide range of results. Thus, selecting an appropriate value for use in further applications such as transient seepage analysis is difficult, as this significantly

affects the accuracy and reliability of the analysis. For example, using values from the lower and upper bounds of the wide range will generate very different results for the transient seepage analysis in terms of the predicted pore pressure distribution and phreatic surface location, leading in turn to further inaccuracies in important applications such as slope stability analysis. Thus, a numerical method based on field measurements of the groundwater table was employed to validate the *k*-values used in the model. The GWT was monitored at the study site, and the experimental results were compared to the results of the seepage analysis model with different values of hydraulic conductivity using MIDAS GTS (MIDAS Information Technology, 2010).

During two different reservoir release events, continuous changes in both the water surface elevation and groundwater table were monitored at a riverbank location using pressure sensors. The monitored data was then compared with the transient seepage analysis results using different hydraulic conductivity values. One event was observed between May 23 and 31, 2008 with the discharge varying from 357 m^3/s to 187 m^3/s through three stepped down stages. The second event occurred between June 20 and 29, 2009 with the discharge changing from 589 m^3/s to 292 m^3/s in a single step. The observed GWT, WSE, and reservoir release hydrograph are presented in Figure 11, revealing that the GWT changes almost instantly in response to WSE changes. The predicted GWTs were determined by numerical modeling using MIDAS GTS (MIDAS Information Technology, 2010) with the different hydraulic conductivities determined using AH, GP and the two laboratory tests. Anisotropy of the riverbanks was taken into account by using a value for the horizontal hydraulic conductivity 10 times larger than the vertical hydraulic conductivity. This anisotropic consideration was only employed for

the models using hydraulic conductivity values measured in the laboratory, as the auger hole and Guelph permeameter methods measure the hydraulic conductivity that has already been affected by the horizontal flow. As can be seen in Figure 11, the results indicate that the highest *k*, which was determined by AH, produced the results which best fit the observed changes in the GWT. Differences between the monitored GWT and the modeling results using the AH values could be due to the uncertainty associated with estimating the modeling parameters and boundary conditions in the seepage analysis. While the modeling results and observed GWTs do not agree perfectly, the agreement is better than the results utilizing the lower *k* values. Considering the wide variations in the permeability values, the comparison between the numerical modeling results and the GWTs monitored in the field supports the validity and utility of in-situ hydraulic conductivity measurements.

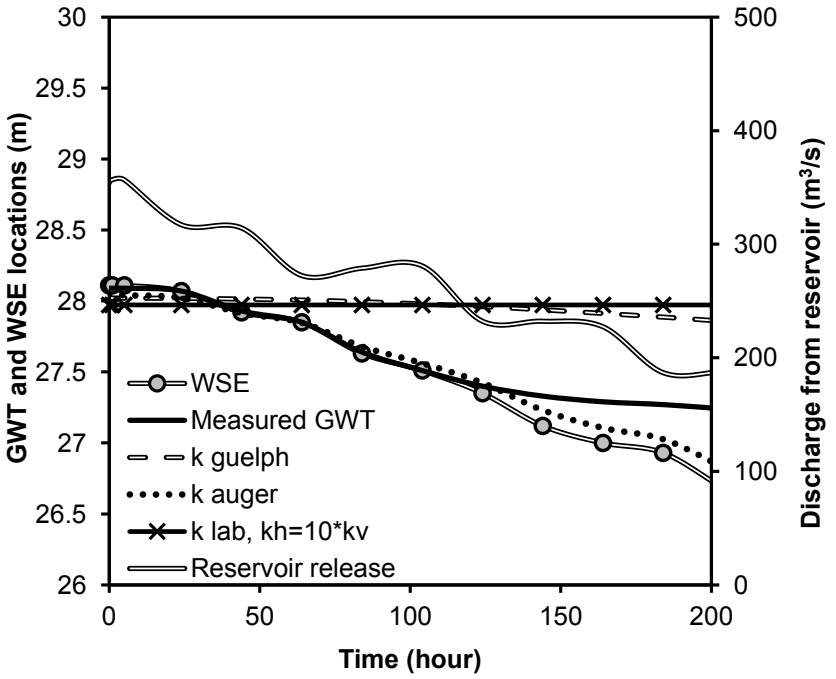

(a) May 23-31, 2008, reservoir release from 354 m^3/s to 187 m^3/s

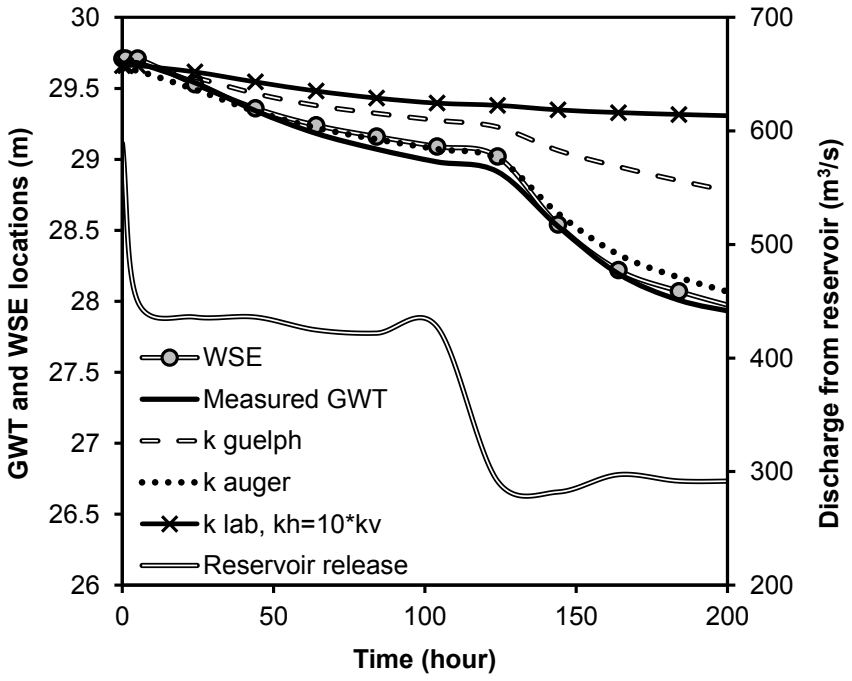

(b) June 20-29, 2009, reservoir release from 589 m^3/s to 292 m^3/s

Figure 11 Changes in the GWT with hydraulic conductivity values determined from field and laboratory tests.

3.9.3 Discussion of the hydraulic conductivity values

Although the numerical results confirmed the validity of hydraulic conductivity from the auger hole method k_{AH}, it is still not clear why k_{AH} should be much higher than typical values for similar soil types, and why the differences between the values produced by k_{AH} and k_L, and k_{AH} and k_L are large. Interestingly, k determined by each method is within a reasonable range regardless of soil type for all the locations. Thus, it is clearly important to identify the factors that contribute to this wide range of values in order to properly select the appropriate test and, ultimately, provide the best possible estimate for k.

Test environment

The values for k from the in-situ tests were higher than those from the lab tests, and of the two in-situ tests, the AH method consistently produced higher values than the GP. Weber (1968) reported that some of the larger k_F/k_L ratios for silty clay and sandy silty clay were 4900 and 46,000, respectively. Reynolds and Zebchuk (1996) also observed higher k with the AH method than with the GP in a clay soil. Dorsey et al. (1990) and Gallichand et al. (1990) reported that the AH results in their study produced values that were about 1.4 to 83.3 times higher for k than the GP method. They attributed this difference to the test environment, as the GP is performed after saturating soils near the bottom of the test hole but above the GWT, whereas the AH is performed in saturated soils below the GWT. Thus, it is generally agreed that the GP measures *field saturated hydraulic conductivity*, which is known to be smaller than *saturated hydraulic conductivity*. Although the soil is assumed to be saturated during the GP tests, air may be entrapped during the saturation process resulting in a value for hydraulic conductivity

that is lower than that for fully saturated hydraulic conductivity (Reynolds et al., 1983, Stephens et al., 1987). The entrapped air is thought to reduce the hydraulic conductivity by as much as 1 to 2 orders of magnitude (Faybishenko, 1997).

The differences in the measured values between the laboratory tests and in situ tests can be also attributed to the difference in flow direction during the tests. Although in situ tests measure the flow rate in all directions, the flow in the test holes is mostly horizontal. In contrast, lab tests measure one dimensional flow rates using soil samples. Thus, the anisotropic characteristics of the riverbank soils are also expected to have contributed to the variability of k in different test methods.

Sample disturbance

In general, the logarithm of hydraulic conductivity increases proportional to the void ratio. However, the consolidation test results indicate that hydraulic conductivity decreased as the void ratio increased at higher void ratios in some tests, as shown in Figure 12. The e vs. log(k) curve tends to change direction at a void ratio of around 1.0, leading to a decrease in hydraulic conductivity, probably due to the sample disturbance that inevitably occurs during sampling and transporting. Although few disturbances are noticeable from the test results, soil samples obtained from lower clay layers such as S1-CL2, S3-CL, and S5-CL in Figure 12 appear relatively undisturbed. When the void ratio becomes small, in areas in which the stress level is higher, the influence of sample disturbance becomes negligible. The shaded box in Figure 12 also shows that several of the test results combine to create a band that represents the e vs. log(k) relationships in the same soil types at different sites. This band can be used to estimate the hydraulic conductivity of undisturbed soil samples by extrapolation from the current results.

Considering the fact that void ratios in the field are larger than the corresponding void ratios in the lab under the stress level prior to the pre-consolidation pressure being applied (Terzaghi et al., 1996), the actual hydraulic conductivity in the field samples that have not experienced sample disturbance should be higher than the values determined in the laboratory.

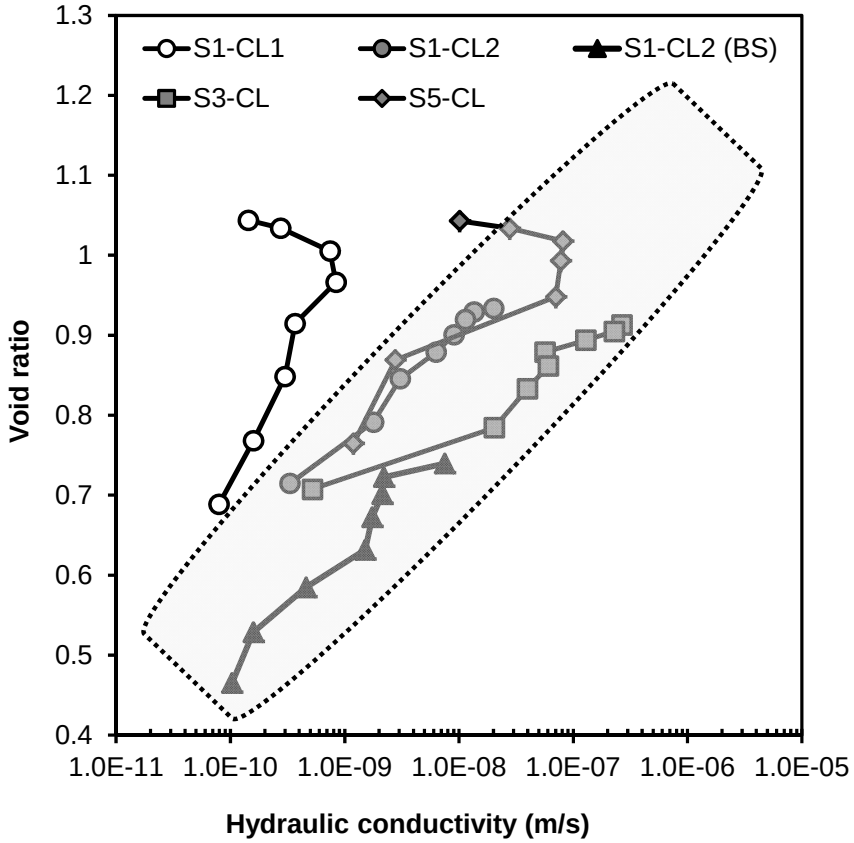

Figure 12 Results of the consolidation tests for CL soils from different locations.

Soil anisotropy

As observed in Figure 10, soil anisotropy is known to affect hydraulic conductivity. Especially in alluvial soils such as those near the study site, where sediment

layers are expected to be deposited by the river periodically overflowing its banks, horizontal k generally exceeds the vertical k (Rycroft and Amer, 1995). According to studies by Wu et al. (1978) and Casagrande and Poulos (1969), the ratio of k_h/k_v for fine grained soils is of the order of 15 and 40, respectively, whereas Mitchell (1993) provided several other references (e.g. Chan and Kenney, 1973, Ladd and Wissa, 1970, Mitchell, 1956, Olsen, 1962) indicating that this ratio varies but less than 10. Although anisotropy in hydraulic conductivity of riverbank soils is common as a result of the stratification of natural soil deposits (Mitchell, 1993), the range of values reported for these ratios remains wide.

Preferential flows

When considering typical values of hydraulic conductivity for clays or silts, which are known to be in the range of 10^{-5} – 10^{-11} m/s (Terzaghi et al., 1996), the larger values determined by in-situ tests as well as the observed rapid response of the GWT are somewhat surprising results. However, similar observations at a natural levee in the Atchafalaya River Basin, LA, were reported by Newman (2010), and Childs et al. (1957) reported saturated hydraulic conductivities for clay soils that had values more usually associated with gravels. Jarvis and Messing (1995) observed higher k in loam soils than in sandy soil but attributed this to the effect of the macrostructure induced by earthworms, plant roots, or shrinkage. Unexpectedly high hydraulic conductivities have been observed even in fine grained soils and have been described using various terms, including preferential flow, bypass flow, macropore drainage, or small-scale channeling flow. The definition of each term may be somewhat different, but all are commonly used to explain unusually high rates of water flow in soil.

As Figure 3 clearly shows, surface cracks and pores are commonly observed in the field, serving as visual indicators of preferential flow paths. In general, wetting and drying cycles may influence soil structures. Beven and Germann (1982) suggested that soil fauna, plants roots, cracks and fissures, and natural soil pipes all contribute to the creation of macropores. They also considered that drought conditions would cause a clay soil to crack, possibly to a considerable depth, and subsequent soil freezing and frost heave would also deepen soil cracks. In addition, Regalado and Munoz-Carpena (2004) pointed out that due to the natural conditions in the field, their in-situ test results contained high spatial variability due to small scale heterogeneities such as structure, texture, flora, fauna, and soil composition. Although there was no analysis of preferential flows for this study, it seems very likely that preferential flow is the major factor responsible for the instantaneous response of the GWT in cohesive riverbank soils.

3.10 Conclusions

The hydraulic conductivity of three silty clays and a clay soil obtained from four locations along the riverbank of the lower Roanoke River was determined using two laboratory and two field test methods. These tests were the constant head permeability test, the consolidation test, the Guelph permeameter and the auger hole method, respectively. Numerical modeling of transient seepage using the resulting values for hydraulic conductivity was then performed to estimate different GWT locations for two different WSE drawdown scenarios, and the results were compared with the actual GWT measured in the field.

The experimental results revealed that the hydraulic conductivity from the auger hole method k_{AH} was about 10^2 times larger than hydraulic conductivity from the Guelph permeameter k_{GP}, and up to 10^4 times larger than the values k_{CHP} and k_{CON} measured from the constant head permeameter and oedometer tests, respectively. Although k_{CHP} and k_{CON} were closer to the typical range of k for the soils, the transient seepage analysis indicates that the highest value, from k_{AH}, produced the GWT prediction closest to the GWT observed in the field.

Roots, cracks and structured soils were observed in the field, all of which could cause preferential flow. These were not quantitatively analyzed, but are generally known to be important factors affecting in-situ hydraulic conductivity. Further analyses of the experimental results, in conjunction with findings reported in the literature, confirmed the natural variability of k as well as the variability between each method. The difference in the hydraulic conductivity between laboratory and in-situ permeability tests can be attributed to anisotropy, sample size and disturbance, and test methods, as suggested by many researchers. It can also be assumed that the combined effect would be more significant than that of a single factor.

This wide range for k has been generally regarded as natural, but it seems to be strongly dependent on test methods. Thus, the determination of k for riverbanks with cohesive soils needs to be performed with care as many in-situ factors that accelerate the seepage may exist in the field. When determining k, especially for non-homogeneous cohesive soils which are common, a single source of information may not adequately represent the actual hydraulic conductivity characteristic of the soils. Thus, it is recommended that additional information be considered, including visual inspection, the

geological and geomorphological background of the site, and numerical modeling, to increase reliability. In addition, long term monitoring of the groundwater table and numerical analysis of seepage are recommended.

3.11 References

[1] ASTM D 2435 (2004). "Standard test methods for one-dimensional consolidation properties of soils using incremental loading." *ASTM International*.

[2] Bagarello, V. (1997). "Influence of well preparation on field-saturated hydraulic conductivity measured with the Guelph Permeameter." *Geoderma*, 80(1-2), 169-180.

[3] Bagarello, V., and Provenzano, G. (1996). "Factors affecting field and laboratory measurement of saturated hydraulic conductivity." *Transactions of the American Society of Agricultural Engineers*, 39(1), 153-159.

[4] Beven, K., and Germann, P. (1982). "Macropores and water flow in soils." *Water Resources Research*, 18(5), 1311-1325.

[5] Bouma, J., and Woesten, J. H. M. (1979). "Flow patterns during extended saturated flow in two, undisturbed swelling clay soils with different macrostructures." *Soil Science Society of America Journal*, 43(1), 16-22.

[6] Boumans, J. H. (1953). "Het bepalen van de drainafstand met behulp van de Boorgaten methode." *Landbouwtijdschrift*, 82-104.

[7] Brown, P. M., Miller, J. A., and Swain, F. M. (1972). "Structural and stratigraphic framework and spatial distribution of permeability of the Atlantic Coastal Plain, North Carolina to New York." *U.S. Geological Survey Professional Paper 796*, U.S. Geological Survey, 79.

[8] Casagrande, L., and Poulos, S. (1969). "On the effectiveness of sand drains." *Canadian Geotechnical Journal*, 6(3), 287-326.

[9] Chan, H. T., and Kenney, T. C. (1973). "Laboratory Investigation of Permeability Ratio of New Liskeard Varved Soil." *Canadian Geotechnical Journal*, 10(3), 453-472.

[10] Chen, X. H. (2004). "Streambed hydraulic conductivity for rivers in south-central Nebraska." *Journal of the American Water Resources Association*, 40(3), 561-573.

[11] Childs, E. C., Collis-George, N., and Holmes, J. W. (1957). "Permeability measurements in the field as an assessment of anisotropy and structure development." *European Journal of Soil Science*, 8(1), 27-41.

[12] Dedrick, R. R., Halfman, J. D., and Brooks McKinney, D. (2000). "An inexpensive, microprocessor-based, data logging system." *Computers & Geosciences*, 26(9-10), 1059-1066.

[13] Desai, C. S. (1975). "Finite element methods for flow in porous media." *Finite elements in fluids, Vol.1: Viscous flows and hydrodynamics*, Wiley, Chichester, Sussex, UK, 157-182.

[14] Diserens, E. (1934). "Beitrag zur Bestimmung der Durchlässigkeit des Bodens in natürlicher Bodenlagerung." *Schweiz. Landw. Monatstr.*, 12.

[15] Dominion (2010). "Roanoke Rapids power station." <http://www.dom.com/about/stations/hydro/roanoke-rapids-power-station.jsp>. (Sep. 29, 2010).

[16] Dorsey, J. D., Ward, A. D., Fausey, N. R., and Bair, E. S. (1990). "A comparison of four field methods for measuring saturated hydraulic conductivity." *Transactions of the ASAE*, 33(6), 1925-1931.

[17] Elrick, D. E., Reynolds, W. D., Lee, D. M., and Clothier, B. E. (1984). "The "Guelph Permeameter" for measuring the field-saturated soil hydraulic conductivity above the water table: I. Theory, procedures and applications." *Proc., the Canadian Hydrology Symposium*, 643-655.

[18] Elrick, D. E., Reynolds, W. D., and Tan, K. A. (1989). "Hydraulic conductivity measurements in the unsaturated zone using improved well analyses." *Ground Water Monitoring & Remediation*, 9(3), 184-193.

[19] Ernst, L. F. (1950). "A new formula for the calculation of the permeability factor with the auger hole method." Agricultural Experiment Station T.N.O., Groningen, The Netherlands.

[20] Faybishenko, B. (1997). "Comparison of laboratory and field methods for determining the quasi-saturated hydraulic conductivity of soils." *Proc., 1997 Riverside International Workshop on Soil Hydraulic Properties*, 14.

[21] Fredlund, D. G., Xing, A., and Huang, S. (1994). "Predicting the permeability function for unsaturated soils using the soil-water characteristic curve." *Canadian Geotechnical Journal*, 31(4), 533-546.

[22] Gallichand, J., Madramootoo, C. A., Enright, P., and Barrington, S. F. (1990). "An evaluation of the Guelph permeameter for measuring saturated hydraulic conductivity." *Transactions of the American Society of Agricultural Engineers*, 33(4), 1179-1184.

[23] Goodall, D. C., and Quigley, R. M. (1977). "Pollutant migration from two sanitary landfill sites near Sarnia, Ontario." *Canadian Geotechnical Journal*, 14(2), 223-236.

[24] Green, R. E., and Corey, J. C. (1971). "Calculation of hydraulic conductivity: A further evaluation of some predictive methods." *Soil Science Society of America Journal*, 35(1), 3-8.

[25] Hupp, C. R., Schenk, E. R., Richter, J. M., Peet, R. K., and Townsend, P. A. (2009). "Bank erosion along the dam-regulated lower Roanoke River, North Carolina." *Geological Society of America Special Papers*, 451, 97-108.

[26] Jarvis, N. J., and Messing, I. (1995). "Near-saturated hydraulic conductivity in soils of contrasting texture measured by tension infiltrometers." *Soil Science Society of America Journal*, 59(1), 27-34.

[27] Kunze, R. J., Uehara, G., and Graham, K. (1968). "Factors important in the calculation of hydraulic conductivity." *Soil Science Society of America Journal*, 32(6), 760-765.

[28] Ladd, C. C., and Wissa, A. E. Z. (1970). "Geology and engineering properties of Connecticut valley varved clays with special reference to embankment construction." Department of Civl Engineering, Massachusetts Institute of Technology.

[29] Lam, L., Fredlund, D. G., and Barbour, S. L. (1987). "Transient seepage model for saturated-unsaturated soil systems: a geotechnical engineering approach " *Canadian Geotechnical Journal*, 24(4), 565-580.

[30] MIDAS Information Technology (2010). "Midas GTS." Seoul, Korea.

[31] Mitchell, J. F. (1956). "The fabric of natural clays and its relation to engineering properties." *Proc., Highway Research Board*, 693-713.

[32] Mitchell, J. K. (1993). *Fundamentals of soil behavior*, John Wiley & Sons, Inc., New York.

[33] Nam, S., Gutierrez, M., Diplas, P., Petrie, J., Wayllace, A., Lu, N., and Munoz, J. J. (2010). "Comparison of testing techniques and models for establishing the SWCC of riverbank soils." *Engineering Geology*, 110(1-2), 1-10.

[34] Newman, A. E. (2010). "Water and solute transport in the shallow subsurface of a riverine wetland natural levee." Master of Science, Louisiana State University, Baton Rouge.

[35] Ng, C. W. W., and Shi, Q. (1998). "A numerical investigation of the stability of unsaturated soil slopes subjected to transient seepage." *Computers and Geotechnics*, 22(1), 1-28.

[36] Olsen, H. W. (1962). "Hydraulic flow through saturated clays." *Proc., the Ninth National Conference on Clays and Clay Minerals*, 131-161.

[37] Olson, R. E., and Daniel, D. E. (1981). "Measurement of the hydraulic conductivity of fine-grained soils." *Proc., Permeability and Groundwater Contaminant Transport, ASTM STP 746*, ASTM, 18-64.

[38] Phonate, V., Malik, R. S., and Kumar, S. (2001). "Anisotropy in some alluvial soils." *Annals of Arid Zone*, 40(4), 425-427.

[39] Regalado, C. M., and Munoz-Carpena, R. (2004). "Estimating the saturated hydraulic conductivity in a spatially variable soil with different permeameters: A stochastic Kozeny-Carman relation." *Soil and Tillage Research*, 77(2), 189-202.

[40] Reynolds, W. D., and Elrick, D. E. (1985). "In situ measurement of field-saturated hydraulic conductivity, sorptivity and the a-parameter using the Guelph permeameter." *Soil Science*, 140(4), 292-302.

[41] Reynolds, W. D., Elrick, D. E., and Topp, G. C. (1983). "A reexamination of the constant head well permeameter method for measuring saturated hydraulic conductivity above the water-table." *Soil Science*, 136(4), 250-268.

[42] Reynolds, W. D., and Zebchuk, W. D. (1996). "Hydraulic conductivity in a clay soil: Two measurement techniques and spatial characterization." *Soil Science Society of America Journal*, 60(6), 1679-1685.

[43] Richards, L. A. (1931). "Capillary conduction of liquids through porous mediums." *Physics*, 1, 318-333.

[44] Riley, T. C., Endreny, T. A., and Halfman, J. D. (2006). "Monitoring soil moisture and water table height with a low-cost data logger." *Computers and Geosciences*, 32(1), 135-140.

[45] Roanoke River Basin Interest Subcommittee (2009). "Comprehensive draft report on the Roanoke River Basin." Virginia Department of Environmental Quality, ed., Virginia Roanoke River Basin Advisory Committee, Richmond, VA.

[46] Rycroft, D. W., and Amer, M. H. (1995). *Prospects for the drainage of clay soils*, Food and Agriculture Organization of the United Nations, Rome, Italy.

[47] Salverda, A. P., and Dane, J. H. (1993). "An examination of the Guelph permeameter for measuring the soil's hydraulic properties." *Geoderma*, 57(4), 405-421.

[48] Soilmoisture Equipment Corp. (2006). "2800K1 Guelph permeameter operating instructions."

[49] Stephens, D. B., Lambert, K., and Watson, D. (1987). "Regression models for hydraulic conductivity and field test of the borehole permeameter." *Water Resources Research*, 23(12), 2207-2214.

[50] Terzaghi, K. (1943). *Theoretical soil mechanics*, John Wiley and Sons, New York.

[51] Terzaghi, K., Peck, R. B., and Mesri, G. (1996). *Soil mechanics in engineering practice*, John Wiley & Sons.

[52] U.S. Army Corps of Engineers Wilmington District (2010). "John H. Kerr project pertinent data." <http://epec.saw.usace.army.mil/kerr.htm>. (09/29, 2010).

[53] van Beers, W. F. J. (1983). *The auger hole method: A field measurement of the hydraulic conductivity of soil below the water table*, International Institute for Land Reclamation and Improvement, Wageningen, the Netherlands.

[54] van Genuchten, M. T. (1980). "A closed-form equation for predicting the hydraulic conductivity of unsaturated soils." *Soil Science Society of America Journal*, 44(5), 892-898.

[55] Vukovic, M., and Soro, A. (1992). *Determination of hydraulic conductivity of porous media from grain-size composition*, Water Resources Publications, Littleton, CO.

[56] Weber, W. G. (1968). "In situ permeabilities for determining rates of consolidation." *Highway Research Record*(243), 49-61.

[57] Weems, R. E., and Lewis, W. C. (2007). "Detailed sections from auger holes in the Roanoke Rapids 1:100,000 map sheet, North Carolina ", U.S. Geological Survey, Reston, Virginia 155.

[58] Weems, R. E., Lewis, W. C., and Aleman-Gonzalez, W. B. (2009). "Surficial geologic map of the Roanoke Rapids 30' x 60' quadrangle, North Carolina: U.S. Geological Survey open-file report 2009–1149, 1 sheet, scale 1:100,000." U.S. Geological Survey.

[59] Wu, T. H., Chang, N. Y., and Ali, E. M. (1978). "Consolidation and strength properties of a clay." *Journal of the Geotechnical Engineering Division-ASCE*, 104(7), 889-905.

CHAPTER 4. Unsaturated Shear Strength of Riverbank Soils Using Multistage Direct Shear Tests[1]

ABSTRACT

The determination of the shear strength of unsaturated soils is generally more complicated, time consuming and expensive than determining the shear strength of saturated soils. Although much research has focused on the development of new unsaturated soil testing methods, these studies have yet to be translated into practice. More importantly, there is a need for further studies on practical testing methods that can reduce both the cost of and time associated with shear strength testing of unsaturated soils. This paper presents a comprehensive evaluation of rapid and practical laboratory methods to determine the shear strength of unsaturated soils. In particular, the validity of using the multistage direct shear test for the determination of shear strength properties of unsaturated soils is examined. Shear strength parameters obtained from the multistage direct shear test are compared with those from conventional direct shear tests using multiple soil specimens. Based on this comparison, recommendations are given on how to apply the multistage direct shear test to ensure reliable unsaturated shear strength measurements. The test is then utilized to determine the shear strength of unsaturated riverbank soils that experience frequent changes in river water surface elevation brought on by controlled reservoir releases.

Keywords: multistage direct shear test, shear strength, unsaturated soils, suction controlled direct shear test

---

[1]This manuscript has been submitted to *Engineering Geology*, and is co-authored by **Soonkie Nam**, Marte S. Gutierrez, Panayiotis Diplas, and John Petrie

4.1 Introduction

A number of studies have been conducted on the experimental determination of shear strength of unsaturated soils (e.g. Escario and Saez, 1986, Feuerharmel et al., 2005, Fredlund et al., 1978, Rahardjo et al., 1995). The fundamental goal of these experimental methods is to establish the shear strength characteristics of an unsaturated soil in terms of net normal stress and matric suction. Matric suction is an important factor that affects the shear strength of unsaturated soils, and is considered to be part of the cohesion in unsaturated soil shear strength (Lu and Likos, 2004). Numerous experimental techniques for creating a suction-controlled environment have been proposed and applied in order to control the stress state (Sheng et al., 2009). For example, osmotic and vapor equilibrium techniques have proven successful in controlling suction in determinations of the shear strength of unsaturated soils (Blatz and Graham, 2000, Boso et al., 2005, Cui and Delage, 1996, Delage and Cui, 2008). More generally, the axis translation technique has also been successfully employed to control suction (e.g. Aversa and Nicotera, 2002, Fredlund and Morgenstern, 1977, Hilf, 1956, Matyas and Radhakrishna, 1968, Sedano et al., 2007). This technique has been applied to the conventional direct shear test, ring shear test, triaxial tests, triaxial systems with self-contained bender elements, resonant column test, and true triaxial tests (Cabarkapa and Cuccovillo, 2006, Feuerharmel et al., 2006, Gan et al., 1988, Ho and Fredlund, 1982, Hormdee et al., 2005, Hoyos et al., 2008, Hoyos et al., 2010, Vassallo et al., 2007). Although many indirect techniques using the soil water characteristic curve (SWCC), saturated shear strength, knowledge-based system or empirical data fitting models are also available to estimate unsaturated shear strength (e.g. Fredlund et al., 1996, Fredlund et al., 1997, Vanapalli and Fredlund, 2000, Vilar,

2006), the determination of the suction-dependent shear strength of unsaturated soils using the axis translation technique remains the most widely used. However, in spite of its general acceptance, the application of the axis translation technique continues to be challenging.

The main problems affecting the determination of the shear strength of unsaturated soils, regardless of the technique used to control suction, are: 1) the large number of tests required to establish the variation of the shear strength with matric suction, and 2) the long testing times needed to establish a suction equilibrium in the soil samples before they can be sheared. Methods for unsaturated shear testing are generally more complicated, more time consuming and more expensive than the conventional test methods used for saturated soils. Although interest in evaluating unsaturated soil characteristics has increased, more studies are required to generalize the application of each method. More importantly, there is a need for further studies on practical testing methods that can reduce the cost and time associated with shear strength testing of unsaturated soils. The multistage direct shear test is a promising laboratory technique that may shorten the time required to determine the shear strength of saturated soils. However, the applicability of the multistage direct shear test for unsaturated soils has not yet been fully evaluated. Thus, the test procedures and interpretation of the results need to be validated.

The main objective of the research presented in this paper is to investigate the validity of the multistage direct shear test for both saturated and unsaturated soils. Shear strength parameters from multistage tests are compared with those obtained from conventional direct shear tests using multiple soil specimens. Based on these

comparisons, recommendations are made for carrying out multistage direct shear tests to ensure reliable shear strength data for unsaturated soils. The resulting method is then applied to investigate the unsaturated shear strength of natural riverbank soil deposits near Scotland Neck, North Carolina, USA, which is an essential step towards understanding the mechanisms responsible for bank failure.

4.2 Shear strength of unsaturated soil

There are several formulations for quantifying the effects of matric suction on the shear strength of unsaturated soils (Vanapalli and Fredlund, 2000). Most originate from the following effective stress equation for unsaturated soils derived by Bishop (1959):

$$\sigma' = (\sigma - u_a) + \chi(u_a - u_w) \quad (1)$$

where σ=total stress, u_a=pore air pressure, u_w=pore water pressure, and χ =parameter related to matric suction with a value of χ =0 for dry soils and χ =1 for saturated soils. This is an extension of Terzaghi's (1943) effective stress equation and accounts for the presence of both gaseous and liquid phases in the voids of the soil. The term $(\sigma - u_a)$ is the net total stress, and $(u_a - u_w) = \psi$ is the matric suction, which is negative since $u_a < u_w$. Although the value of χ is known to be affected by soil structure, stress changes, and cycles of wetting and drying (Bishop, 1961), the degree of saturation is the dominant factor in determining the matric suction ψ, and ultimately, the effective stress. Suction increases the effective stress, and in turn, the shear strength of unsaturated soils. Substituting Eq. (1) in the Mohr-Coulomb failure criterion for frictional-cohesive soil:

$$\tau = c' + \sigma_n' \tan\phi' \quad (2)$$

yields:

$$\tau = c' + [(\sigma_n - u_a) + \chi(u_a - u_w)]\tan\phi' \quad (3)$$

where τ= shear strength of unsaturated soil, ϕ' = effective friction angle, and c' = effective cohesion.

Several researchers have shown the difficulty of quantifying the value of χ in Eq. (3) both theoretically and experimentally (Burland, 1965, Fredlund and Morgenstern, 1977, Jennings and Burland, 1962, Matyas and Radhakrishna, 1968). To circumvent this difficulty, Fredlund et al. (1978) proposed a shear strength equation for unsaturated soils that incorporated two independent strength parameters corresponding to $(u_a - u_w)$ and $(\sigma_n - u_a)$:

$$\tau = c' + (u_a - u_w)\tan\phi^b + (\sigma_n - u_a)\tan\phi' \quad (4)$$

where ϕ^b = angle of shearing resistance with respect to matric suction.

When a soil is fully saturated, the pore air pressure becomes equal to the pore water pressure, and the matric suction component is eliminated. Then, Eq. (4) reduces to the conventional Mohr-Coulomb shear strength equation for saturated soils (Eq. (2)). For an unsaturated soil, the matric suction ψ and angle ϕ^b are the additional parameters that increase the shear strength compared to Eq. (2). Thus, the shear strength of an unsaturated soil can be determined by ψ and ϕ^b in addition to the saturated shear strength parameters.

The shear strength of an unsaturated soil as a function of matric suction ψ can be estimated experimentally. The effective friction angle ϕ' and cohesion c' are determined by conventional direct shear or triaxial tests on saturated soil specimens. Specimens at

different degrees of saturation are then tested, and the shear strength recorded for each specimen is plotted against matric suction. The slope of the shear strength vs. matric suction failure envelope is the angle of shearing resistance with respect to matric suction ϕ^b. Initially, the angle ϕ^b is assumed to be constant resulting in a linear variation of shear strength with matric suction. A simple approximation is $\phi^b = \phi'$ (Fredlund and Rahardjo, 1993). However, subsequent experimental studies have shown that $\phi^b \neq \phi'$ for many soils and ϕ^b is not constant but varies nonlinearly with suction i.e., $\phi^b = \phi^b(\psi)$. Consequently, shear strength varies nonlinearly with respect to soil suction (Escario and Saez, 1986, Feuerharmel et al., 2005, Fredlund et al., 1987, Gan et al., 1988, Ridley, 1995, Rohm and Vilar, 1995, Wheeler, 1991).

It is also generally assumed that the angle ϕ^b changes bi-linearly. That is, ϕ^b is equal to the friction angle ϕ' for matric suction values lower than the air entry value (AEV) of the soil and decreases for matric suction values above the AEV. However, there are also cases where ϕ^b is larger than ϕ'. It has been suggested that ϕ' may also be affected by suction changes (Abramento and Carvalho, 1989, Rohm and Vilar, 1995).

Due to the practical difficulties of testing unsaturated soils, such as the long test periods and the need for special test apparatus, and the consequent higher cost, many studies have suggested alternative techniques for establishing the shear strength properties of unsaturated soils. One approach is to directly link the shear strength criterion to the degree of saturation via the soil water characteristic curve (SWCC), which relates matric suction to soil saturation.

Vanapalli et al. (1996) assumed that the contribution of matric suction to the shear strength is proportional to the product of matric suction and the normalized area of water, and that the normalized area of water is proportional to the normalized volumetric water content with a fitting parameter:

$$\tau = (u_a - u_w)(a_w \tan\phi') = (u_a - u_w)\left[\Theta^{\kappa} \tan\phi'\right] \quad (5)$$

where a_w = normalized area of water, Θ = normalized volumetric water content (=degree of volumetric saturation), and κ = a fitting parameter.

Thus, the final form of the equation proposed for the estimation of the shear strength of an unsaturated soil using the SWCC can be written as follows:

$$\tau = c' + (\sigma_n - u_a)\tan\phi' = (u_a - u_w)\left[\Theta^{\kappa} \tan\phi'\right] \quad (6)$$

Vanapalli et al. (1996) also proposed a similar equation without the fitting parameter, but this approach requires the residual degree of saturation S_r, which is difficult to determine for clay soils:

$$\tau = c' + (\sigma_n - u_a)\tan\phi' + (u_a - u_w)\left[\tan\phi'\left(\frac{S - S_r}{100 - S_r}\right)\right] \quad (7)$$

A comparison of the use of Eqs. (6) and (7) to predict the unsaturated shear strengths of two different soils for a range of suction values is provided by Vanapalli and Fredlund (2000). Their results indicate that both equations agree well with experimental data.

4.3 Experimental procedures

The unsaturated shear strength characteristics of riverbank soils that change with degree of saturation were studied in the laboratory using the multistage direct shear test. These laboratory tests benefited from a newly-constructed modified direct shear test

apparatus that allows independent control of matric suction, referred to as a suction controlled multistage direct shear test. The shear strength was established using multistage loading over a range of net normal stresses and matric suction values.

4.3.1 Construction of suction-controlled direct shear test equipment

To investigate the relationship between matric suction and shear strength of unsaturated soils, a new direct shear box to be placed inside a pressure chamber was constructed for unsaturated soil shear testing (Figure 1). The pressure chamber allows for the matric suction to be controlled over a wide range during testing. The pressure chamber is 190 mm wide, 190 mm long and 150 mm high, and the shear box is 90 mm wide, 90 mm long and 55 mm high.

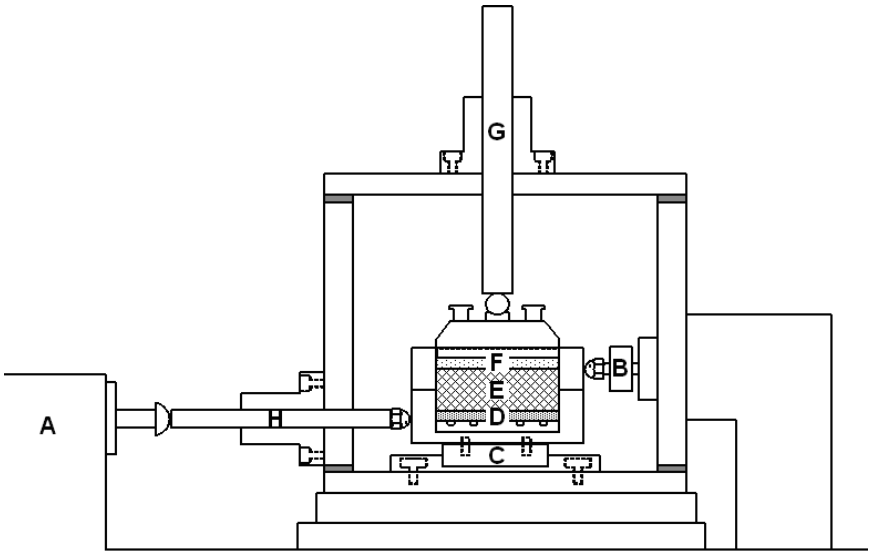

Figure 1 Schematic diagram of the modified suction-controlled direct shear test equipment.

The shear box holds a cylindrical-shaped soil specimen 63.5 mm in diameter and 25 mm thick. A high air entry ceramic disc (HAECD) with an AEV of either 100 kPa or

300 kPa, manufactured by Soilmoisture Equipment Corp., is placed at the bottom of the soil specimen to provide continuity of the water phase in the soil with the atmosphere. A grooved channel is located beneath the HAECD for drainage from the soil sample and to remove diffused air below the HAECD. Both ends of the channel are open to the atmosphere, which makes the pore water pressure of the soil equal to atmospheric pressure independent of the applied air pressure. This setup is also used for injecting water to remove air bubbles.

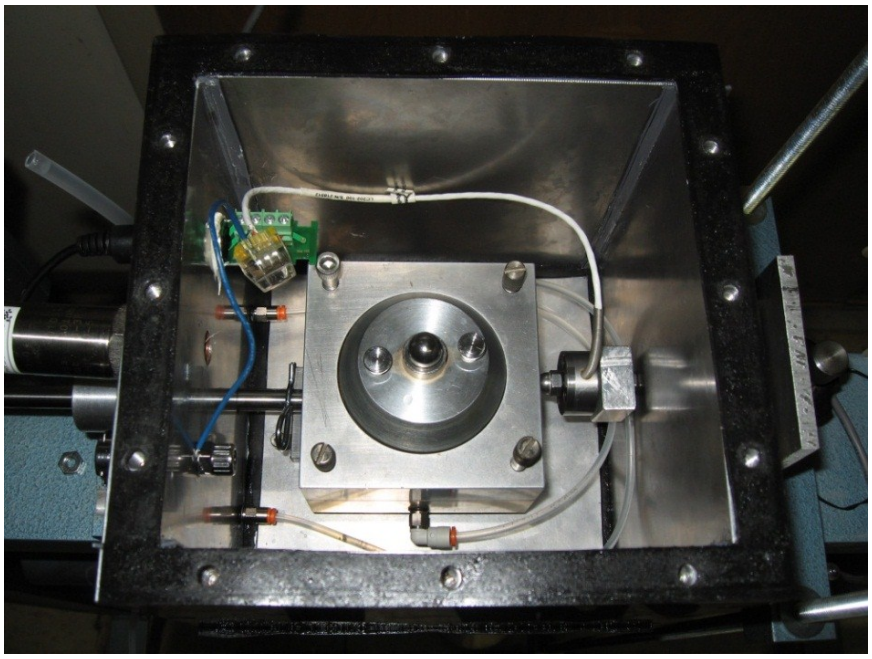

Figure 2 A plan view of the modified direct shear test apparatus within the pressure chamber.

The bottom shear box is seated on a linear guide for horizontal shearing, and the top shear box is in contact with a load cell to measure the shear load. Although ASTM D 3080 (2004) states that a counter force to support the top shear box may be required, the shear box used for these tests is not equipped with a counter support system. Thus, there is a possibility that the measured shear strength might have been influenced by the weight

of the upper shear box when the applied normal stress is low. Loading and shearing rams are connected through the pressure chamber with O-rings and linear bearings to prevent air leaks. A pressure transducer and a low profile load cell are mounted inside the chamber to monitor pressure changes and shear load, respectively (Figure 2). The top plate of the pressure chamber is made of transparent polycarbonate to provide a view into the chamber. The new pressure chamber with the modified shear box can be used with a conventional direct shear loading frame with height adjustment for shearing ram alignment.

4.3.2 Multistage direct shear test

Unlike conventional shear strength tests for soils that use several soil specimens, a multistage test uses a single soil specimen and shears the sample in stages with increasing normal stresses. The multistage test is not an ASTM standard method for obtaining total or effective stress parameters, but has been widely used in practice. The multistage test approach has been adapted for both triaxial and direct shear tests and is especially useful when there are difficulties in sampling and sample preparation. It has been applied to rocks (Kim and Ko, 1979, Tisa and Kovári, 1984), undisturbed submarine soils (Nambiar et al., 1985), undisturbed silty sand (Saeedy and Mollah, 1988), and undisturbed residual soils (Gan et al., 1988). The benefits of the multistage tests are: 1) the effects of sample variability are eliminated, 2) the time required for sample preparation and testing is minimized, and 3) the overall cost for the tests is reduced. As a single sample is used throughout the test, it is important that the sample be representative of the site of interest.

Multistage tests were first introduced by Taylor (1951) to measure the shear strength of undisturbed, partially saturated silty clay using both consolidated and

unconsolidated, undrained triaxial tests with pore pressure measurements. At each stage, a single soil sample was sheared until failure, followed by an increase in the confining pressure leading to the next stage of shearing. The results were considered satisfactory. However, Taylor noted that multistage tests should be limited to soils that are relatively insensitive to changes in structure. Kenny and Watson (1961) performed consolidated-drained triaxial tests and consolidated-undrained triaxial tests with pore pressure measurements on both undisturbed and remolded soils. Their conclusions also supported the benefits and reliability of multistage tests, but did not recommend it for drained compression tests on sensitive soils. Lumb (1964) emphasized the benefits of using multistage triaxial tests on undisturbed residual soils in Hong Kong, mainly decomposed rhyolite and decomposed granite, which have great variation in their properties. He also concluded that the results are practically indistinguishable from ordinary tests. Parry and Nadarajah (1973) also performed consolidated-undrained multistage triaxial tests for remolded and undisturbed clays, and reached the same conclusion, noting that the errors in results from multistage tests are insignificant compared to those from single stage tests using multiple specimens. Soranzo (1988) completed a series of multistage unconsolidated undrained and isotropically consolidated undrained triaxial compression tests on natural complex clayey soils, and concluded that the multistage test results were highly comparable to those of traditional triaxial tests.

The multistage loading method is ideally suited for unsaturated soil testing, where each individual stage requires increased testing time due to the long equilibrium period (Futai et al., 2006, Gan and Fredlund, 1988, Huat et al., 2005a). Ho and Fredlund (1982) measured the shear strength of unsaturated residual soils in Hong Kong with modified

triaxial test equipment. The modified equipment was able to control matric suction up to 500 kPa using the axis translation technique. Ho and Fredlund (1982) suggested that the samples should not be sheared excessively during the early stage of loading. The shear strength with respect to matric suction increased linearly, although the measured strength at the last stage was smaller than the projected value determined by the results at lower suctions. This was initially interpreted as a possible reduction in shear strength due to the multistage test, but on further reflection was ascribed to the nonlinear matric suction vs. shear strength relationship. A number of studies have shown the feasibility of using multistage tests with triaxial test equipment modified for unsaturated soil tests (Aversa and Nicotera, 2002, Cabarkapa and Cuccovillo, 2006, Drumright and Nelson, 1995, Futai and Almeida, 2005, Lu and Wu, 2006, Rahardjo et al., 1995).

Although the triaxial test is generally more advanced and versatile for research purposes, including being adapted for multistage tests, the direct shear test is preferred for unsaturated soil testing as the drainage path of soil samples in the direct shear test is much shorter than that of the triaxial test, especially for soils with low permeability (Gan et al., 1988). Several researchers have also adapted the direct shear test to unsaturated soils (Boso et al., 2005, De Campos and Carrillo, 1995, Escario and Saez, 1986, Feuerharmel et al., 2005, Hormdee et al., 2005). However, there have been few investigations of the application of the multistage shearing technique to the direct shear test for unsaturated soils (Gan and Fredlund, 1988, Huat et al., 2005b).

4.4 Experiments

The validity of suction controlled multistage direct shear test procedures to determine the unsaturated shear strength of riverbank soils was investigated using

undisturbed soil samples obtained from the riverbank of the lower Roanoke River near Scotland Neck, North Carolina, in the eastern U.S. The surface soil consists of Quaternary alluvium deposits up to 7.6 m and Upper Cretaceous sedimentary materials underlying the alluvium soil layer (Weems et al., 2009). This location has been exposed to frequent changes of water surface elevation due to an upstream hydropower dam. It has also undergone extensive levels of riverbank erosion and failure as documented by Hupp et al. (2009).

4.4.1 Soil samples and physical properties

Undisturbed soil samples for direct shear tests were extruded from Shelby tubes and block soil samples obtained from the study site. Disturbed soil samples were also collected and tested for grain size distribution, Atterberg limits, specific gravity, and classification by the United Soil Classification System (USCS). A representative soil profile of the riverbank, where the soil samples were collected, consists of silty sand SM (0-0.6 m), low plasticity clay CL (0.6-2.5 m), high plasticity silt MH (2.5-3.8 m), and low plasticity clay CL (3.8-4.5 m). In this study, the upper and lower clays are referred to as CL1 and CL2 respectively for the classification. Tables 1 and 2 summarize the physical properties of the soil samples used in the study, and the SWCCs of these soils are presented in Figure 3. The SWCCs of the four soil types were originally obtained by Nam et al. (2010), and were established using the pressure plate test, dew point potentiameter, vapor equilibrium technique, osmotic method, Tempe cell test and filter paper test. The AEV were determined from the curves.

Table 1 Soil properties of the site.

Soil properties	Units	Soil type			
		SM	CL1	MH	CL2
Depth, D	m	0-0.6	0.6 - 2.5	2.5 – 3.8	3.8-4.5
Specific gravity, G_s	-	2.69	2.72	2.73	2.72
Liquid Limits, LL	%	N.P.	39-48	50-57	37-43
Plasticity Index, I_p	%		16-25	18-24	15-20
Sand content	%	68-71	4-24	5-14	4-18
Silt content	%	20-24	28-58	41-48	50-66
Clay content	%	8-9	30-48	42-50	23-43

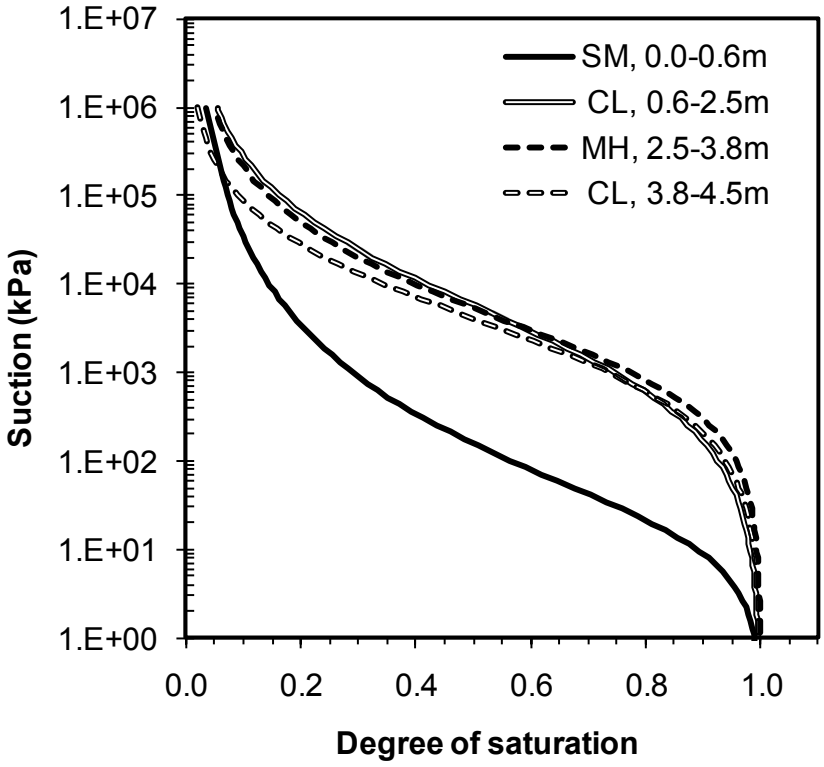

Figure 3 SWCCs for the four soil types.

Table 2 Average soil properties and test results of multistage direct shear tests.

Soil condition	Soil property	Soil type				Remark
		SM	CL1	MH	CL2	
Saturated conditions	w_{ini}, %	9.7	34.3	30.7	30.5	measured before saturation
	$\gamma_{t\ ini}$, g/cm^3	1.67	1.79	1.82	1.78	
	e_{ini}	0.82	1.04	0.96	1.01	
	ϕ', °	35	32.4	32	28.4	
	c', kPa	4.3	5.0	15.8	22.5	
Unsaturated condition	w_{ini}, %	10.6	36.4	29.0	29.4	
	$\gamma_{t\ ini}$, g/cm^3	1.59	1.79	1.85	1.74	
	e_{ini}	0.83	1.06	0.91	1.02	
	ψ_a, kPa	60	180	280	200	Air Entry Value (AEV)
	α, kPa	50	50	50	100	Inflection point
	$\sigma_n - u_a$, kPa	43	43	43*	43	
	ϕ^b, ° ($\psi_M < \alpha$)	38.7	46.6	44.9*	16.0	
	ϕ^b, ° ($\psi_M > \alpha$)	13.3	10.2	14.7*	9.0	
	τ_{sat}, kPa	36.3	33.6	42.3	39.7	
	a	4.68	10.18	8.13	12.34	$\tau = a\psi^b + \tau_{sat}$
	b	0.54	0.39	0.46	0.35	
	R^2	1.00	0.96	1.00	1.00	
	a	5.64	5.84	6.45	5.84	when b is fixed at 0.5
	R^2	1.00	0.90	1.00	0.96	

* Estimated from measurements from 21 and 68 kPa of matric suction.

4.4.2 Laboratory tests

The conventional direct shear test procedures followed ASTM D 3080 (2004), except in the case of the multistage tests. The multistage direct shear tests were performed for both saturated and unsaturated tests. A single specimen was used for each multistage test, and the shear stress vs. shear displacement response was continuously monitored during the test. When the slope of the shear stress vs. shear displacement curve approached zero, that test stage was terminated and the measurement moved on to the next stage. Typically, the shear stress vs. shear displacement curve became almost flat after 1 to 2 mm of shear displacement. In the final stage, the sample was sheared until strain softening was observed at a shear displacement of about 5 mm. For unsaturated samples, instead of increasing the normal stress, the matric suction was increased for the next stage. When the air pressure was increased for the matric suction at a given stage, an additional vertical load was applied to counteract the increased air pressure, maintaining a constant net normal stress $(\sigma_n - u_a)$ throughout the unsaturated test. The soil sample was sheared at a rate of 0.005 mm/min for silt (MH) and clay (CL), and 0.008 mm/min for silty sand (SM).

Special procedures were followed to control the matric suction when testing unsaturated soils. The high air entry ceramic disc (HAECD) fixed in the shear box was saturated before testing and stored in a saturation chamber filled with water and maintained at 60 kPa of vacuum pressure. Before setting a soil sample, the shear box with the flooded HAECD was checked for leaks with a high air pressure. Then the soil sample was placed in the shear box and moved to the saturation chamber for a further 7 to 14 days for saturation. A porous stone was placed on top of the soil specimen and an

additional weight was placed above the shear box. The additional weight was not applied to the soil directly and thus did not compress the sample, but served to restrict and minimize volume changes in the sample during the saturation process. The samples did not exhibit noticeable volume change during consolidation. After the saturation process, the shear box was moved into the pressure chamber and the sample was consolidated. After the consolidation process, a designated air pressure was applied to create the suction controlled environment. The loading steps of the matric suction for the multistage tests were 25, 50, 100, 200, and 290 kPa. Under higher pressures, typically above 200 kPa, water in the grooved channel and connecting tubes was flushed every 8 to 12 hours to remove air bubbles from the system. The weight of drained water was monitored to determine if the sample had reached equilibrium. The equilibrium period is known to differ with applied pressure, soil type, void ratio and other soil properties. A typical equilibrium period was 1 to 3 days for air pressures less than 100 kPa, and 5 to 12 days for higher air pressures. As the system was not equipped with a diffused air volume measurement system, the weight of water was measured for three hours after each flushing to minimize any error caused by the diffused air in the channel and tubes. Following the equilibrium period, the soil samples were sheared.

4.5 Results and discussion

Multistage direct shear tests for saturated and unsaturated soils were successfully performed for three different soil types: silty sand (SM), high plasticity silt (MH), and low plasticity clay (CL). Results are presented for (1) the validation of the multistage technique, (2) the shear strength of saturated soils obtained from consolidated drained direct shear tests, and (3) the shear strength of unsaturated soils obtained from suction-

controlled consolidated drained direct shear tests. The experimentally determined shear strengths of the unsaturated soils were compared to those estimated using the SWCC and the saturated shear strength.

4.5.1 Validation of the multistage direct shear test

Figure 4 shows typical results from a multistage direct shear test on a saturated sample of the MH soil. The normal stress was increased from 43 to 164 kPa in 5 shearing stages. Shearing at each loading stage was stopped when the change in shear stress became almost minimal with an increase in shear displacement. The sample was then unloaded to zero shear stress and the normal stress was increased to the next level. Once the sample had been consolidated under the new effective normal stress level, the shearing process was repeated until the shear stress vs. shear displacement curve again became almost horizontal. For unsaturated soils, the matric suction was increased instead of the normal stress while maintaining a constant net normal stress during the multistage test, and the sample was sheared after it reached equilibrium under the new matric suction level.

The most important requirement for the multistage test is that the loading at each stage should never extend beyond the peak shear stress into the strain softening regime. Figure 5 shows typical examples of multistage tests for saturated and unsaturated soils that did not comply with this requirement. In Figure 5a, a saturated sample was subjected to a large shear displacement beyond the peak shear stress, sheared in the opposite direction, and returned to zero shear displacement. The normal stress was then increased from 71 to 96 kPa and the sample was allowed to consolidate before the shearing process was repeated. As the figure shows, despite the increase in the normal stress, the shear

stress did not increase and the response followed essentially the same shear stress vs. displacement curve from the prior shearing at the normal stress of 71 kPa. Figure 5b shows the response of a highly strain softening unsaturated sample, where strain softening suddenly occurred before the slope of the shear stress vs. shear displacement curve approached zero. The sample was re-sheared after the matric suction was increased in two stages from the initial value of 60 kPa to 87 kPa and then 106 kPa. Although the increase in matric suction would be expected to increase the shear strength, no such gain in shear strength is visible. Figure 5a and 5b emphasize the importance of ensuring that multistage shearing is monitored to guarantee the peak strength is not surpassed, and proceeding to the next stage before strain softening occurs to ensure correct results.

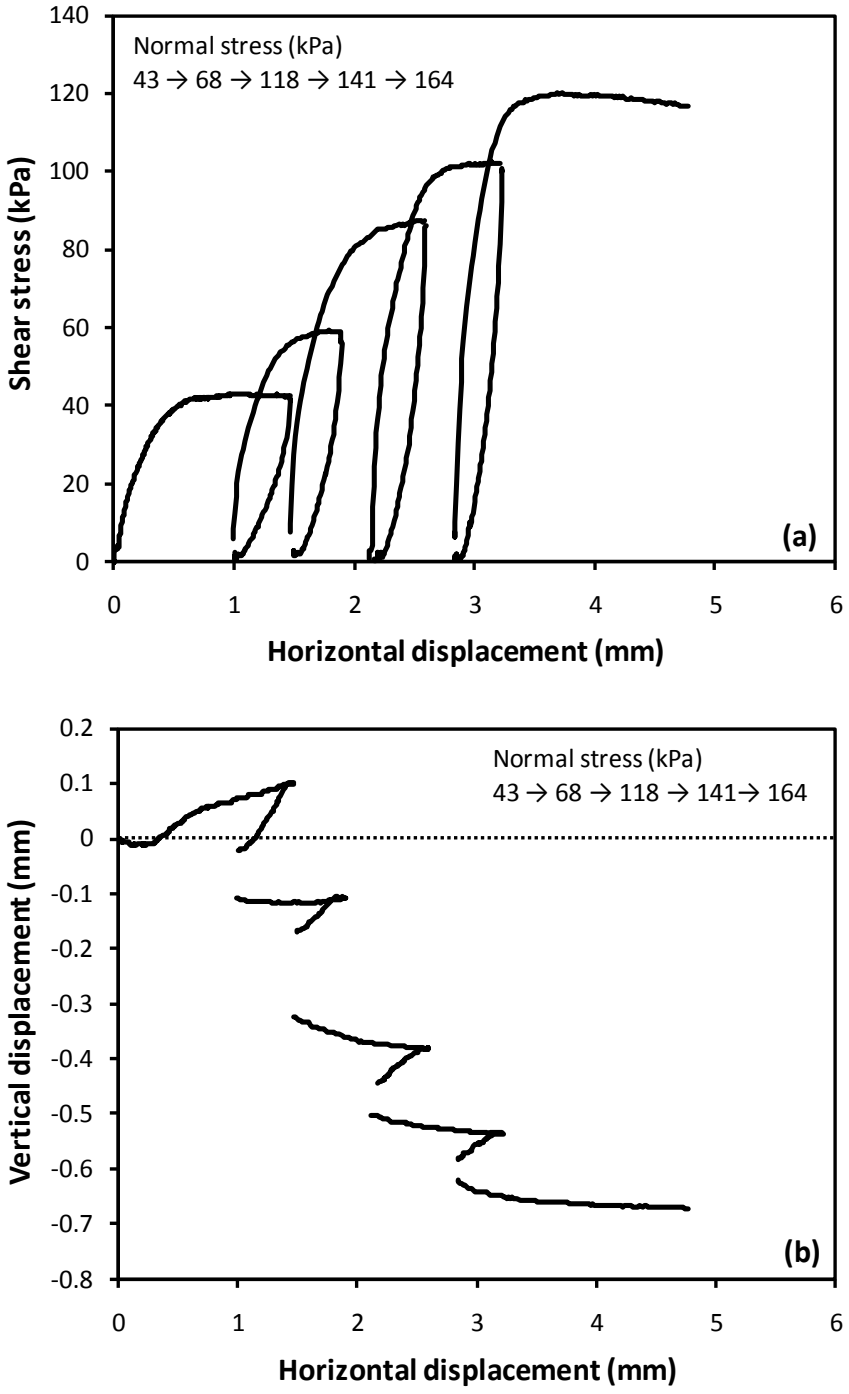

Figure 4 Results of multistage direct shear test for saturated MH soil (Negative volumetric strain indicates dilation). (a) shear stress vs. horizontal displacement, and (b) vertical displacement vs. horizontal displacement

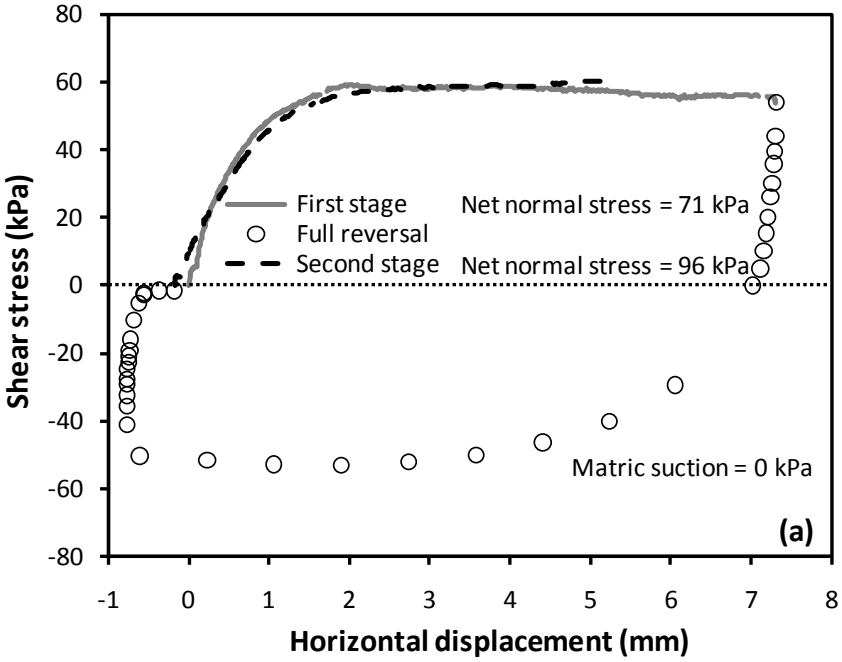

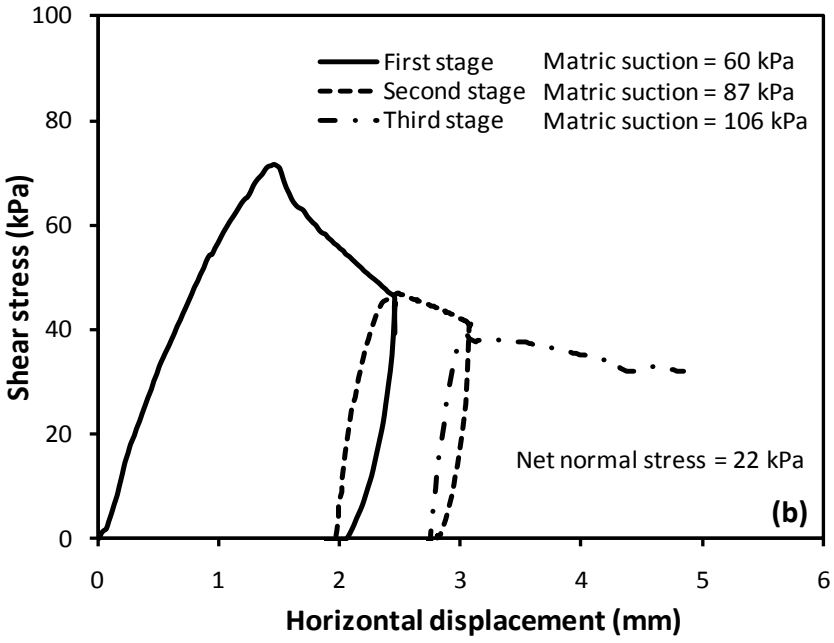

Figure 5 Examples of incorrect multistage test results. (a) Multistage test with full and reverse shearing under different normal stresses (saturated), and (b) Multistage test with different matric suctions applied after the peak stress.

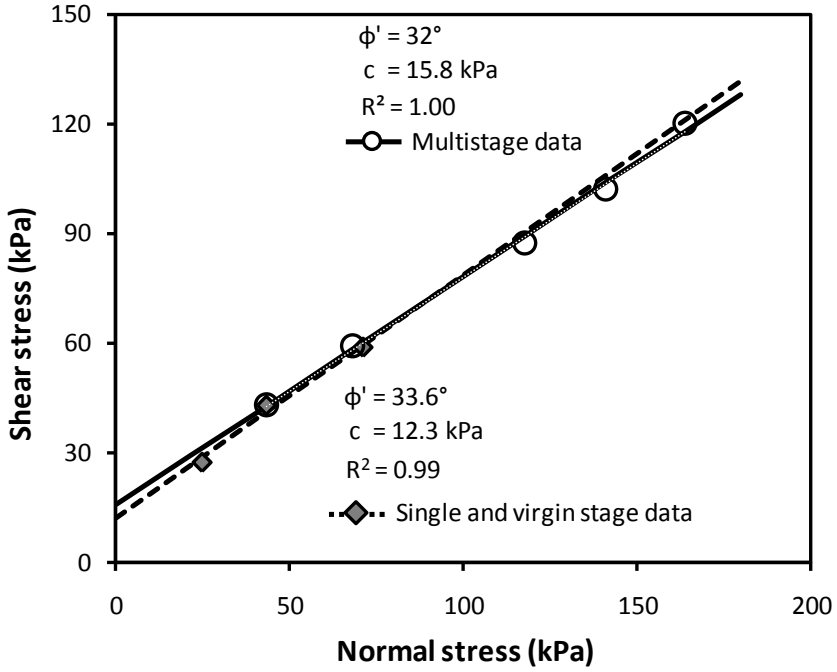

Figure 6 Validation of results from the multistage direct shear tests for saturated MH.

To investigate the validity of the multistage direct shear tests, the test results were compared to those from single stage loading and virgin stage shearing of soil samples. The single stage test is a conventional direct shear test using one soil sample per normal stress. The virgin stage is the first stage of a multistage test before the sample has been subjected to any re-shearing. Figure 6 shows an example of this comparison for the MH soil. The failure envelope determined from the combined results of the single stage and virgin stage direct shear tests is shown as a dotted line, while the failure envelope determined from the multistage tests is shown as a solid line. As the figure shows, the friction angle of ϕ=32° from the multistage test is slightly lower than that from the single and virgin loading tests of ϕ=33.6°. On the other hand, the cohesion of c=15.8 kPa for the multistage test is higher than the cohesion of c=12.3 kPa for the single and virgin loading tests. The differences are, however, small and it may be concluded that the multistage test

yields results that are reasonably accurate for use in practical applications. Similar results were obtained for the tests on the upper clay (CL1). Based on the results for both the silt and clay, it was assumed that the test would also be valid for the lower clay (CL2).

As noted previously, it is very important to avoid exceeding the complete shear failure of the soil sample during a multistage direct shear test. Each shearing stage was terminated when the shear stress had almost reached the maximum stress and stabilized. This maximum shear stress is defined as the "failure shear stress" in this study. As shown in Figure 7, the failure shear stress from each stage of loading was determined at a shear displacement of about 1.5 mm from the start of the re-shearing. To determine how close this failure shear stress is to the true peak shear stress, samples were sheared until strain softening occurred in the final stage of shearing. Figure 7 illustrates typical behavior of two samples of the upper clay from the same Shelby tube, where the samples were subjected to large shear displacements at the last stage of shearing. One sample was sheared in four stages while the other was sheared in five stages. The shear stresses at 1.5 mm shear displacement and the true peak shear stress are indicated by circles in the final stages. Looking at the second circles, the peak shear stresses occurred at shear displacements larger than 1.5 mm. However, the failure shear stresses corresponding to 1.5 mm of shear displacement were only 3% lower than the true peak shear stress. Similar results were also observed in the other soils. Thus, the error from determining the failure friction angle and cohesion from the shear stresses at an earlier stage of displacement appears to be minimal. Figure 7 illustrates the importance of carrying out the last stage of shearing under large shear deformation to check the validity of selecting the failure shear stress at a smaller shear displacement.

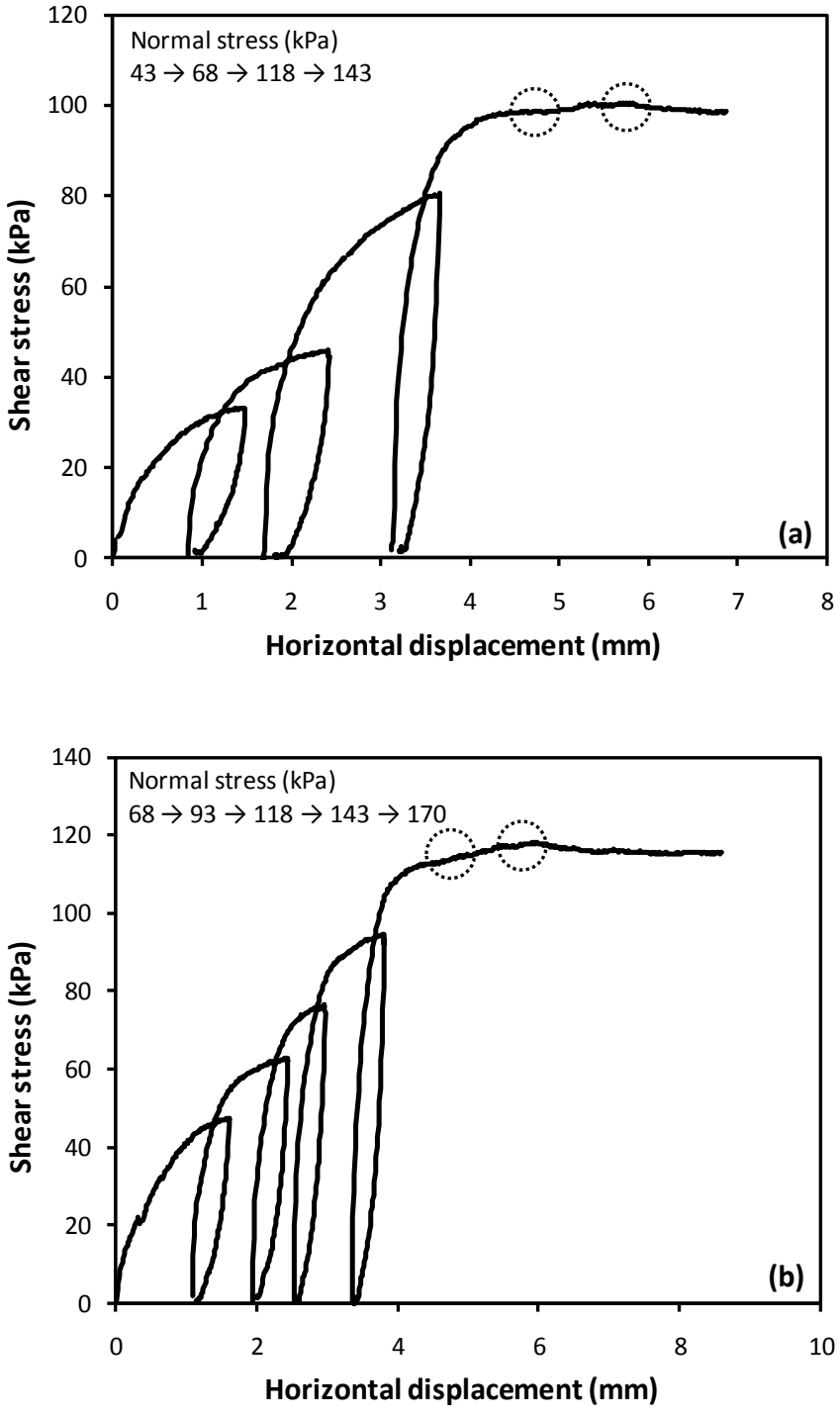

Figure 7 Repeatability of the multistage direct shear test for saturated CL1. (a) Multistage test with four stages and (b) Multistage test with five stages.

Another crucial factor in determining the validity of the multistage direct shear test is the repeatability of the test. This is demonstrated in Figure 8, which is constructed from the same results as those shown in Figure 7. As described above, two samples from the same Shelby tube were sheared in four and five stages under different normal stress histories (Figure 7). The failure envelopes obtained from the two tests, summarized in Figure 8, are nearly identical despite the fact that the two samples have undergone different loading histories. The results shown in Figure 8 indicate that the multistage loading test provides results that are both consistent and repeatable. The results also demonstrate that the multistage test can be carried out using up to five loading stages and still yield results that can be relied upon in engineering practice.

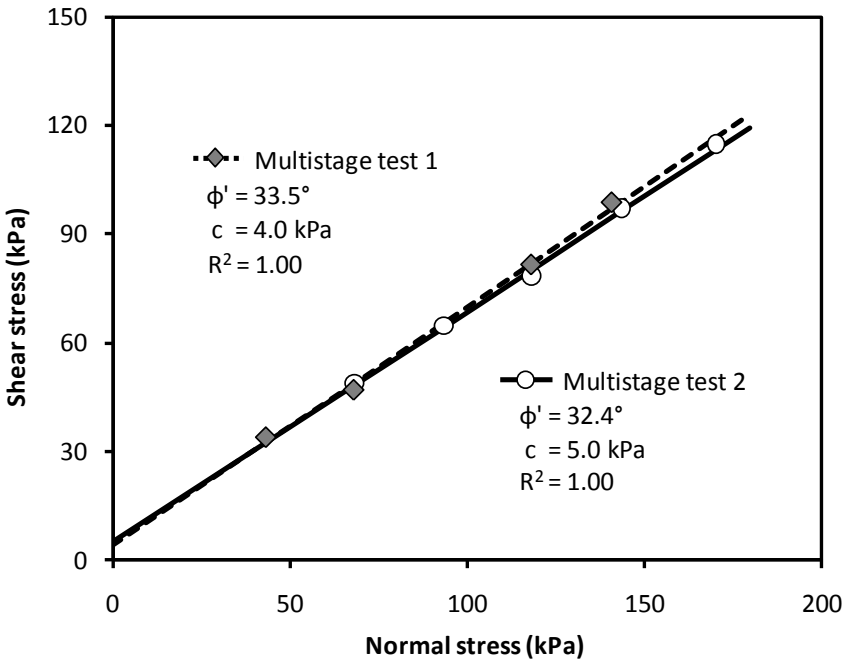

Figure 8 Results of two multistage direct shear tests on samples of CL1 soil with different loading histories.

4.5.2 Shear strength of saturated soil samples

The failure envelopes, cohesions and friction angles of the saturated soils for the four soil types, all determined using the multistage direct shear test, are summarized in Figure 9 and in Table 2. The results appear to be consistent, and linear failure envelopes fit the data well for the range of effective normal stresses used in the tests. The friction angle appears to decrease with increasing depth of the sample, while cohesion increases with increasing sample depth. Surprisingly, the friction angle of the upper clay CL1 was relatively high and the cohesion was low when compared to those of the much stiffer lower clay CL2. These shear strength values for CL1 were closer to those of the MH soil than CL2, although the CL1 and CL2 have comparable index properties.

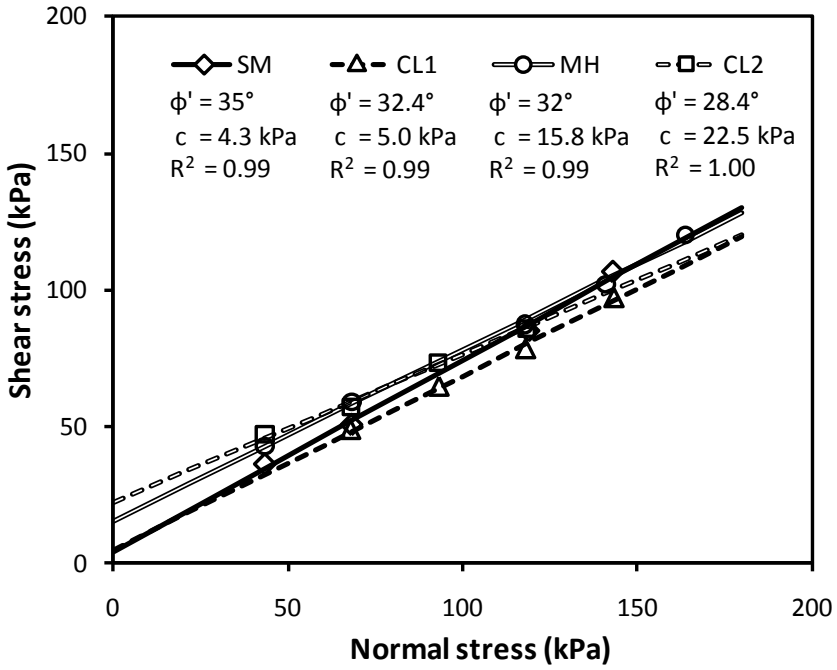

Figure 9 Failure envelopes determined from the multistage direct shear tests on saturated soil samples from the four soil types.

4.5.3 Shear strength of unsaturated soil samples

The relationship between shear strength and matric suction for unsaturated soil sample was obtained from suction-controlled multistage direct shear tests. The testing procedures were similar to those used for the saturated samples except that the matric suction was changed instead of the normal stress. While maintaining a constant net normal stress, the first stage of matric suction generally began with 25 kPa. The suction was doubled at each stage up to 200 kPa, and in the final stage the suction was raised to the limit of the HAECD, which was 290 kPa.

Typical results for the multistage direct shear test using increasing magnitudes of matric suction are illustrated in Figure 10 for the SM soil. The solid lines represent the results from the multistage tests at a constant net normal stress $(\sigma_n - u_a)$ of 43.3 kPa, while the hollow lines represent the results at the last loading stage which were tested at a matric suction ψ of 290 kPa and an increased net normal stress of 68 kPa. The volume changes during the suction-controlled tests were different from those in the saturated direct shear tests. The samples typically contracted during shearing in the saturated soil samples, whereas the samples seemed to initially contract then dilate under unsaturated conditions regardless of the soil type.

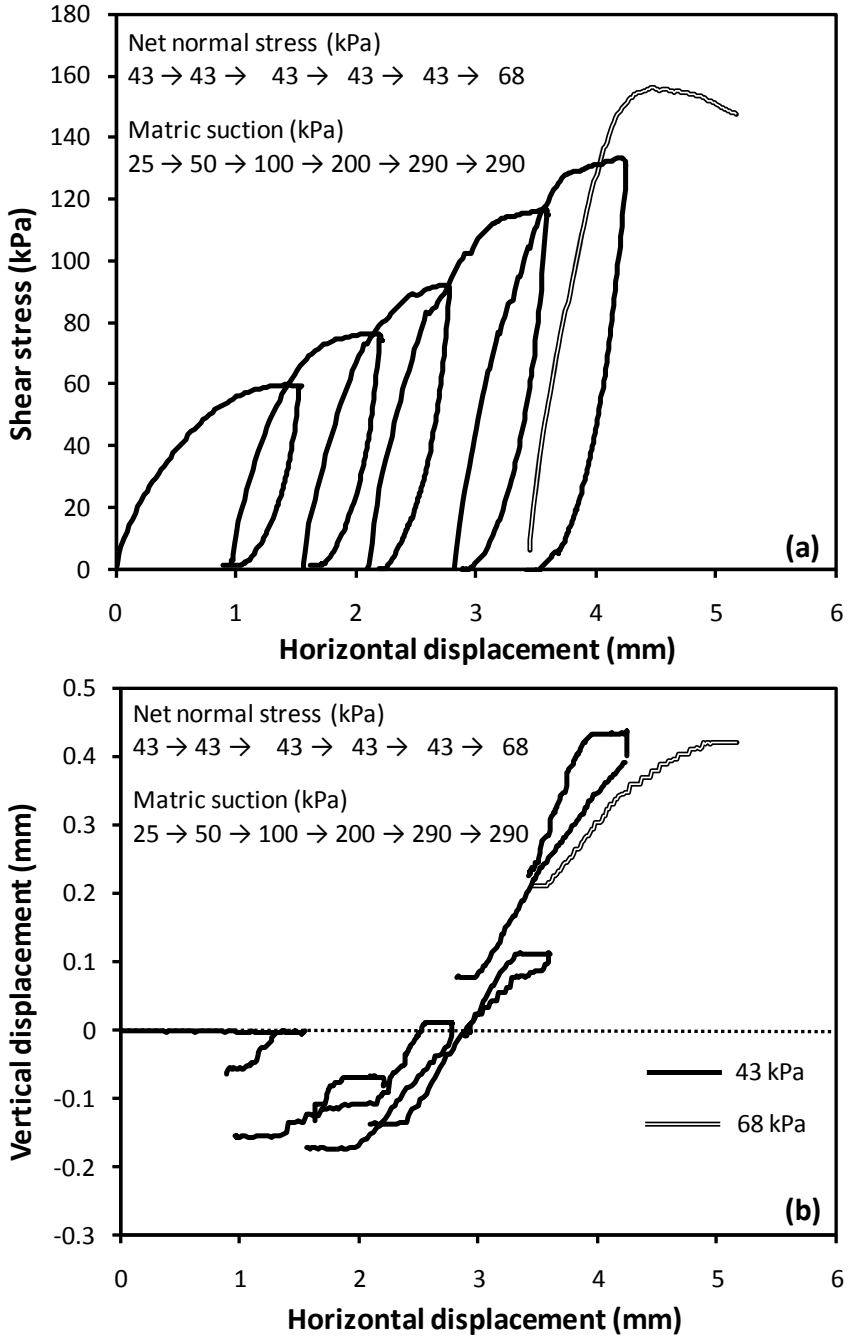

Figure 10 Multistage direct shear test results for unsaturated SM soil under different suction values. (a) Shear stress vs. horizontal displacement, and (b) Vertical displacement vs. horizontal displacement.

Figure 11 shows the effect of matric suction on the shear strength of unsaturated soils. The shear strengths shown are for a constant net normal stress of 43.3 kPa. Consistent with the observations of many researchers, the shear strength increased nonlinearly with increasing matric suction. Fredlund et al. (1987) suggested the use of a bilinear failure envelope to model the effect of matric suction on the shear strength of unsaturated soils. The bilinear criterion assumes that the slope of the τ vs. ψ failure envelope ϕ^b is equal to ϕ' when the suction is lower than the AEV, whereas the slope is smaller when suction is larger than the AEV. Thus, ϕ' and ϕ^b are the upper and lower bound values, respectively, of the matric suction dependent friction angle of unsaturated soils. Assuming a constant ϕ^b above the AEV results in a linear failure envelope and smaller, but conservative, unsaturated shear strengths.An alternative to the bilinear failure envelope is to fit a nonlinear equation through the experimental data. The experimental results were found to be well represented by a power equation of the form:

$$\tau = a\psi^b + d \tag{8}$$

where a, b = fitting parameters and $d = \tau_{sat}$ =saturated shear strength.

Eq. (8) is similar to a model proposed by Abramento and Carvalho (1989) except that they set *b* to 0.5. As can be seen in Figure 11, Eq. (8) adequately fits the experimental data for the SM soil. Comparisons of Eq. (8) with the shear strength of the MH soil at net normal stresses of 21.6 and 68.1 kPa, together with the estimated failure envelope for a net normal stress of 43.3 kPa, are shown in Figure 12.

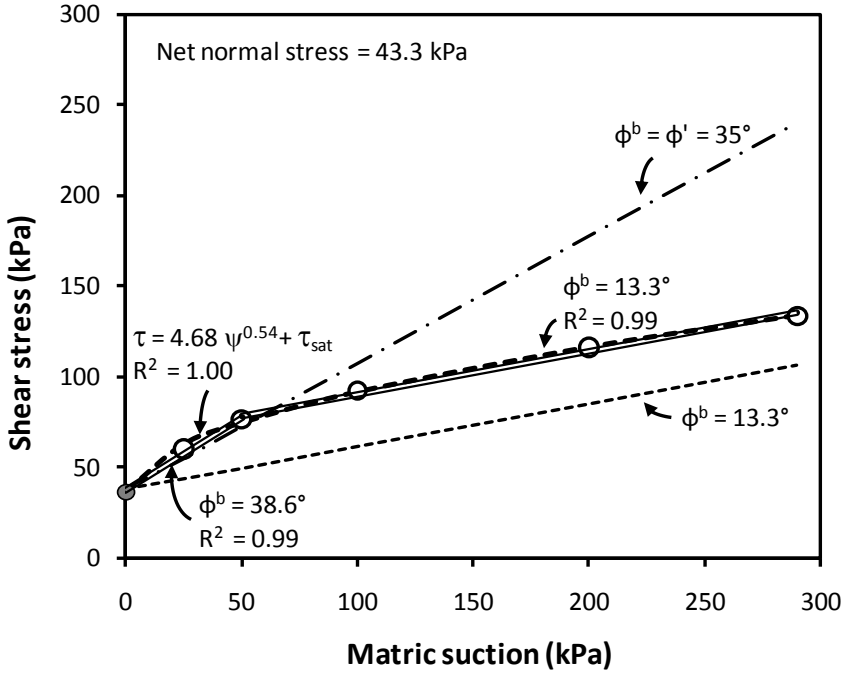

Figure 11 Different interpretations of shear strength vs. matric suction relationship for SM soil.

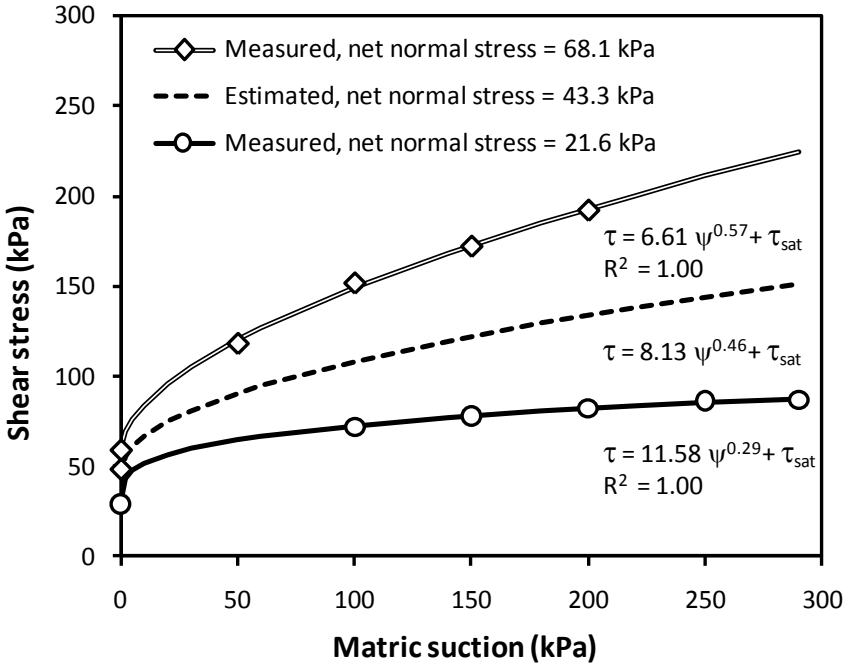

Figure 12 Estimation of shear stress vs. suction relationship for $\sigma_n - u_a$ = 43 kPa for MH soil.

Figure 13 shows how Eq. (8) can be used to model the unsaturated shear strength of the CL1 soil. The fitting parameters a and b for the four soil types are summarized in Table 2. As the calculated values of b were 0.54, 0.39, 0.46, and 0.35 for silty sand SM, upper clay CL1, silt MH, and lower clay CL2, respectively, setting the value of b to 0.5 as in the model of Abramento and Carvalho (1989) seems to be a reasonable approach to simplify the equation. As shown in Figure 13, there are no significant differences between the case where b is fixed at 0.5, and the case where b is allowed to vary to obtain a best fit regression of Eq. (8) through the experimental data, although the differences could be larger in a higher suction range.

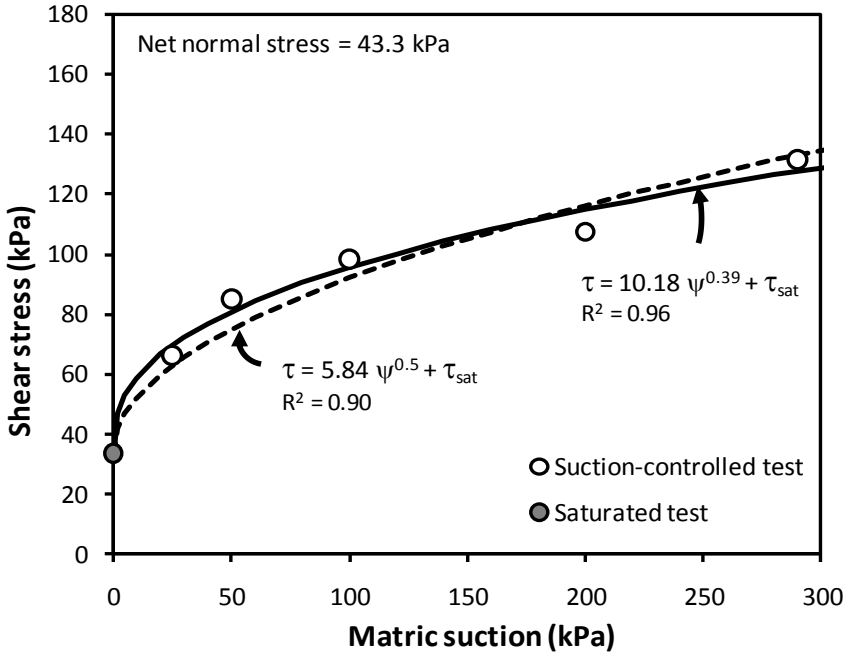

Figure 13 Shear stress and matric suction for CL1 soil.

4.5.4 Unsaturated shear strength estimated from the SWCC

Following the procedures proposed by Vanapalli et al. (1996) and Fredlund et al. (1996), the unsaturated shear strength of the soil samples can also be estimated using Eq.

(6). Strictly speaking, the parameter κ is obtained by fitting Eq. (6) through the SWCC and the unsaturated shear strength data. In the absence of the shear strength and suction data, Vanapalli and Fredlund (2000) developed a correlation of κ with plasticity index I_p for cohesive soils. For non-plastic soils, κ is assumed to be equal to unity. Experimental data for the unsaturated shear strength and the best fit curve in the form of Eq. (8) are presented in Figure 14 along with the estimated curves using Eq. (6) with values of κ equal to 2.06, 2.2, 4.31, 4.81 and 5.57. The value of κ equal to 2.2 was determined from the plasticity index and the other κ values were determined using four different suction ranges in the SWCC of the soil. When the suction was less than 200 kPa, there was little difference among the predicted shear strengths using the different values of κ. However, the difference became larger as the suction increased. It is also noticeable in Figure 15 that the fitting parameter κ varies with the suction range of interest. For example, as can be seen in Figure 15, the fitting parameter κ of the lower clay CL2 varies from 2.06 to 5.57 depending on the suction range considered. Typically, the range of suction is equal to that of the available experimental data for unsaturated shear strength, which is necessary to determine κ. If a nonlinear best fit curve for the unsaturated shear strength can be obtained (i.e., using Eq. 8), a wider range of suction can be considered for the shear strength estimation. However, if the plasticity index is used to determine κ and, ultimately, to predict the unsaturated shear strength of the soil, a large error could be generated, especially for higher suction because the κ vs. I_p correlation suggested by Vanapalli and Fredlund (2000) does not consider differences in suction range. Thus, the correlation between κ and plasticity index needs to be improved to include the applicable

suction range information. Otherwise, soils with a single plasticity index can have several different fitting parameters depending on the suction range, as shown in Figure 15.

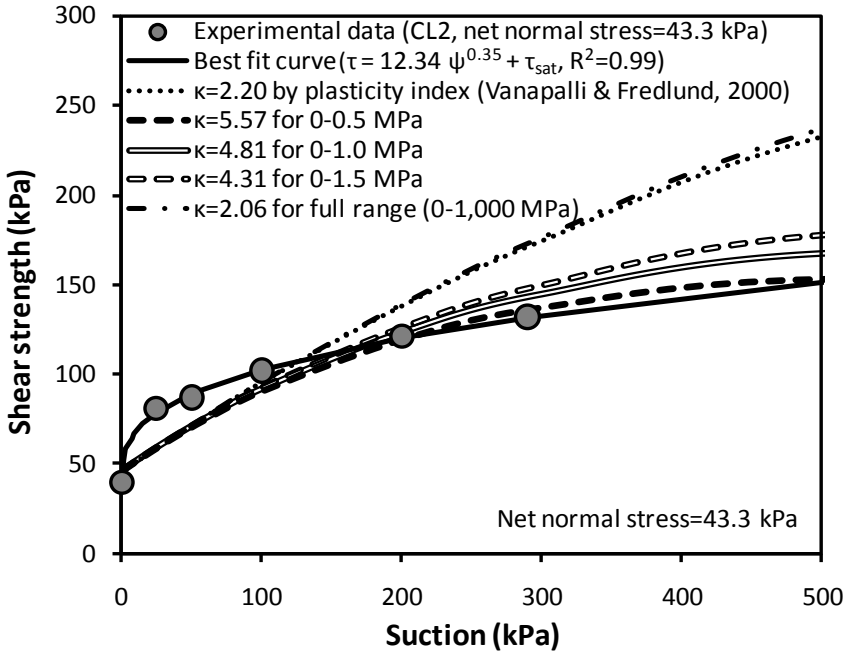

Figure 14 Estimation of unsaturated shear strength from SWCC for CL2 soil.

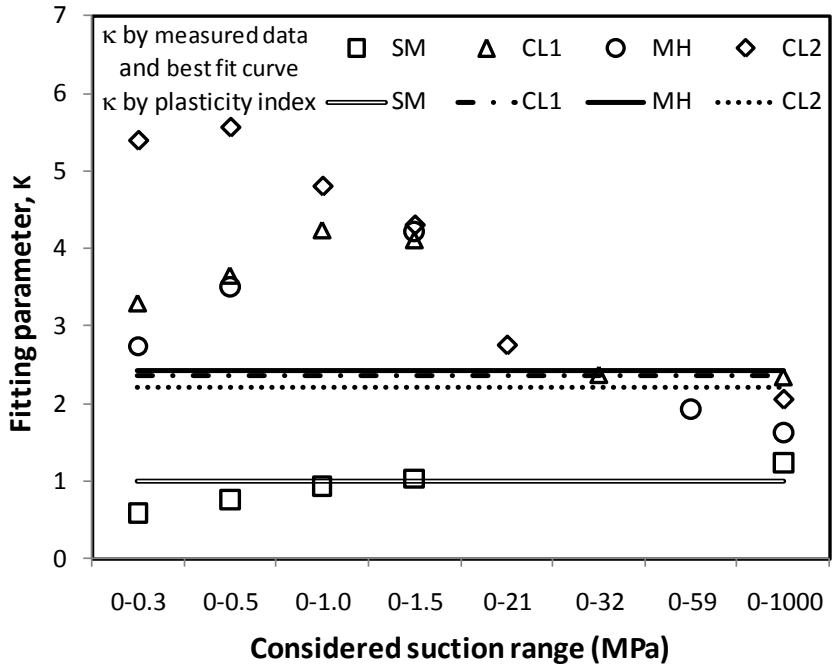

Figure 15 Variation of fitting parameter for different soil types and suction range.

4.6 Conclusions

An extensive investigation was carried out to study the validity of rapid procedures in obtaining shear strength parameters of saturated and unsaturated soils using the multistage direct shear test. The study was carried out using soil samples from the four main layers of alluvial deposits at the riverbank along the lower Roanoke River. The results from the rapid test procedures were compared with those obtained from conventional direct shear tests using multiple soil samples. Additional comparisons were made between the experimental unsaturated shear strength data and estimated data using the SWCC and saturated shear strength. The main conclusions from the study are as follows.

The multistage shearing technique was successfully applied to both saturated and unsaturated direct shear tests. The multistage direct shear test provided friction angles that are slightly lower and cohesion values that are slightly higher than those obtained from the conventional direct shear test. The observed differences are generally negligible for engineering practice. It was shown that reliable shear strengths parameters for both saturated and unsaturated soil samples can be obtained from the multistage shearing test if some precautions are followed during testing. These precautions include avoiding excessive shearing of the soil sample beyond the peak shear stress into the strain softening region, and ensuring that the samples completely reach equilibrium at every new matric suction. Potential errors in the shear strength parameters from the multistage loading can be assessed by carrying out the last stage of shearing under large shear deformation to confirm the validity of selecting the failure shear stress at smaller shear displacements. The results demonstrated that the multistage direct shear test can be

carried out using up to five loading stages, yielding results that can be relied upon in engineering practice.

The experimental results confirmed the non-linear relationship between the unsaturated shear strength and matric suction. The friction angle with respect to matric suction ϕ^b was higher than the effective friction angle ϕ' at suction values below the AEV, and decreased as suction increased. The bilinear relationship proposed by Fredlund et al. (1987), while simple, failed to adequately represent the experimental unsaturated shear strength vs. suction data. This study found a better representation of the experimental data to be either an empirical power function or the square-root function proposed by Abramento and Carvalho (1989).

The unsaturated shear strength was also estimated from the SWCC, saturated shear strength parameters c' and ϕ', and a fitting parameter κ. The value of κ can be determined from experimental unsaturated shear strength data, or empirically using the plasticity index. The latter seems to provide reasonable estimates of shear strength only at low suction values, i.e. less than approximately 200 kPa in this study. The fitting parameter κ varied with the suction range, indicating that different unsaturated shear strengths could be estimated for a soil if the applicable suction range is not defined in the determination of the κ-value. This observation is in disagreement with the approach suggested by Vanapalli and Fredlund (2000) of using a constant κ-value determined from the plasticity index regardless of suction range.

4.7 References

[1] Abramento, M., and Carvalho, C. S. (1989). "Geotechnical parameters for the study of natural slopes instabilization at `Serra do Mar', Brazil." *Proc., the International Conference on Soil Mechanics and Foundation Engineering*, A.A. Balkema, Rotterdam, Netherlands, 1599-1602.

[2] ASTM D 3080 (2004). "Standard test method for direct shear test of soils under consolidated drained conditions." *ASTM International*.

[3] Aversa, S., and Nicotera, M. V. (2002). "A triaxial and oedometer apparatus for testing unsaturated soils." *Geotechnical Testing Journal*, 25(1), 3-15.

[4] Bishop, A. W. (1959). "The principle of effective stress." *Teknisk Ukeblad*, 106(39), 859-863.

[5] Bishop, A. W. (1961). "The measurement of pore pressure in the triaxial test." *Proc., the Conference on Pore Pressure and Suction in Soils*, Butterworth, 38-46.

[6] Blatz, J., and Graham, J. (2000). "A system for controlled suction in triaxial tests." *Geotechnique*, 50(4), 465-469.

[7] Boso, M., Tarantino, A., and Mongiovì, L. (2005). "A direct shear box improved with the osmotic technique." *Proc., the International Symposium on Advanced Experimental Unsaturated Soil Mechanics*, Taylor & Francis, 85-91.

[8] Burland, J. B. (1965). *Some aspects of the mechanical behaviour of partly saturated soils*, Butterworths, Sydney.

[9] Cabarkapa, Z., and Cuccovillo, T. (2006). "Automated triaxial apparatus for testing unsaturated soils." *Geotechnical Testing Journal*, 29(1), 21-29.

[10] Cui, Y. J., and Delage, P. (1996). "Yielding and plastic behaviour of an unsaturated compacted silt." *Geotechnique*, 46(2), 291-311.

[11] De Campos, T. M. P., and Carrillo, C. W. (1995). "Direct shear testing on an unsaturated soil from Rio de Janeiro." *Proc., the 1st International Conference on Unsaturated Soils*, A. A. Balkema, 31-38.

[12] Delage, P., and Cui, Y. J. (2008). "An evaluation of the osmotic method of controlling suction." *Geomechanics and Geoengineering*, 3(1), 1-11.

[13] Drumright, E. E., and Nelson, J. D. (1995). "The shear strength of unsaturated tailings sand." *Proc., Proceedings of the 1st international conference on Unsaturated Soils*, A.A. Balkema, 45-50.

[14] Escario, V., and Saez, J. (1986). "The shear strength of partly saturated soils." *Géotechnique*, 36(3), 453-456.

[15] Feuerharmel, C., Bica, A. V. D., Gehling, W. Y. Y., and Flores, J. A. (2005). "A study of the shear strength of two unsaturated colluvium soils." *Proc., the International Symposium on Advanced Experimental Unsaturated Soil Mechanics*, Taylor & Francis, 169-174.

[16] Feuerharmel, C., Pereira, A., Gehling, W. Y. Y., and Bica, A. V. D. (2006). "Determination of the shear strength parameters of two unsaturated colluvium soils using the direct shear test." *Proc., the 4th International Conference on Unsaturated Soils* ASCE, 1181-1190.

[17] Fredlund, D. G., and Morgenstern, N. R. (1977). "Stress state variables for unsaturated soils." *American Society of Civil Engineers, Journal of the Geotechnical Engineering Division*, 103(5), 447-466.

[18] Fredlund, D. G., Morgenstern, N. R., and Widger, R. A. (1978). "Shear strength of unsaturated soils." *Canadian Geotechnical Journal*, 15(3), 313-321.

[19] Fredlund, D. G., and Rahardjo, H. (1993). *Soil mechanics for unsaturated soils*, Wiley, New York.

[20] Fredlund, D. G., Rahardjo, H., and Gan, J. K. M. (1987). "Non-linearity of strength envelope for unsaturated Soils." *Proc., 6th International Conference on Expansive Soils* 49-54.

[21] Fredlund, D. G., Xing, A., Fredlund, M. D., and Barbour, S. L. (1996). "The relationship of the unsaturated soil shear strength to the soil-water characteristic curve." *Canadian Geotechnical Journal*, 33(3), 440-448.

[22] Fredlund, M. D., Fredlund, D. G., and Wilson, G. W. (1997). "Estimation of unsaturated soil properties using a knowledge-based system." *Proc., the 4th Congress on Computing in Civil Engineering*, ASCE, 501-510.

[23] Futai, M. M., and Almeida, M. S. S. (2005). "An experimental investigation of the mechanical behaviour of an unsaturated gneiss residual soil." *Geotechnique*, 55(3), 201-213.

[24] Futai, M. M., Almeida, M. S. S., and Lacerda, W. A. (2006). "The shear strength of unsaturated tropical soils in Ouro Preto, Brazil." *Proc., the 4th International Conference on Unsaturated Soils* ASCE, 1200-1211.

[25] Gan, J. K. M., Fredlund, D. G., and Rahardjo, H. (1988). "Determination of the shear strength parameters of an unsaturated soil using the direct shear test." *Canadian Geotechnical Journal*, 25(3), 500-510.

[26] Gan, K. J., and Fredlund, D. G. (1988). "Multistage direct shear testing of unsaturated soils." *Geotechnical Testing Journal*, 11(2), 132-138.

[27] Hilf, J. W. (1956). "An investigation of pore-water pressure in compacted cohesive soils." U.S. Department of the Interior, Bureau of Reclamation, Design and Construction Division, Denver, CO.

[28] Ho, D. Y. F., and Fredlund, D. G. (1982). "A multistage triaxial test for unsaturated soils." *Geotechnical Testing Journal*, 5(1/2), 18-25.

[29] Hormdee, D., Ochiai, H., and Yasufuku, N. (2005). "Advanced direct shear testing for collapsible soils with water content and matric suction measurement." *Proc., the Geo-Frontiers 2005 Congress*, ASCE, 25-25.

[30] Hoyos, L., Laloui, L., and Vassallo, R. (2008). "Mechanical testing in unsaturated soils." *Geotechnical and Geological Engineering*, 26(6), 675-689.

[31] Hoyos, L. R., Velosa, C. L., and Puppala, A. J. (2010). "A novel suction-controlled ring shear testing apparatus for unsaturated soils." *Proc., 2010 GeoShanghai International Conference - Experimental and Applied Modeling of Unsaturated Soils*, American Society of Civil Engineers, 32-39.

[32] Huat, B. B. K., Ali, F. H., and Abdullah, A. (2005a). "Shear strength parameters of unsaturated tropical residual soils of various weathering grades." *Electronic Journal of Geotechnical Engineering*, 10 D, 6.

[33] Huat, B. B. K., Ali, F. H., and Hashim, S. (2005b). "Modified shear box test apparatus for measuring shear strength of unsaturated residual soil." *American Journal of Applied Sciences*, 2(9), 1283-1289.

[34] Hupp, C. R., Schenk, E. R., Richter, J. M., Peet, R. K., and Townsend, P. A. (2009). "Bank erosion along the dam-regulated lower Roanoke River, North Carolina." *Geological Society of America Special Papers*, 451, 97-108.

[35] Jennings, J. E. B., and Burland, J. B. (1962). "Limitations to the use of effective stresses in partly saturated soils." *Geotechnique*, 12(2), 125-144.

[36] Kenney, T. C., and Watson, G. H. (1961). "Multiple-stage triaxial test for determining c' and Phi' of saturated soils." *Proc., 5th International Conference on Soil Mechanics and Foundation Engineering*, 191-195.

[37] Kim, M. M., and Ko, H. Y. (1979). "Multistage triaxial testing of rocks." *Geotechnical Testing Journal*, 2(2), 98-105.

[38] Lu, N., and Likos, W. J. (2004). *Unsaturated soil mechanics*, J. Wiley, Hoboken, N.J. USA.

[39] Lu, N., and Wu, B. (2006). "Unsaturated shear strength behavior of a fine sand." *Proc., the 2nd Japan-U.S. Workshop on Testing, Modeling, and Simulation in Geomechanics*, ASCE, 488-499.

[40] Lumb, P. (1964). "Multi-stage triaxial tests on undisturbed soils." *Civil Engineering (London)*, 59(694), 591-595.

[41] Matyas, E. L., and Radhakrishna, H. S. (1968). "Volume change characteristics of partially saturated soils." *Geotechnique*, 18(4), 432-448.

[42] Nam, S., Gutierrez, M., Diplas, P., Petrie, J., Wayllace, A., Lu, N., and Munoz, J. J. (2010). "Comparison of testing techniques and models for establishing the SWCC of riverbank soils." *Engineering Geology*, 110(1-2), 1-10.

[43] Nambiar, M. R. M., Venkatappa Rao, G., and Gulhati, S. K. (1985). "Multistage triaxial testing: A rational procedure." ASTM, 274-293.

[44] Parry, R. H. G., and Nadarajah, V. (1973). "Multistage triaxial testing of lightly overconsolidated clays." *Journal of Testing & Evaluation*, 1(5), 374-381.

[45] Rahardjo, H., Lim, T. T., Chang, M. F., and Fredlund, D. G. (1995). "Shear-strength characteristics of a residual soil." *Canadian Geotechnical Journal*, 32(1), 60-77.

[46] Ridley, A. M. (1995). "Strength-suction-moisture content relationships for kaolin under normal atmospheric conditions." *Proc., the first international conference on Unsaturated Soils*, Balkema, 645-651.

[47] Rohm, and Vilar, O. M. (1995). "Shear strength of an unsaturated sandy soil." *Proc., the 1st international conference on Unsaturated Soils*, A.A. Balkema, 189-193.

[48] Saeedy, H. S., and Mollah, M. A. (1988). "Application of multistage triaxial test to Kuwaiti soils." *Symposium on advanced triaxial testing of soil and rock*, R. T. Donaghe, R. C. Chaney, and M. L. Silver, eds., ASTM, Louisville, KY, USA, 512-538.

[49] Sedano, J. A. I., Vanapalli, S. K., and Garga, V. K. (2007). "Modified ring shear apparatus for unsaturated soils testing." *Geotechnical Testing Journal*, 30(1), 39-47.

[50] Sheng, D., Zhou, A., and Fredlund, D. (2009). "Shear strength criteria for unsaturated soils." *Geotechnical and Geological Engineering*, 29(2), 145-159.

[51] Soranzo, M. (1988). "Results and interpretation of multistage triaxial compression tests." *Advanced Triaxial Testing of Soil and Rock, ASTM STP 977*, R. T. Donaghe, R. C. Chaney, and M. L. Silver, eds., American Society for Testing and Materials, Philadelphia, Pa, USA, 353-362.

[52] Taylor, D. W. (1951). "A triaxial shear investigation on a partially saturated soil." *Triaxial testing of soils and bituminous mixtures ASTM STP 106*, 180-187.

[53] Terzaghi, K. (1943). *Theoretical soil mechanics*, John Wiley and Sons, New York.

[54] Tisa, A., and Kovári, K. (1984). "Continuous failure state direct shear tests." *Rock Mechanics and Rock Engineering*, 17(2), 83-95.

[55] Vanapalli, S. K., and Fredlund, D. G. (2000). "Comparison of different procedures to predict unsaturated soil shear strength." *Proc., Advances in Unsaturated Geotechnics*, ASCE, 195-209.

[56] Vanapalli, S. K., Fredlund, D. G., Pufahl, D. E., and Clifton, A. W. (1996). "Model for the prediction of shear strength with respect to soil suction." *Canadian Geotechnical Journal*, 33(3), 379-392.

[57] Vassallo, R., Mancuso, C., and Vinale, F. (2007). "Effects of net stress and suction history on the small strain stiffness of a compacted clayey silt." *Canadian Geotechnical Journal*, 44(4), 447-462.

[58] Vilar, O. M. (2006). "A simplified procedure to estimate the shear strength envelope of unsaturated soils." *Canadian Geotechnical Journal*, 43(10), 1088-1095.

[59] Weems, R. E., Lewis, W. C., and Aleman-Gonzalez, W. B. (2009). "Surficial geologic map of the Roanoke Rapids 30' x 60' quadrangle, North Carolina: U.S. Geological Survey open-file report 2009–1149, 1 sheet, scale 1:100,000." U.S. Geological Survey.

[60] Wheeler, S. J. (1991). "Alternative framework for unsaturated soil behaviour." *Geotechnique*, 41(2), 257-261.

CHAPTER 5. Effect of Reservoir Releases on Riverbank Stability[1]

ABSTRACT

The increasing number of extreme climate events has necessitated changes in, the operation of reservoirs to accommodate large changes in the volume of water, sometimes within short periods of time. Such extreme conditions generally result in drastic changes in the flow releases from reservoirs, which in turn mean downstream riverbanks experience more rapid and frequent changes of the river water surface elevation (WSE). These changes in the WSE affect pore water pressures in the riverbanks, directly influencing slope stability. This study presents an analysis of seepage and slope stability for riverbanks under the influence of steady state, drawdown, and peaking operations of the Roanoke Rapids Hydropower dam on the lower Roanoke River, North Carolina, USA. Although the riverbanks were found to be stable under all the discharge conditions tested, which indicates that normal operations of the reservoir have no adverse effects on riverbank stability, the factor of safety decreases as the WSE decreases. When the role of fluvial erosion is considered, the stability of the riverbank is found to decrease. Drawdown and fluctuation also decrease the safety factor, though the rate of the decrease depends on the hydraulic conductivity of the soils rather than the discharge pattern.

Keywords: riverbank stability, unsaturated shear strength, limit equilibrium method, shear strength reduction method, transient seepage

---

1 This manuscript has been prepared for submission to a journal, and is co-authored by **Soonkie Nam**, Marte S. Gutierrez, Panayiotis Diplas, and John Petrie

5.1 Introduction

The stability of a slope is generally expressed in terms of its "Factor of Safety" (FS), which is defined as the ratio of the available shear strength of the soil to the equilibrium shear stress that is required to maintain a just-stable slope (Duncan and Wright, 2005). Several major factors contribute to stability, namely soil weight, soil shear strength, location of the phreatic surface and degree of saturation. When considering a riverbank, these factors are all directly affected by the water surface elevation (WSE). The WSE acts as an external force on the slope surface confining the riverbanks and affects the location of the phreatic surface, which in turn influences pore water pressure and the weight of the soil. The WSE also affects the shear stress applied to the riverbank, thus influencing fluvial erosion. The decrease in riverbank stability due to fluvial erosion and the associated changes in bank geometry are well documented in the literature (Lawler et al., 1997, Simon et al., 2000, Thorne and Abt, 1993) and cumulative fluvial erosion at the toe of a slope is known to trigger mass failures (Hubble, 2004). Thus, a critical evaluation of the influence of reservoir releases on the stability of the downstream riverbank can provide a useful tool for reservoir managers.

In recent decades, the global climate has changed dramatically, resulting in an increased frequency of extreme events, such as hurricanes, heavy rains, and snows. Storms have become both more intense and longer in duration (Emanuel, 2005), and the proportion of category 4 and 5 hurricanes has doubled since 1970 (Webster et al., 2005). Thus, there is a higher likelihood that, in response to these events, reservoir releases may need to be adjusted and more instantaneous reservoir releases may be required to maintain the safety of both the reservoir and the downstream floodplain. However,

instantaneous releases create flow conditions that are not commonly found during normal operations of the reservoir. Instead, extreme flows or drastic changes in the downstream WSE may lead to overbank flow or transient drawdown conditions. As a result, riverbank stability under prolonged high flow conditions or drawdown reservoir releases needs to be considered in terms of slope stability analysis.

The designated sites for the study presented in this paper have been exposed to these types of release due to the operation of an upstream hydropower dam, the Roanoke Rapids Dam, which directly controls the downstream WSE. The area has experienced even more extreme conditions due to a prolonged drought followed by high flow releases in recent years. Thus, it is very important to understand how the reservoir release patterns impact the downstream flow conditions and, consequently, the stability of riverbanks, and how the reservoir releases can best be managed to minimize the potential negative impacts on the riverbank.

The objective of this study is to compare the stability of riverbanks under normal reservoir operations of an upstream hydropower dam and extreme reservoir operations that can cause overbank conditions, frequent changes of the WSE, and transient drawdown. The results can be directly interpreted to determine the optimum dam operational modes to minimize bank retreat. The unique contribution of this study is that: i) riverbank stability analysis is performed taking into account actual reservoir operations and downstream conditions; ii) unsaturated soil properties are considered for the transient seepage and slope stability analysis; and iii) the riverbank stability is predicted taking fluvial erosion into account, using actual erosion rates measured by the U.S. Geological Survey (USGS).

5.2 Background

5.2.1 Site information and bank geometry

The study sites, shown in Figure 1, are located on the lower Roanoke River near Scotland Neck, North Carolina, about 72 km downstream from the Roanoke Rapids Dam. Since construction of the dam was completed in 1955, the flow in the river has been regulated resulting in a decrease in extreme high flow events, as shown in Figure 2. The WSE at the study sites is primarily controlled by flow releases from the dam because of the lack of major tributaries (see Fig. 1b), the limited effect of precipitation due to the narrow watershed, and the heavy vegetation and swamps that surround the study sites.

Five study sites were selected based on evidence of past bank retreat. Sites 2, 4, and 5 are located on relatively straight reaches, while Site 1 and Site 3 are located on the outer and inner banks of meander bends, respectively. The sites were close enough to the dam to be directly affected by peaking releases. Several field trips were made between 2007 and 2010 to perform in situ tests and collect hydraulic and geotechnical data that represent field conditions under reservoir release rates ranging from 57 m^3/s to 566 m^3/s. Visual observation during the field trips confirmed that the riverbanks are relatively steep, indicating that fluvial erosion likely occurs at these sites. In addition, the presence of trees rooted in the submerged slopes within the river channel indicates that deep seated mass failure events had already occurred. Small scale local failures near the WSE were also noticeable, but both failure types seemed to be randomly distributed throughout the study reach. This has been noted by other researchers: Hupp et al. (2009) observed and documented bank erosion and mass failure in their study of the same reach, while the

USGS also monitored bank erosion at several locations along the study reach between 2005 and 2009 (Schenk et al., 2010).

Hydraulic properties such as flow velocity and discharge rate in the field, as well as bathymetry, were obtained by acoustic Doppler current profiler (ADCP) and echosounder. Combining the bathymetric data with ground-based light detection and ranging (LIDAR) data at each site, the complete bank geometry required for the numerical modeling was obtained.

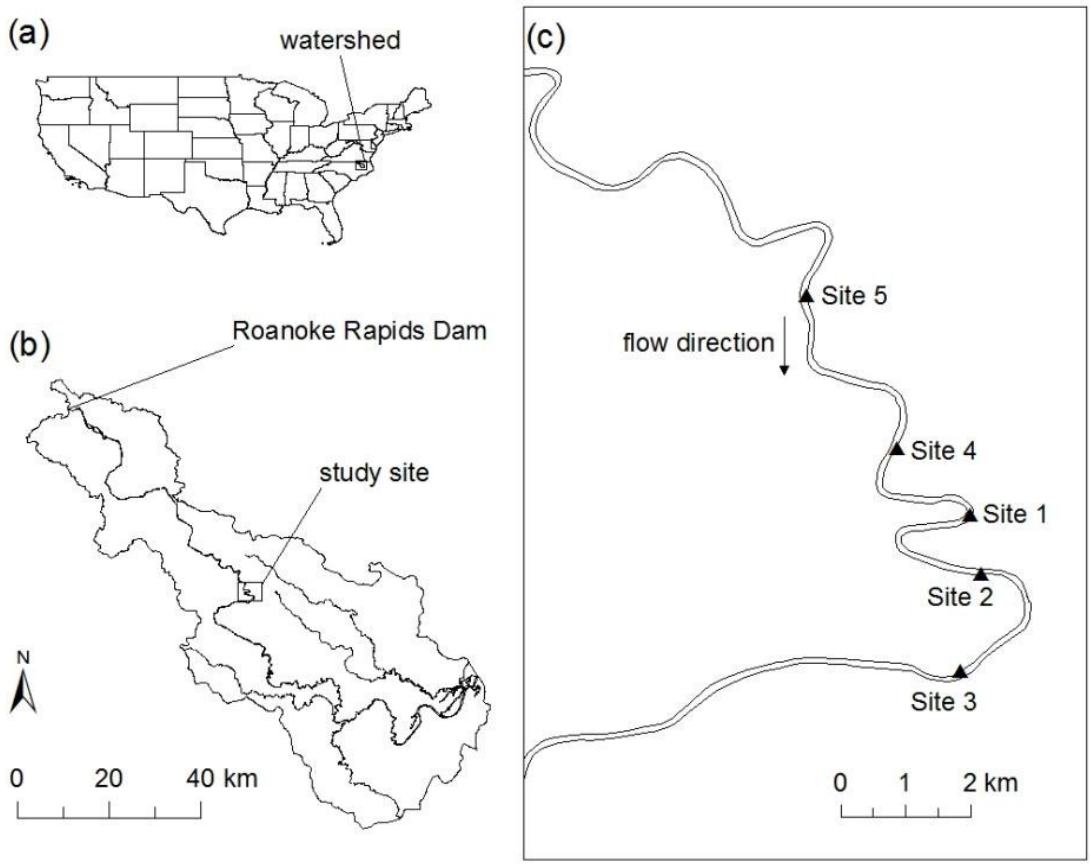

Figure 1 Location of study area. (a) the United States and the location of the lower Roanoke River watershed in N.C., (b) the Roanoke River watershed below the Roanoke Rapids Dam, and (c) the study sites on the lower Roanoke River.

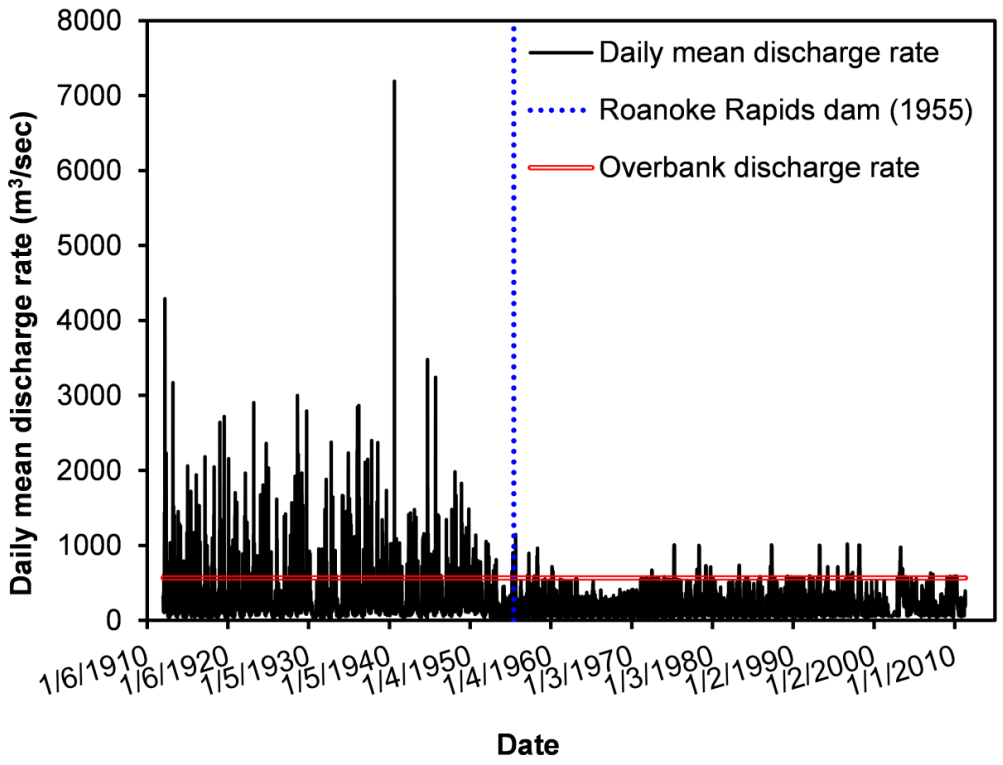

Figure 2 Hydrograph before and after the construction of Roanoke Rapids Dam, NC (modified from Hupp et al. (2009)).

5.2.2 Soil properties

After selecting the study reach and five study sites, disturbed and undisturbed soil samples were collected during the field trips. The soil samples were then analyzed for basic physical properties, hydraulic conductivity, and shear strength for both saturated and unsaturated conditions. The shear stress parameters for the saturated and unsaturated soils were determined by conventional and suction controlled multistage direct shear tests. The hydraulic conductivity was determined after comparing the results from the experimental measurements, transient seepage analysis, and ground water table observation. The soil water characteristic curves (SWCC) were obtained from Tempe cell tests and pressure plate tests to characterize the relationship between suction and water

content. The SWCC from the study sites were reported previously in Nam et al. (2010a). Some additional in situ tests, including the borehole shear test, Guelph permeameter test, and auger hole test, were also performed to provide additional in situ values. Due to the restricted site access and limited availability of samples and testing apparatus, some of the input parameters for modeling were assumed. All values used for the modeling are listed in Table 1, and the assumed values are marked with an asterisk.

Table 1 Soil properties for seepage and riverbank stability modeling.

Site	USCS Soil Type	γ_t (kN/m^3)	ϕ' (°)	c' (kPa)	AEV (kPa)	ϕ^b (°)	VWC (%)	k_{Lab} (m/s)	k_{Auger} (m/s)
S1	SM	16.4	33	5.4	10	13.3	46.1	5.09E-07	1.84E-04
	CL	17.7	28.3	13.3	120	10.2	50.3	1.65E-08*	2.64E-05
	MH	18	32.1	18.4	160	13.5	48.3	4.99E-09	1.35E-05
	CL	18.5	28.1	18.8	200	9	47.8	1.26E-09	2.58E-05
S2	CL	18.2	29.5	7.5	120*	10.2*	48.5	1.65E-08*	2.64E-05*
	CL	19.1	34.1	12.8	180*	11.3*	47.7	3.13E-09*	1.97E-05*
S3	ML	17.6	28.8	6.3	120*	10.2*	52.5	1.65E-08	2.13E-05
	CL	18.7	33.7	8.7	180*	11.3*	49.7	8.30E-09	1.97 E-05*
S4	ML	17.9	28.2	9.5	120*	10.2*	49.5	1.72E-08	2.13E-05*
	CL	18.3	34.5	8.9	180*	11.3*	48.1	3.13E-09*	1.97E-05*
S5	ML	17.4	32.9	8.2	120*	10.2*	48.5	5.90E-09	3.15E-05
	CL	17.9	31.6	10	180*	11.3*	47.3	5.13E-09	1.97E-05*
S1-S5	Impervious layer	22	37	200	0	0	26	1.26E-10*	1.26E-07*

**assumed based on the values from other sites.*

Surface soil in the area is primarily Quaternary alluvium deposits up to 7.6 m depth, with Upper Cretaceous sedimentary materials underlying the alluvium soil layer (Weems et al., 2009). A loose layer of silty sand exists at the top of the riverbank, and a firm and thick cohesive soil layer underlies it. The underlying layer is classified as CL, ML or MH by the Unified Soil Classification System (USCS). The average values of the test results and bank geometries used for the transient seepage analysis and slope stability analysis are provided in Table 1 and Figure 3.

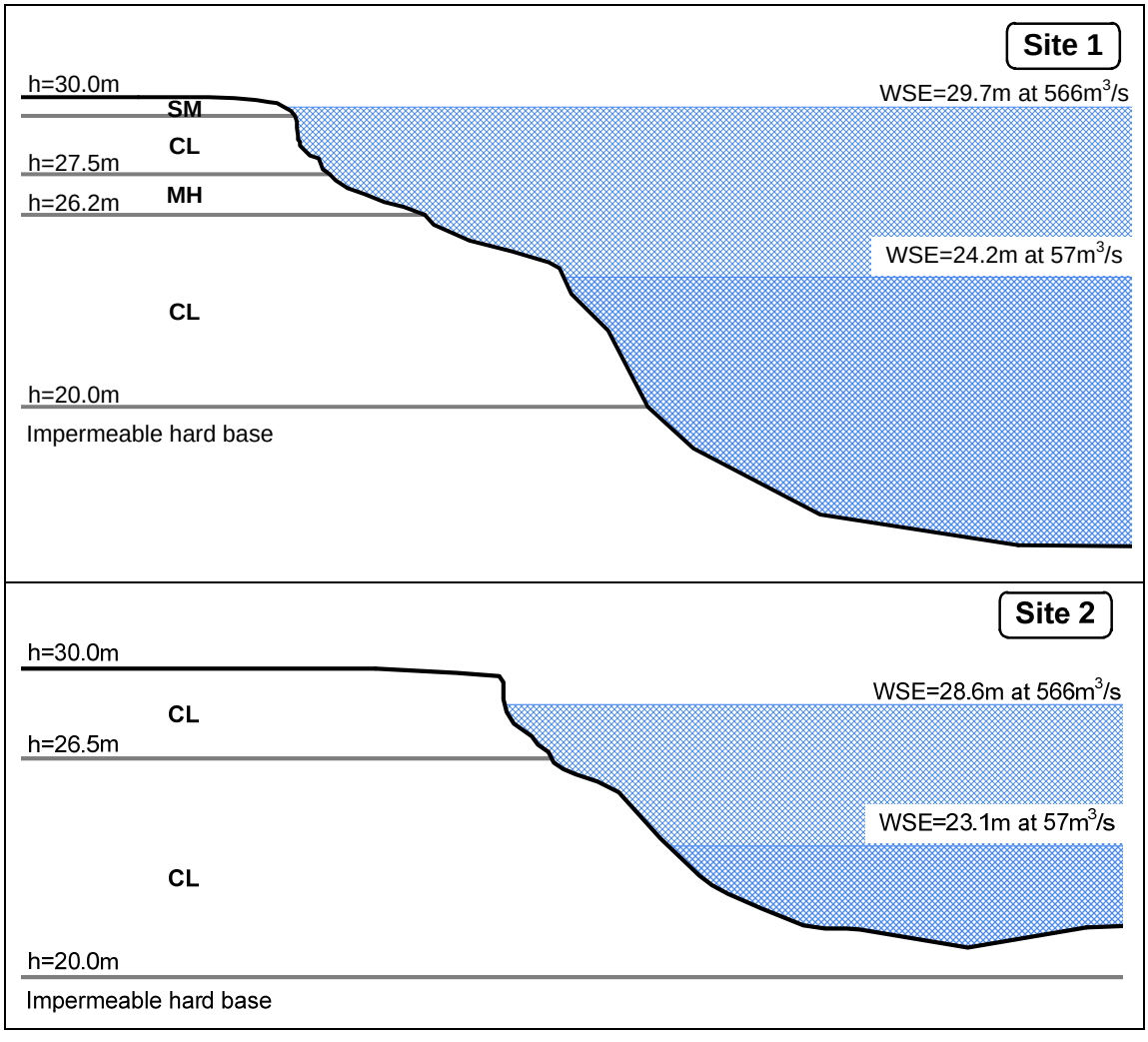

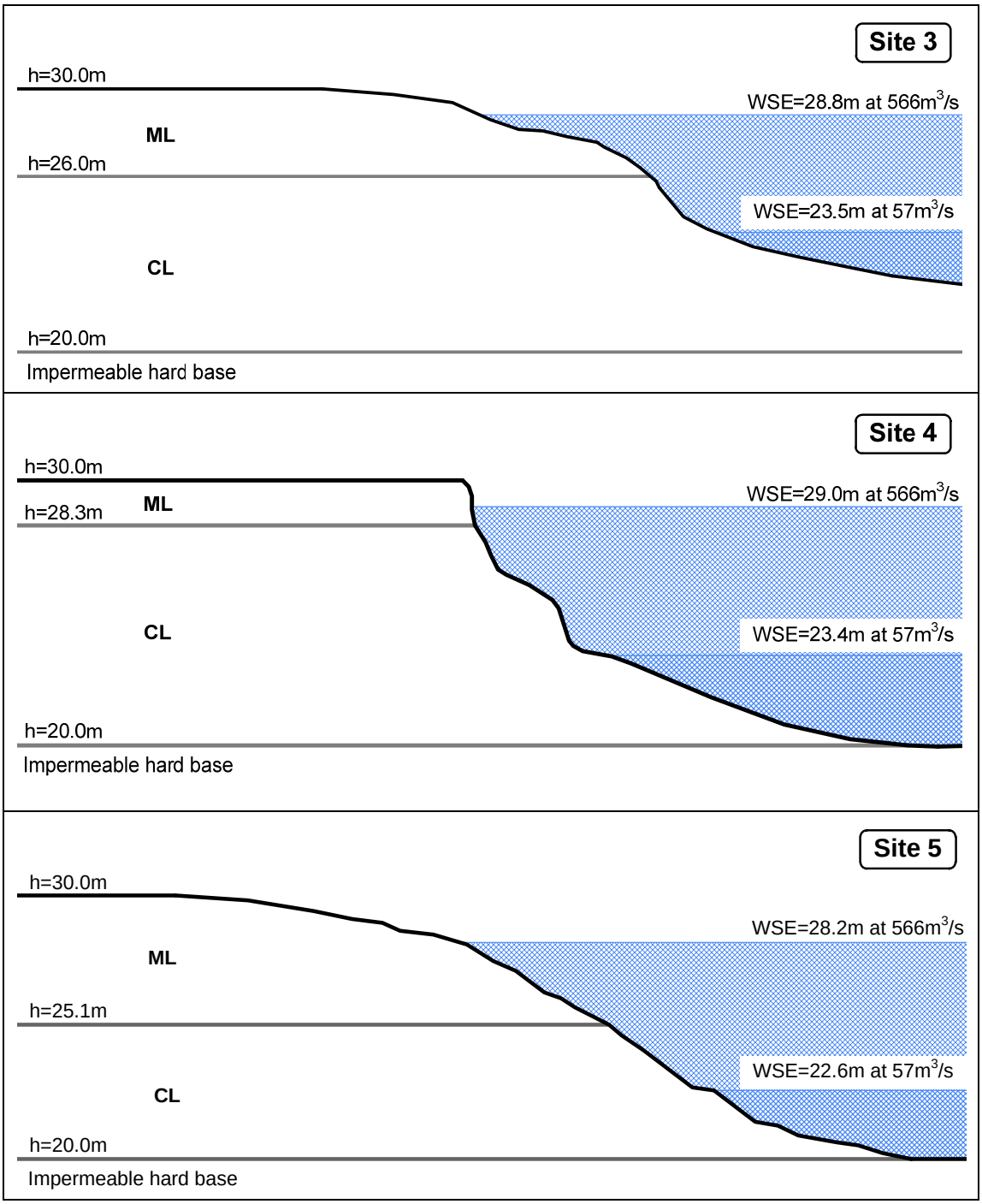

Figure 3 Riverbank cross section and profile with WSE location.

5.2.3 Reservoir release patterns

The Roanoke Rapids Dam has four operational modes: normal, fish spawning, drought control and flood control modes (see Table 2). During normal operation, which occurs throughout the year except during the fish spawning season, the reservoir release rate can vary from 57 to 566 m^3/s and is limited only by the hydraulic capacity of the power station (Dominion, 2010). Thus, the discharge is expected to be dependent on the seasonal inflow rate to the dam, although more periodic and frequent peaking is expected in order to generate power. During spawning season, between March 1 and June 15, the downstream WSE is managed to maintain a relatively uniform flow with only small variations allowed in order to minimize WSE fluctuations. If drought or flood conditions are declared, the flow release is governed by the discharge from the John H. Kerr Dam, which is located further upstream and is controlled by the U.S. Army Corps of Engineers. During drought operations, the flow tends to remain at 57 m^3/s and peaking events are reduced, resulting in a low steady downstream WSE. Flood control does not limit the minimum flow but can release up to 991 m^3/s or more depending on the inflow to the reservoir. Figure 4 depicts an example of the actual release rate at the dam and resulting downstream WSE near Scotland Neck, North Carolina as monitored by the USGS between October 2005 and November 2009. As the figure shows, although the dam has four distinct operational modes for regulating the release rate, the actual release rate and downstream WSE are not easily categorized in terms of these modes. Thus, for this study several representative release rates and flow events were selected based on historical data.

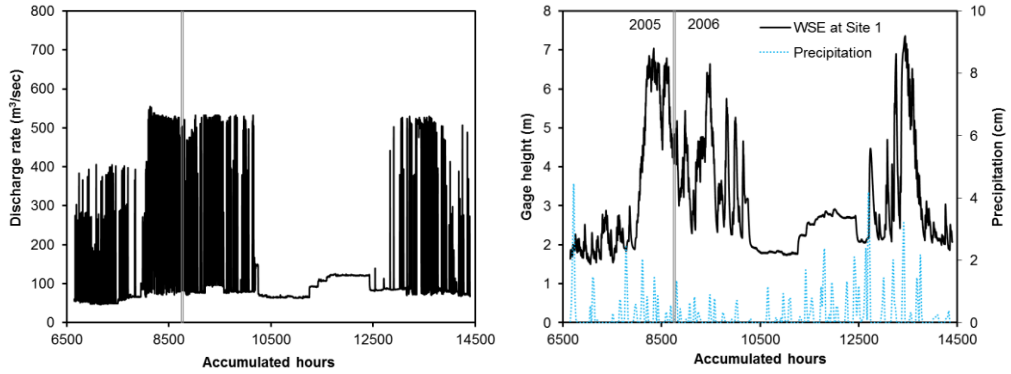

(a) Oct. 2005 - Aug.2006

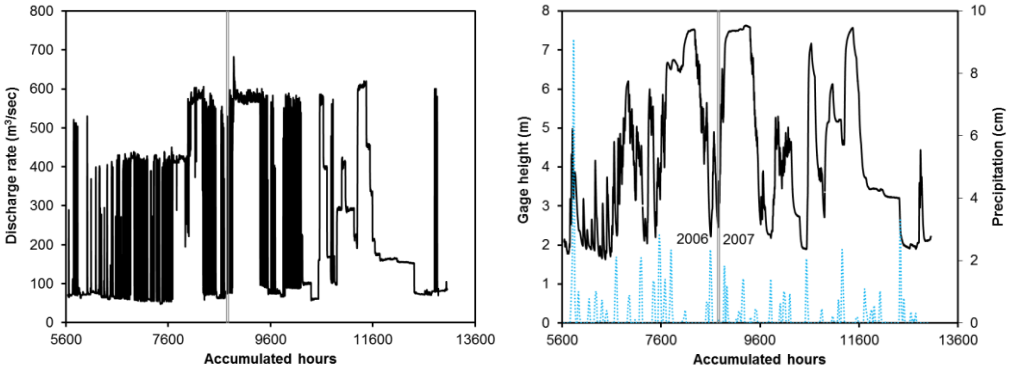

(b) Aug. 2006 - Jun.2007

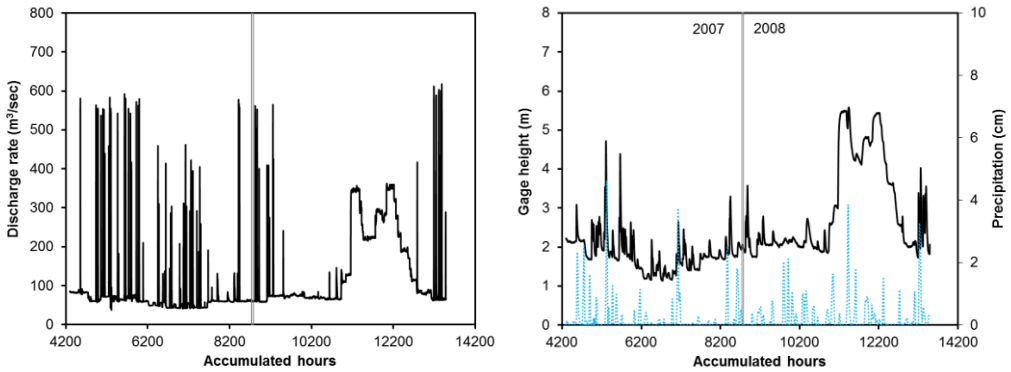

(c) Jul. 2007-Jul. 2008

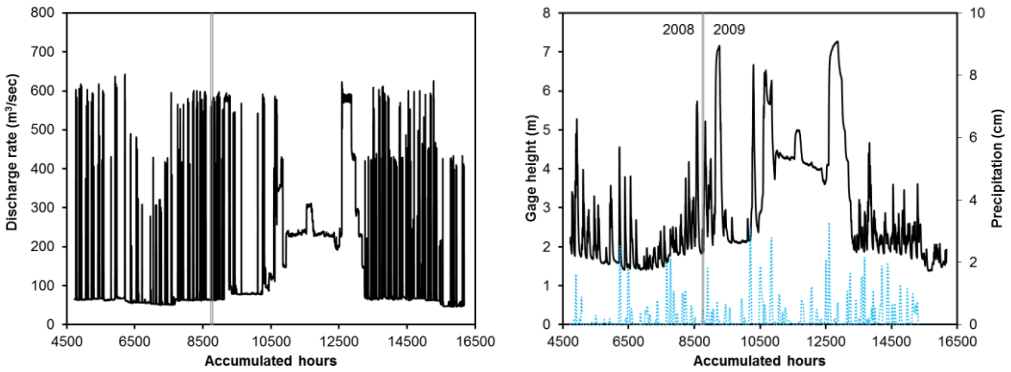

(d) Jul. 2008-Nov. 2009

Figure 4 Roanoke Rapids hydropower dam discharge rates between 2005-2009.

5.3 Seepage and slope stability analyses

5.3.1 Transient seepage analysis

Transient seepage analysis is utilized in this study to analyze the impact of fluctuating WSE on riverbank stability. When a riverbank is exposed to rapid changes in the WSE, the pore water pressure inside the riverbank becomes an important factor determining slope stability. Excess pore water pressure develops and dissipates over time, which directly affects the effective shear stress of the soil and, thus, the riverbank stability. Depending on the soil properties and bank geometry, the influence of excess pore water pressure may become critical for slope stability. Thus, transient seepage analysis is applied to estimate how the excess pore water pressure changes with time.

Transient seepage analysis is typically performed using numerical methods based on Darcy's Law. Darcy's Law was originally derived for the flow of water through saturated soil, but it can be extended to include flows in unsaturated soil. The governing equation for two dimensional transient flow through unsaturated soils is as follows:

$$\frac{\partial}{\partial x}\left(k_x \frac{\partial h}{\partial x}\right)+\frac{\partial}{\partial y}\left(k_y \frac{\partial h}{\partial y}\right)+Q=\frac{\partial \theta_w}{\partial t} \qquad (1)$$

where, h = total hydraulic head, k_x and k_y = hydraulic conductivity in the x and y directions, respectively, Q = external boundary flux, and θ_w = volumetric water content.

The major difference between the flow of water in saturated and unsaturated soils is that the hydraulic conductivity varies with the degree of saturation in unsaturated soils, whereas for saturated flow hydraulic conductivity remains constant.

5.3.2 Slope stability analysis

The limit equilibrium method (LEM) is a classical approach that is used to evaluate the stability of a slope, and was developed before the application of computers. Although more advanced techniques using numerical methods have since been developed for slope stability analysis using more powerful computational resources, LEM remains by far the most widely used slope stability analysis method due to its simplicity and ease of use.

LEM presents the stability of a slope in terms of the factor of safety (FS). Duncan and Wright (2005) defined FS as the ratio of the available shear strength of soil to the shear stress required to maintain a just-stable slope, expressed as follows:

$$FS = \frac{s}{\tau} \tag{2}$$

where s = available shear strength and τ = equilibrium shear stress

Leshchinsky (1990) described the calculation of the FS of a slope in terms of a two-step process: (1) assuming a potential slip surface and (2) assembling and solving the limit equilibrium equations for the soil mass defined by the surface. Both processes have benefitted by the application of numerical methods. A large number of potential slip surfaces, including non-circular types, can be examined, and various methods applying different assumptions when defining equilibrium can be utilized. As a result, LEM provides more accurate results and has been used more frequently than advanced numerical methods.

Once the basic concepts of unsaturated soil mechanics were proposed, slope stability analyses could be performed using the shear strength of unsaturated soils. This is logical, as most man-made and natural slopes are not fully saturated. Additional factors

such as precipitation, evaporation, or changes in boundary conditions alter the degree of saturation in soils so that the unsaturated shear strength must be taken into account when performing a slope stability analysis for more realistic modeling. Thus, the concept of matric suction, which is not considered in classical slope stability analysis, is now being incorporated into slope stability analyses. Matric suction can be related to the degree of saturation or volumetric water content using the SWCC. The shear strength of an unsaturated soil can be described by the modified Mohr-Coulomb failure criterion as follows (Fredlund et al., 1978):

$$\tau = c' + (\sigma_n - u_a)\tan\phi' + (u_a - u_w)\tan\phi^b \quad (3)$$

where τ=shear strength of unsaturated soil, c'=effective cohesion, ϕ'=effective friction angle, σ_n=normal stress, u_a=pore air pressure, u_w=pore water pressure, ϕ^b=angle of shearing resistance with respect to matric suction.

The calculations for transient seepage analysis and slope stability analysis using LEM have improved with advances in computational resources and recent studies have shown how these analyses can successfully be applied to solve a variety of problems (e.g. Dapporto et al., 2001, Fredlund et al., 2011, Huang and Jia, 2009, Ng and Shi, 1998, Pauls et al., 1999).

5.3.3 Coupling with fluvial erosions

One of the unique characteristics of riverbank stability is that fluvial erosion may also affect the bank stability, altering the bank geometry by creating steeper slopes. This often occurs through erosion of the bank toe, which may trigger mass failure. However,

fluvial erosion is a very complex phenomenon that involves both geotechnical and hydraulic characteristics and thus is difficult to estimate.

A common approach to estimating the erosion rate of fine grained cohesive soils is to apply the linear excess shear stress equation as follows (Hanson and Cook, 1997, Partheniades, 1965):

$$\varepsilon = k_d\left(\tau_e - \tau_c\right) \tag{4}$$

where ε = erosion rate, k_d = erodibility coefficient, τ_e = effective shear stress applied by the flow, and τ_c = critical shear stress of the soil.

Although the threshold concept in Eq. (4) may not represent the actual physical phenomenon, the equation has been used to predict the erosion rate of cohesive soils, often in conjunction with the results of submerged jet tests (Clark and Wynn, 2007, Hanson and Cook, 2004). However, it is not straightforward to estimate all the parameters in the excess shear stress equation. Although the effective shear stress in the equation may be simplified, for example by assuming that shear stress increases linearly with depth, the actual effective shear stress by the flow is much more complex for three dimensional flows. The critical shear stress and erodibility coefficient are also difficult to estimate due to the spatial and temporal variability of natural soils and the complex interparticle forces in cohesive soils (Nam et al., 2010b, Wynn et al., 2008).

Schenk et al. (2010) installed and monitored a series of pins to estimate the erosion rate in the lower Roanoke River between 2005 and 2009. The study sites presented here coincided with the locations of the erosion pins, except for Site 4. At each site, 6 to 8 erosion pins were installed normal to the local bank slope, in positions ranging from near the WSE for drought conditions to near the bank crest (Figure 7). Each erosion

pin is approximately 1 m in length and 1 cm in diameter. If erosion occurs, the exposed portion is measured and then the pins are pushed back to the slope surface. Pins buried due to deposition are located using a metal detector and their depth beneath the new surface is measured. Further details of the techniques involved in measuring erosion pin data are provided in Schenk et al. (2010). Using the erosion pin data collected in the summers of 2006, 2007, 2008, and 2009, the annual average erosion rates were calculated. Although the actual erosion rates and profiles were different each year, these were averaged in order to predict erosion at the five study sites for the next 10 years.

Although fluvial erosion can be challenging for numerical modeling of slope stability, in practice it is possible to neglect erosion for short times periods due to the fact that in terms of hours or days erosion is too small to induce changes in the pore water pressure distribution and bank geometry sufficient to affect the calculation of slope stability. Thus, riverbank stability with fluvial erosion was considered as a separate modeling case for different bank geometries, assuming that the monitored annual mean erosion rate is maintained for the next 10 years and creates noticeable changes in the bank geometry.

5.4 Numerical modeling

Seven steady state discharges and three transient operations were considered as representative flow scenarios for the modeling. Riverbank stability with changing water surface elevation (WSE) was analyzed using the Slide software package developed by Rocscience (Rocscience Inc., 2010a). This is capable of both transient seepage analysis using the finite element method and slope stability analysis using the limit equilibrium

method, with the factor of safety calculated by the Morgenstern-Price methods with half sign interslice force function (Morgenstern and Price, 1965).

For numerical modeling, it is important for the boundary conditions to be carefully defined in addition to the soil properties. The far field boundary was assumed to be the constant head boundary condition, and the initial location of the ground water table at the boundary was assumed to be located 1.3 m below the surface, which is the annual average location of the ground water table (GWT) as shown in Figure 5. Solid dots in Figure 5 present the depths of GWT below surface between October 1994 and June 2010 at Roxobel, NC, monitored by USGS. Each box-and-whisker plot also shows the upper extreme, upper quartile, median, lower quartile, and lower extreme values for that month. The USGS station (USGS 361420077111407 BE-080) is about 12 km away from the lower Roanoke River and 14 km away from Site 1, and thus is assumed to adequately represent the initial location of GWT for the modeling.

The boundary condition of the riverbank surface was defined in terms of the given total head with time function simulating the fluctuation of the WSE. The local WSE at each study site was determined by correlating the USGS gaging station data with the estimated WSE using steady state HEC-RAS simulation and the WSE measured by differential pressure sensors at Site 1, 2, 4 and 5. The real-time surface water data at the USGS gaging stations is available from the USGS website (U.S. Geological Survey, 2010). The discharge from the dam was measured at the USGS gaging station near Roanoke Rapids, NC (USGS 02080500) and the relative WSE data for areas near Scotland Neck, NC (USGS 02081000) and Oak City, NC (USGS 02081028) are also available.

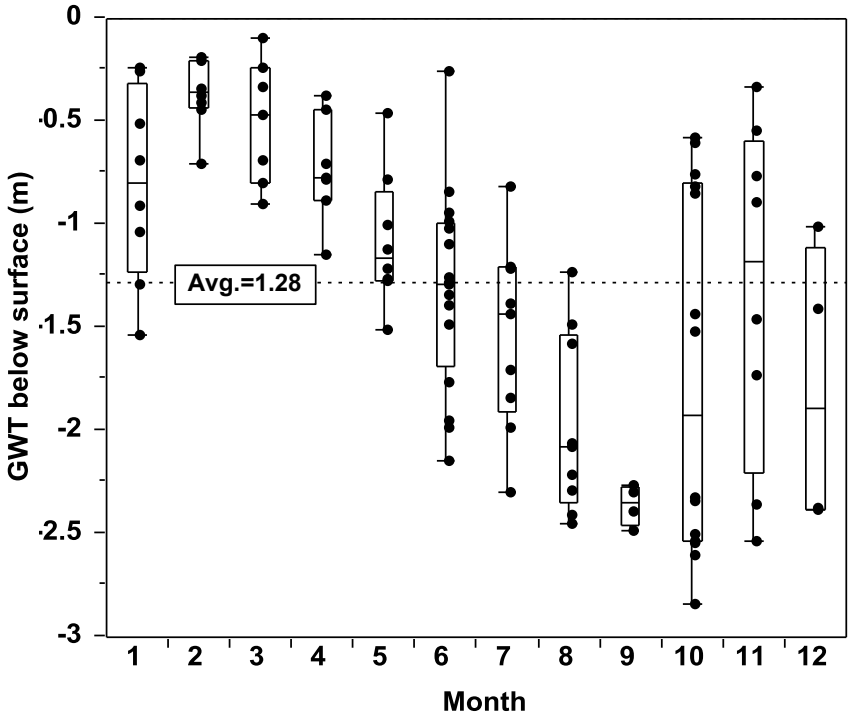

Figure 5 Average and monthly locations of ground water table between Oct. 1994 and Jun. 2010 at Roxobel, NC, monitored by USGS (USGS Sta. 361420077111407 BE-080).

5.4.1 Steady state condition

The steady state condition assumes that the downstream WSE remains stable even after peaking occurs at the dam. Thus, steady state conditions represent seasonal variations in the riverbank stability rather than a single event. Based on the regulations for each operational mode, summarized in Table 2, seven different flow rates representing the full range of fish spawning, flood control, draught control, and normal operational modes, along with an overbank flow representing an extreme flood control scenario, were considered for the steady state slope stability analysis and are listed in Table 3.

Table 2 Dam operational modes and the range of flow rates (modified from Dominion, 2010).

Operation Mode	Drought Control		Fish Spawning		Normal		Flood Control	
	From	To	From	To	From	To	From	To
Discharge rate (m^3/s)	57*	N/A	99	388	57	566	566	991**

*42 m^3/s between September and November
** Greater of 100% of inflow to the dam or 991 m^3/s

Table 3 Representative flow rates for modeling and expected corresponding water surface elevation at Site 1.

Discharge rate (m^3/s)	Discharge rate (ft^3/s)	Relative WSE at Site 1 (m) (Bank top = 0.00m)	Representing operational mode
57	2,000	-5.80	Normal, drought
142	5,000	-4.35	Normal, spawning
227	8,000	-3.16	Normal, spawning
311	11,000	-2.29	Normal
425	15,000	-1.36	Normal
566	20,000	-0.30	Normal, flood
991	35,000	+1.10	Flood

5.4.2 Transient condition – peaking

Peaking discharge is a common release pattern for hydropower dams that generate electricity to satisfy periods of high power demand. These peaks in demand typically

occur during the hottest and coldest days in the year and on a daily basis in the morning and late afternoon (Bob Graham, personal communication, July 7, 2008). During the monitored period between 2005 and 2009, the prolonged peaking event shown in Figure 6(a) was selected as an example of a regular peaking discharge pattern. This event occurred between February 13 and 28, 2007. Prior to the peaking period, the discharge rate was maintained at around 70 m^3/s for 7 days (Feb. 6-12, 2007). Then, repetitive peaks ranging from 57 m^3/s to 566 m^3/s were observed over the next 16 days. The discharge rate generally reached 566 m^3/s and dropped instantly, resulting in a typical peaking cycle of about 6 hours. However, the discharge often remained at the highest rate for several hours, extending the cycle to up to 12 hours. On a daily basis, the monitored peaking events typically occurred twice a day, once starting in the morning around 6 AM and again in the early evening around 6 PM.

5.4.3 Transient condition – drawdown

In general, drawdown of the external water surface level in a slope may lead to one of the most critical conditions affecting slope stability. Especially in a slope with cohesive soils, poor drainage causes slow changes in the pore water pressures in the slope. When the WSE drops, the external force that works as a stabilizing factor is lost while excess pore pressures in the riverbank are slow to dissipate, leaving the slope in a critical condition. Thus, estimating changes in the pore water pressures during transient flow releases is essential for checking the critical conditions of riverbank stability. The drawdown rate selected from the historical records between January 19 and 27, 2009 presented in Figure 6(b) represents the fastest drawdown rate that occurred between 2005 and 2009.

5.4.4 Transient condition – step-down

The step-down release is a kind of drawdown pattern that includes buffer periods to minimize the environmental impacts induced by drastic changes of flow rate. In general, after a prolonged high flow, drawdown is performed with several buffer stages, as shown in Figure 6(c), instead of reducing the discharge to base flow instantly. The step-down rates and stages are predetermined and take into account the anticipated inflow and outflow of the dam, and the ecological and environmental impacts. The step-down scenario presented in this study occurred between June 20 and July 9, 2009. Prior to the step-down event, the release rate was around 580 m^3/s and the downstream WSE had maintained a bankfull condition for 12 consecutive days, providing the initial steady state condition. The release rate was then dropped to 85 m^3/s via 4 buffer stages. At each stage, the release rate was maintained for about 4 days on average as a buffer period. The buffer period was longer at the higher rate (4.7 days at 430 m^3/s) and shorter at the lower rate (2.8 days at 147m^3/s).

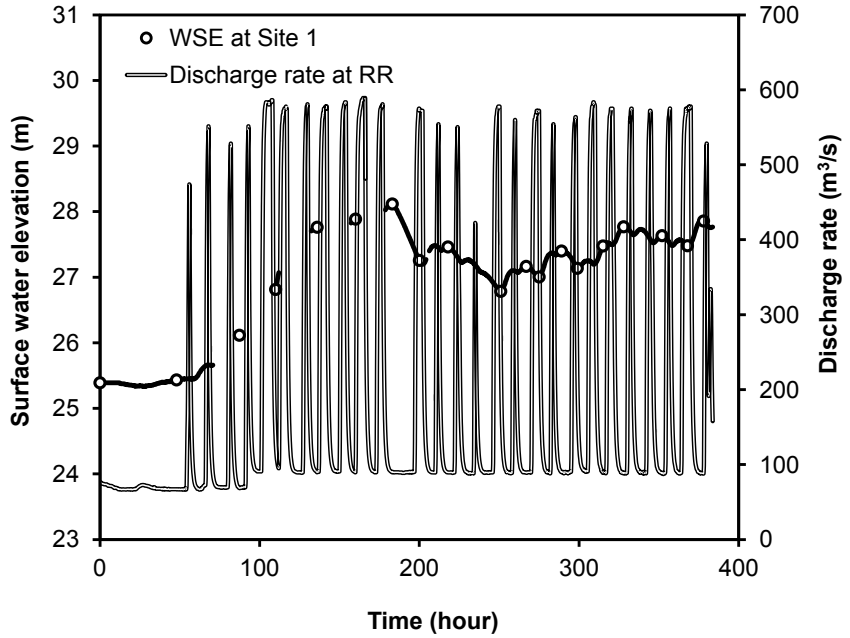

(a) Peaking (February 2007)

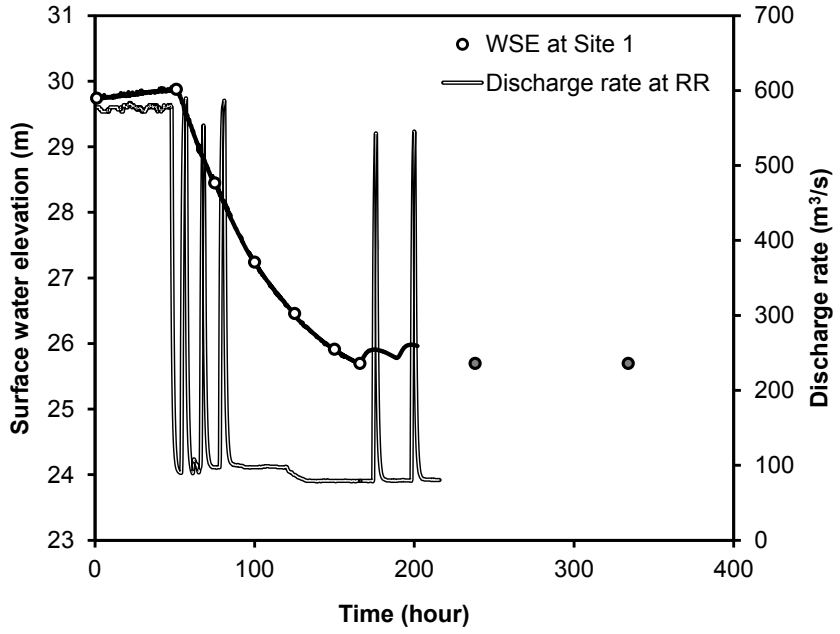

(b) Drawdown (January 2009)

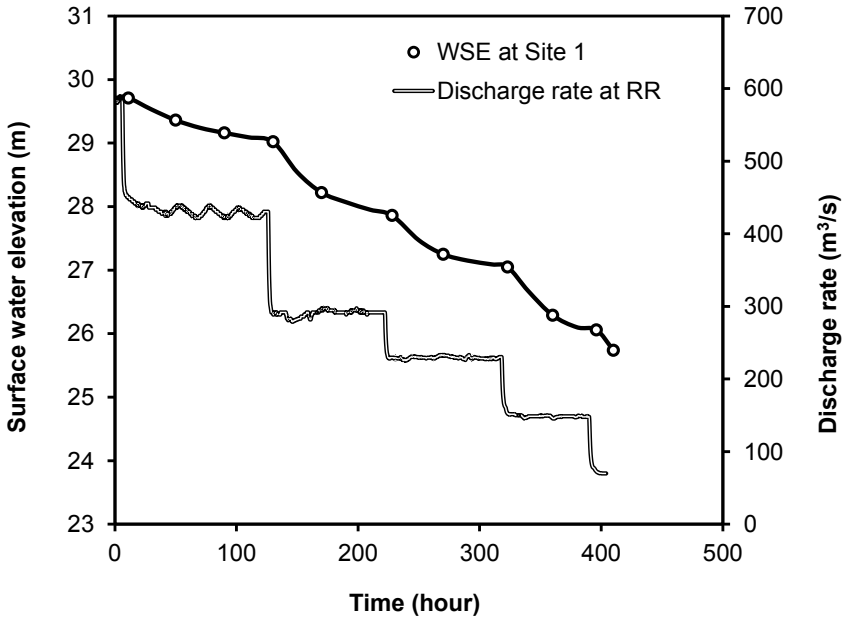

(c) Step-down (June-July 2009)

Figure 6 Actual discharge patterns and corresponding changes of WSE at Site 1.

5.4.5 Fluvial erosion

Fluvial erosion was estimated by interpreting the USGS erosion pin data. The average annual erosion rate was calculated from the data for the 4 years from 2005 to 2009 gathered by (Schenk et al., 2010). As presented in Table 4, the maximum erosion was measured at the lowest part of the riverbanks, while the minimum erosion, or deposition in a few locations, occurred in the middle or upper part of the banks. Using the current bank geometry and the average annual erosion rate, the eroded bank geometry after 10 years was predicted as shown in Figure 7. The slope stability of the riverbank with the new geometry was analyzed for two steady state, one peaking and one step-down conditions, for a total of four scenarios.

Table 4 Erosion rate calculated from USGS erosion pin data.

Site	Bank Location	Maximum erosion		Minimum erosion	
		Rate (cm/year)	Location	Rate (cm/year)	Location
Site 1	Outside	-23.0	Pin 1	-3.0	Pin 6
Site 2	Straight	-5.4	Pin 2	+3.5	Pin 3
Site 3	Inside	-5.9	Pin 2	-0.2	Pin 4
Site 5	Straight	-8.1	Pin 1	-0.05	Pin 6

No erosion pins near Site 4
+: deposition, -: erosion

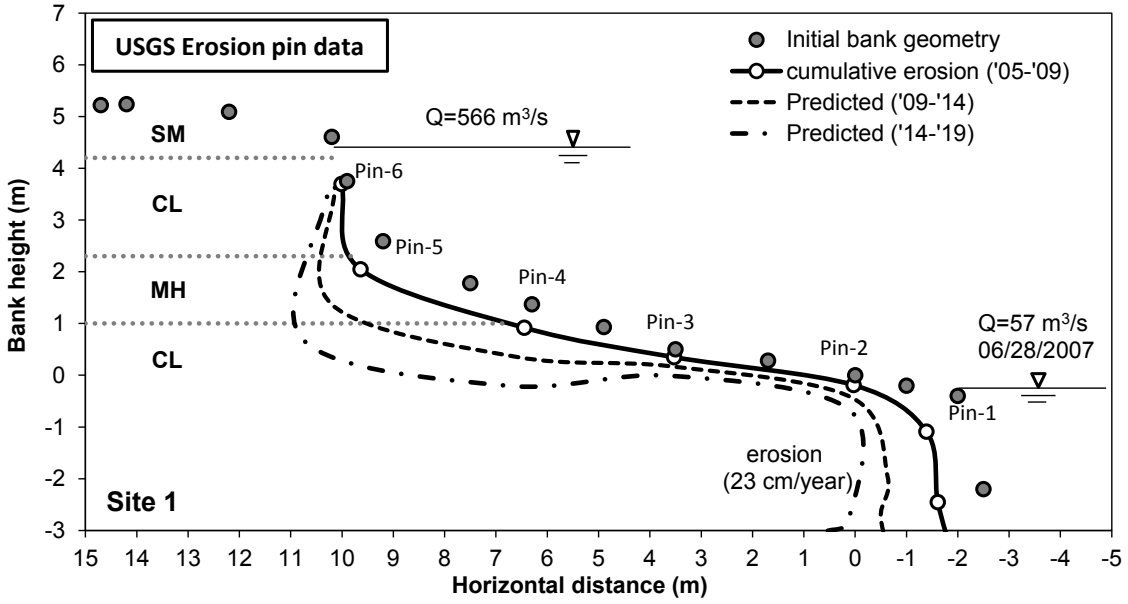

(a) Site 1

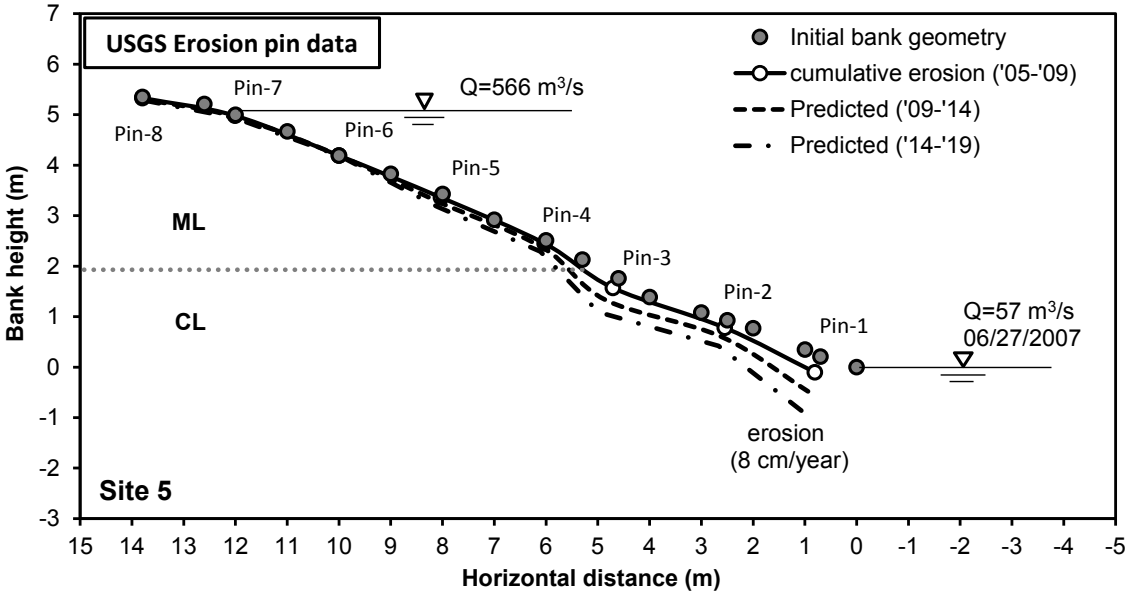

(b) Site 5

Figure 7 Cumulative and predicted erosion and bank profile at Site 1 and Site 5.

5.5 Results and discussion

Transient seepage analysis was applied to calculate the pore water pressures in the riverbanks. The stability of the riverbanks was then analyzed using the pore water pressures for different flow scenarios that represent the field conditions under the different dam operations. As the stability depends directly on the hydraulic conductivity of the soils, the riverbanks were also reviewed for critical cases that used the lowest values determined by either constant head permeability tests or consolidation tests.

5.5.1 Steady state

Riverbank stability at all five sites was analyzed for the steady state flow conditions listed in Table 3, representing typical operational modes in different seasons including one overbank flow condition. Examples of the slip surface at Site 1 and Site 4 are presented in Figure 8, indicating different depths of failures. Figure 9 illustrates the relationship between discharge rates and riverbank stability under steady state flow conditions. All slopes were found to be stable, and generally became more stable as the water surface elevation (WSE) rose. The WSE was confirmed to be the dominant factor governing riverbank stability under steady state conditions. A few cases showed slightly larger values of the factor of safety at the lowest WSE (Site 1, Site 2 and Site 4), which seems to be due to the effect of negative values of effective normal stress on the slices. The factor of safety estimated by both saturated and unsaturated shear strengths are compared in Figure 10, indicating that the actual riverbank stability in the field would be safer than the numerical model due to the unsaturated soil conditions. The influence of unsaturated soil shear strength appeared to be larger for a steeper slope (Site 4) than for a gentle slope (Site 1).

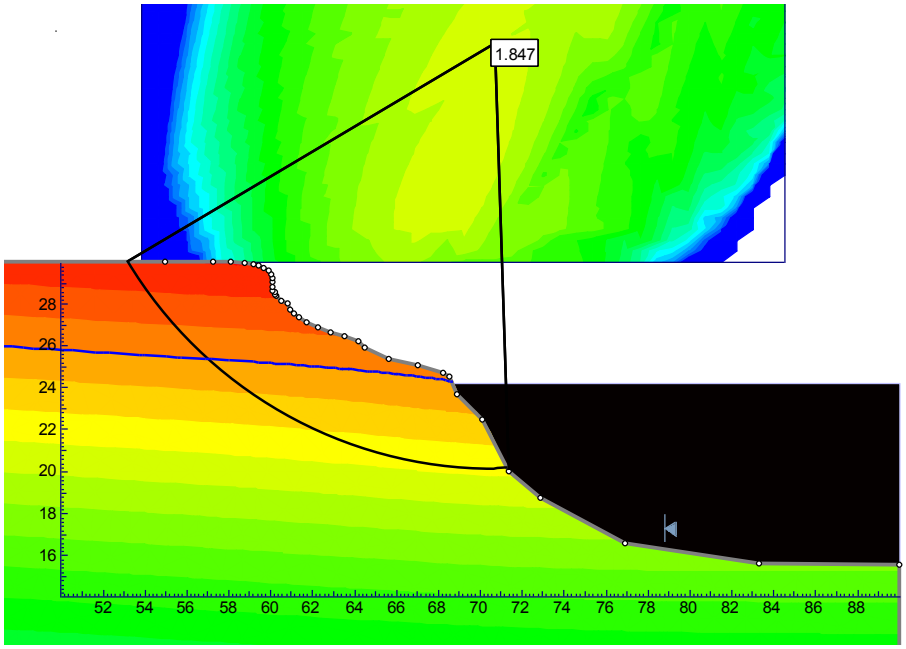

(a) Site 1

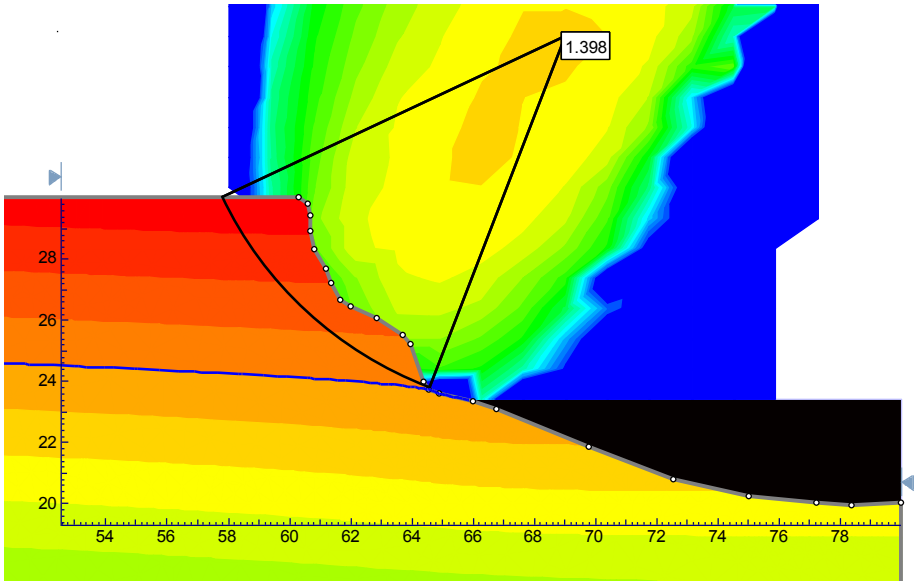

(b) Site 4

Figure 8 Results of slope stability analysis under 57 m^3/s steady state flow.

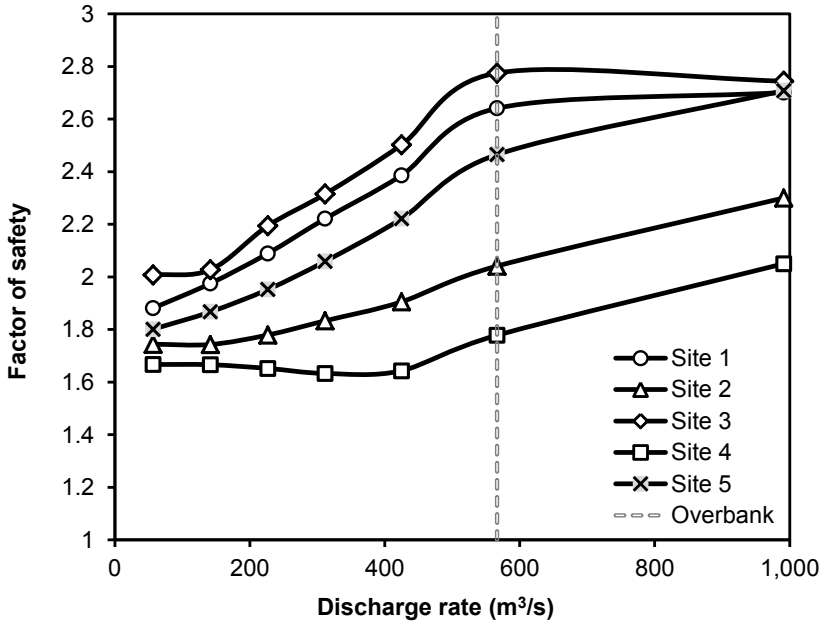

Figure 9 The relationship between discharge rate and factor of safety.

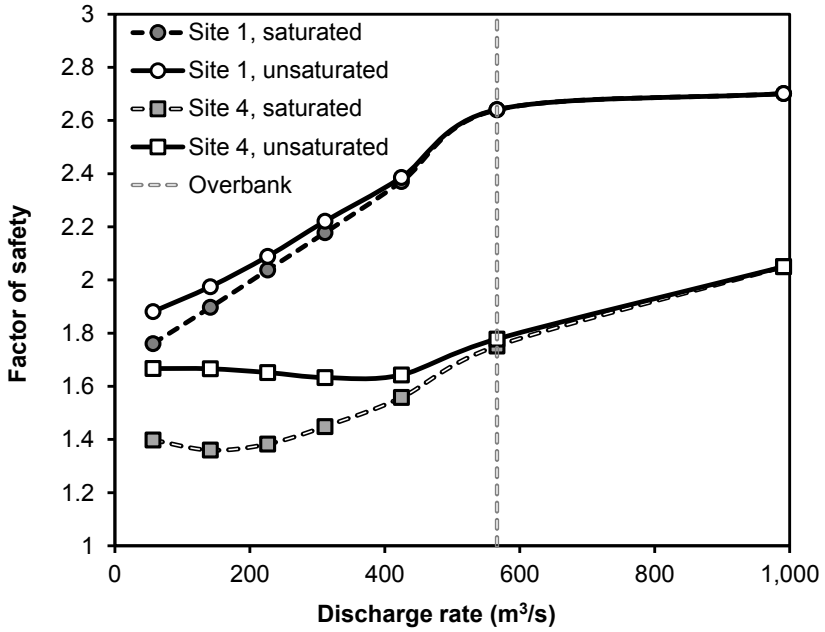

Figure 10 Comparison of saturated and unsatruated soil conditions under steady state flows.

5.5.2 Peaking

The riverbank at Site 1 was found to be stable during the peaking events, as shown in Figure 11(a). The values of the factor of safety varied, responding directly to changes in the WSE, and this variation was larger when lower hydraulic conductivity was taken into account. The FS was lower when hydraulic conductivity of the soil was larger, indicating more water seeped into the soils as the WSE rose and the area where matric suction has been eliminated became larger, thus decreasing the shear strength of the soil. However, if peaking started when the initial steady state condition was assumed to be higher, as presented in Figure 11(b), the FS dropped more rapidly in the model with lower hydraulic conductivity (k_{LAB}). This can be attributed to the fact that pore water pressure dissipation in poorly drained soils takes longer. As the rate and magnitude of the WSE changes during peaking events are smaller than those in a drawdown event, it is reasonable to assume that the peaking is less critical than drawdown in terms of slope stability. This transient drawdown is effectively a mild case of rapid drawdown, which will be discussed next, but it is not expected to create an instantaneous rise of downstream WSE.

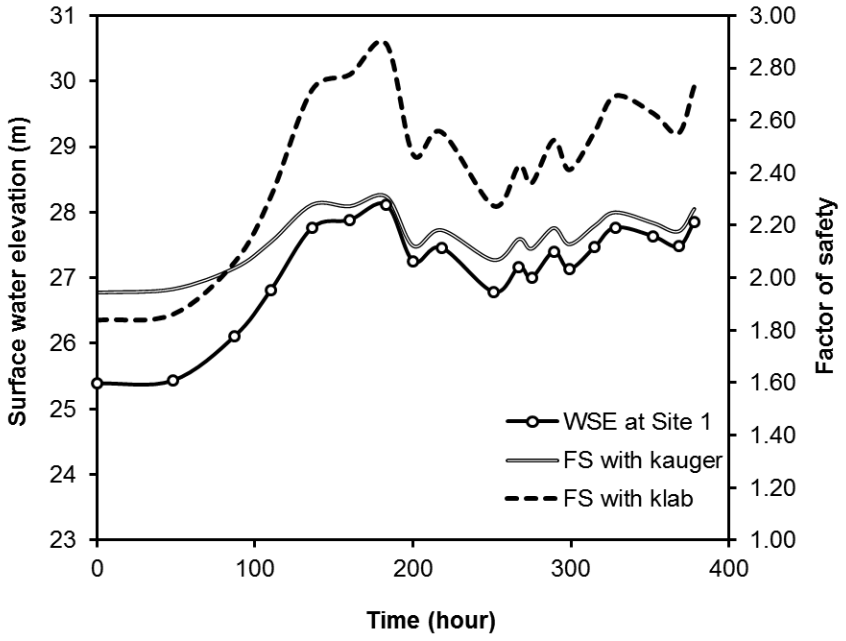

(a) Actual data with initially low phreatic surface

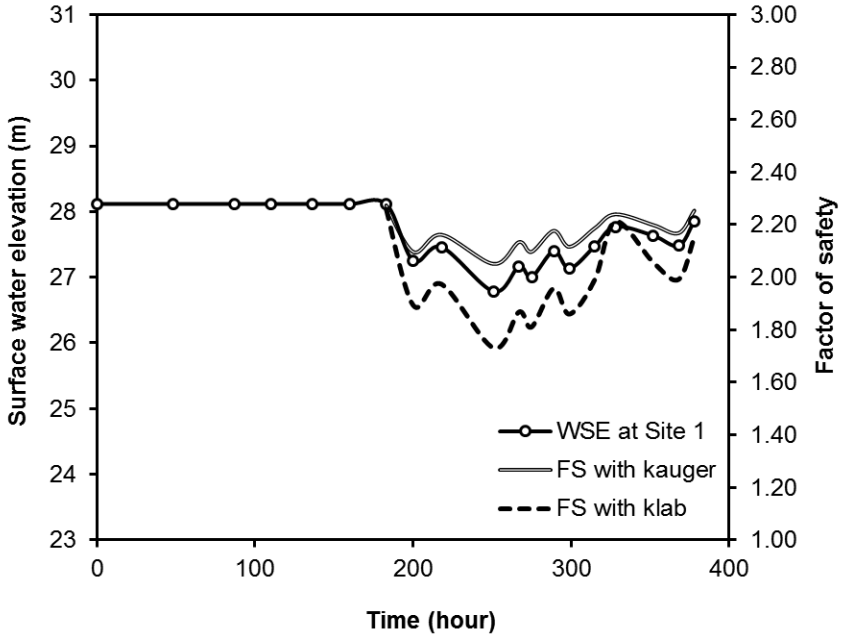

(a) Assumed initially high phreatic surface until 189 hours

Figure 11 Changes of the factor of safety during continuous peaking events in February, 2007.

5.5.3 Drawdown

For the drawdown event studied here, which occurred in January 2009, the riverbanks at all five study sites experienced a reduction in their factor of safety, as shown in Figure 12. However, the values remained above 1.0 for all sites, indicating stable conditions. This finding seems to be due to the relatively high hydraulic conductivity values of the soil used for the model, which allow the pore pressure to dissipate. The lower hydraulic conductivities suggested by laboratory tests indicate a much higher sensitivity to WSE changes, but the FS could not be quantified due to several numerical issues. These will be discussed later in more detail.

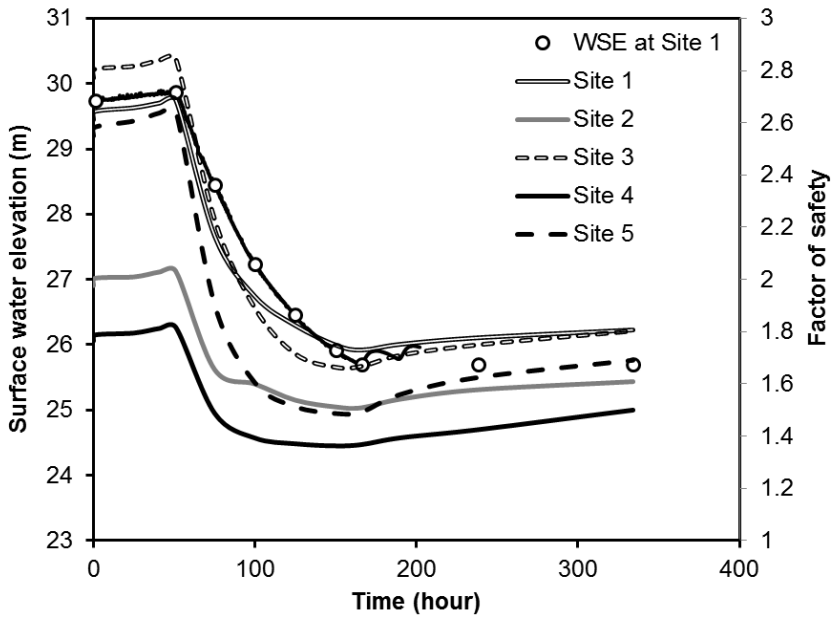

Figure 12 Changes in factor of safety over time during a transient drawdown event.

5.5.4 Step-down

Similar to the results of the drawdown analysis, the step-down scenario (Figure 13) resulted in a decreasing factor of safety as the WSE decreased. However, while the factor of safety did decrease during step-down releases, the banks were found to remain stable. The amount of time at each discharge rate seems to have been sufficient to allow the pore water pressure to dissipate. Larger values of the hydraulic conductivity measured by in situ auger hole tests appear to be responsible for the nearly instantaneous changes in factor of safety. Excess pore pressure dissipates faster in easily drainable soils, and thus the factor of safety is directly related to the magnitude of confining pressure by the river. Additionally, the drawdown rate of the WSE during the step-down scenario was lower than that of the drawdown case, resulting in a more stable riverbank. Therefore, the riverbank appears to be relatively insensitive to step-down rate when considering large-scale instability.

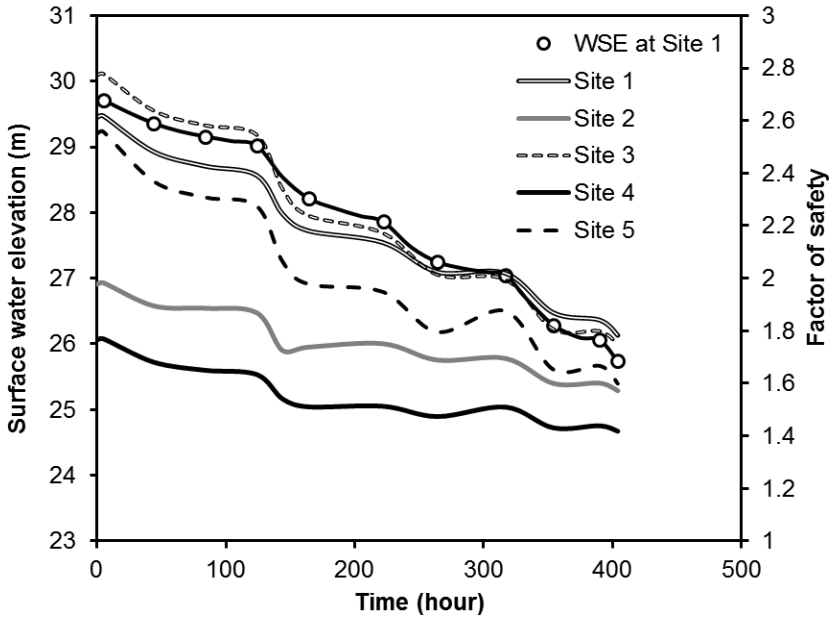

Figure 13 Factor of safety at each site for step-down flow conditions.

5.5.5 Bank stability with fluvial erosion

Erosion rates were determined for all study sites except Site 4, where no erosion pin data was available. The highest annual average erosion rate was 230 mm/year, monitored at the lowest pin at Site 1. However, this seems to be largely due to mass failures, as 750 mm out of the 920 mm erosion at the pin was measured between 2006 and 2008 by Schenk et al (2010). The average of the highest erosion rates at the other sites were 64 mm/year, which were mostly observed at the lowest pins as well. Some deposits were also measured at upper pins in Site 2. Using the mean erosion rate and erosion profile estimated by the USGS erosion pin data shown in Figure 7 as an example, the bank geometry after 10 years was predicted and the stability of the predicted riverbanks was analyzed for 57 m^3/s steady state flow. This flow rate was selected because it produced the lowest factor of safety in the steady state modeling. As the results in Table 5 show, Site 1, Site 3 and Site 4 are predicted to become more unstable as erosion progresses, mainly due to the initial bank geometry and predicted erosion, which mostly originates from the lower sections of the slopes. In contrast, Site 2 and Site 5 are predicted to maintain a similar FS, primarily due to their mild slopes and very low erosion rates.

Table 5 Factor of safety changes after ten years of erosion estimated by USGS erosion pin data.

Site	Current		After 10 years	
	Maximum erosion (m) (2005 – 2009)	FS at 57 m^3/s	Cumulative erosion (m)	FS at 57 m^3/s
Site 1	0.92	1.92	2.3	1.58
Site 2	0.22	1.84	0.55	1.83
Site 3	0.2*	2.07	1.0	1.83
Site 4	N/A	1.74	1.2 (assumed)	1.61
Site 5	0.33	1.80	0.83	1.81

* 2007-2009.

5.5.6 Discussion

Although most slope stability analyses provided reasonable results in terms of factor of safety, a few issues such as inconsistent test results, unrealistic body force estimates from equilibrium equations, or unrealistic values of factor of safety were identified when lower values of hydraulic conductivity were applied.

Both transient drawdown and step-down scenarios using the lowest hydraulic conductivity values resulted in less stable conditions. Most of the failure envelopes seem to be located within the range of normal stresses in the direct shear tests. However, some of the calculated factor of safety values appear to be invalid, containing numerical errors that imply a rapid drop in the factor of safety that may not represent the actual stability of slopes. These errors may occur when the calculated effective normal stress is negative.

Among the potential causes for these errors are high pore pressure in the soil due to the lower hydraulic conductivity and a steep base angle of the slices in the limit equilibrium method (LEM) (Rocscience Inc., 2010b). Poor drainage of the soils with lower hydraulic conductivity means that they experience larger excess pore water pressure for some time after a drawdown event, resulting in negative values of normal stress calculated at the bottom of each slice. Consequently, the factor of safety becomes unrealistically low.

Another possible source of error is the development of tensile strength due to cohesion. In cohesive soils, as the tension develops it induces negative normal forces and the reversal of interslice normal and shear forces as a result of the cohesion, which is large in comparison with the magnitude of the other forces. These negative interslice forces also produce discontinuities in the line of the thrust. This seems to be especially true for relatively shallow slices in soils, where cohesion dominates the shear strength of soils (Ching and Fredlund, 1983).

Typically, it is recommended that a tension crack be created to eliminate such negative values. However, negative normal forces may be calculated even below the tension zone and this situation frequently occurs with relatively shallow slip surfaces and high cohesion. In addition, matric suction in unsaturated soil also increases tensile strength values, which ultimately increases the depth of the assumed tension cracks (Ching and Fredlund, 1983). In low profile slopes like riverbanks, deep tension cracks may not be feasible, as increasing the crack depth decreases the factor of safety significantly, shortening the length of resistible slip lines and increasing the weight of the soil mass. Dry tension cracks may reduce the rate at which FS decreases, but it may still be necessary to eliminate portions of the slip line.

This may be avoided by adopting a different method to calculate slope stability under rapid drawdown, as suggested by Duncan et al. (1990). However, due to the different parameters required for their analysis, Duncan, Wright, and Wong's method could not be applied in the current study.

5.6 Conclusions

The actual reservoir release rates of a hydropower dam were first analyzed to identify representative flow patterns and then transient seepage and slope stability analyses were performed to highlight the influence of dam operations on downstream riverbank stability using input parameters determined by laboratory tests, in situ tests, and empirical methods. The seven steady state flow rates modeled represented the range of seasonal and operational modes throughout a typical year and included one overbank flow case. The model provided a useful picture of the influence of water surface elevation (WSE), unsaturated shear strength parameters, and hydraulic conductivity.

These analyses revealed that the riverbanks at the study sites were stable for all their present flow conditions, including steady state, peaking, drawdown, and step-down conditions. A flow rate of 991 m^3/s would result in overbank flow throughout much of the lower Roanoke River. Even here, though, the increase in confining pressure would most likely result in the banks remaining stable. However, the banks were predicted to be less stable if they consisted of less permeable soils due to the development of excess pore water pressures. The hydraulic conductivity determined by laboratory tests tends to be considerably lower than that determined by in situ tests. Although the lab values are close to the typical values for similar types of soils, the in situ hydraulic conductivity seems to represent the flow of water in the riverbanks better as seen from the GWT modeling

results and can thus be used for modeling. However, as noted earlier, if low permeability soils are present, this may create more unstable conditions, especially when the riverbanks are exposed to transient drawdown or step-down flow conditions. Areas of low permeability soil may exist in the riverbanks and this likely explains the occasional small scale bank failures observed along the study reach.

Although the major analyses conducted for this study provided reasonable results, several numerical issues were identified. These are related to the apparently unrealistic values for the factor of safety, and are possibly due to the negative normal stress calculated at the slip line. Cohesion seems to be responsible for the negative values and, thus, the application of unsaturated shear strength may increase the possibility of such errors, as the matric suction is regarded as a part of total cohesion. Further investigation of the role and influence of unsaturated shear strength is required for limit equilibrium slope stability analysis.

5.7 References

[1] Ching, R. K. H., and Fredlund, D. G. (1983). "Some difficulties associated with the limit equilibrium method of slices." *Canadian Geotechnical Journal*, 20(4), 661-672.

[2] Clark, L. A., and Wynn, T. M. (2007). "Methods for determining streambank critical shear stress and soil erodibility: Implications for erosion rate predictions." *Transactions of the ASABE*, 50(1), 95-106.

[3] Dapporto, S., Rinaldi, M., and Casagli, N. (2001). "Failure mechanisms and pore water pressure conditions: Analysis of a riverbank along the Arno River (Central Italy)." *Engineering Geology*, 61(4), 221-242.

[4] Dominion (2010). "Description of operational modes." <http://www.dom.com/about/stations/hydro/operational-modes.jsp>. (Sep 29, 2010).

[5] Duncan, J. M., and Wright, S. G. (2005). *Soil strength and slope stability*, John Wiley & Sons, Inc. , Hoboken, N.J. :.

[6] Duncan, J. M., Wright, S. G., and Wong, K. S. (1990). "Slope stability during rapid drawdown " *Proceedings of the H. Bolton Seed Memorial Symposium*, 253-273.

[7] Emanuel, K. (2005). "Increasing destructiveness of tropical cyclones over the past 30 years." *Nature*, 436(7051), 686-688.

[8] Fredlund, D. G., Morgenstern, N. R., and Widger, R. A. (1978). "Shear strength of unsaturated soils." *Canadian Geotechnical Journal*, 15(3), 313-321.

[9] Fredlund, M., Lu, H., and Feng, T. (2011). "Combined seepage and slope stability analysis of rapid drawdown scenarios for levee design." ASCE, 1595-1604.

[10] Hanson, G. J., and Cook, K. R. (1997). "Development of excess shear stress parameters for circular jet testing." *Proc., 1997 ASAE Annual International Meeting*, ASAE, 97-2227.

[11] Hanson, G. J., and Cook, K. R. (2004). "Apparatus, test procedures, and analytical methods to measure soil erodibility in situ." *Applied Engineering in Agriculture*, 20(4), 455-462.

[12] Huang, M. S., and Jia, C. Q. (2009). "Strength reduction FEM in stability analysis of soil slopes subjected to transient unsaturated seepage." *Computers and Geotechnics*, 36(1-2), 93-101.

[13] Hubble, T. C. T. (2004). "Slope stability analysis of potential bank failure as a result of toe erosion on weir-impounded lakes: an example from the Nepean River, New South Wales, Australia." *Marine and Freshwater Research*, 55(1), 54-65.

[14] Hupp, C. R., Schenk, E. R., Richter, J. M., Peet, R. K., and Townsend, P. A. (2009). "Bank erosion along the dam-regulated lower Roanoke River, North Carolina." *Geological Society of America Special Papers*, 451, 97-108.

[15] Lawler, D. M., Thorne, C. R., and Hooke, J. M. (1997). "Bank Erosion and Instability." *Applied Fluvial Geomorphology for River Engineering and Management*, C. R. Thorne, R. D. Hey, and M. D. Newson, eds., John Wiley and Sons Ltd., 137-172.

[16] Leshchinsky, D. (1990). "Slope stability analysis: Generalized approach." *Journal of Geotechnical Engineering*, 116(5), 851-867.

[17] Morgenstern, N. R., and Price, V. E. (1965). "An analysis of the stability of general slip surfaces." *Geotechnique*, 15(1), 79-93.

[18] Nam, S., Gutierrez, M., Diplas, P., Petrie, J., Wayllace, A., Lu, N., and Munoz, J. J. (2010a). "Comparison of testing techniques and models for establishing the SWCC of riverbank soils." *Engineering Geology*, 110(1-2), 1-10.

[19] Nam, S., Petrie, J., Diplas, P., and Gutierrez, M. S. (2010b). "Effects of spatial variability on the estimation of erosion rates for cohesive riverbanks." *Proc., River Flow 2010*.

[20] Ng, C. W. W., and Shi, Q. (1998). "A numerical investigation of the stability of unsaturated soil slopes subjected to transient seepage." *Computers and Geotechnics*, 22(1), 1-28.

[21] Partheniades, E. (1965). "Erosion and deposition of cohesive soils." *American Society of Civil Engineers Proceedings, Journal of the Hydraulics Division*, 91(HY1, Part 1), 105-139.

[22] Pauls, G. J., Sauer, E. K., Christiansen, E. A., and Widger, R. A. (1999). "A transient analysis of slope stability following drawdown after flooding of a highly plastic clay." *Canadian Geotechnical Journal*, 36(6), 1151-1171.

[23] Rocscience Inc. (2010a). "Slide v6 2D Limit equilibrium slope stability analysis."Toronto, Canada.

[24] Rocscience Inc. (2010b). "SLIDE v6.0 Online help." <http://www.rocscience.com/downloads/slide/webhelp/Slide.htm>. (Dec. 19 2010, 2010).

[25] Schenk, E. R., Hupp, C. R., Richter, J. M., and Kroes, D. E. (2010). "Bank erosion, mass wasting, water clarity, bathymetry, and a sediment budget along the dam-regulated lower Roanoke River, North Carolina." U.S. Geological Survey 112p.

[26] Simon, A., Curini, A., Darby, S. E., and Langendoen, E. J. (2000). "Bank and near-bank processes in an incised channel." *Geomorphology*, 35(3-4), 193-217.

[27] Thorne, C. R., and Abt, S. R. (1993). "Analysis of Riverbank Instability due to Toe Scour and Lateral Erosion." *Earth Surface Processes and Landforms*, 18(9), 835-843.

[28] U.S. Geological Survey (2010). "USGS Real-time water data for the nation." < http://waterdata.usgs.gov/nwis/uv>. (Dec. 15, 2010).

[29] Webster, P. J., Holland, G. J., Curry, J. A., and Chang, H.-R. (2005). "Changes in tropical cyclone number, duration, and intensity in a warming environment." *Science*, 309(5742), 1844-1846.

[30] Weems, R. E., Lewis, W. C., and Aleman-Gonzalez, W. B. (2009). "Surficial geologic map of the Roanoke Rapids 30' x 60' quadrangle, North Carolina: U.S. Geological Survey open-file report 2009–1149, 1 sheet, scale 1:100,000." U.S. Geological Survey.

[31] Wynn, T. M., Henderson, M. B., and Vaughan, D. H. (2008). "Changes in streambank erodibility and critical shear stress due to subaerial processes along a headwater stream, southwestern Virginia, USA." *Geomorphology*, 97(3-4), 260-273.

CHAPTER 6. Conclusions

The main objective of this research was to investigate the effects of reservoir releases on slope stability and bank erosion. Extensive field work and laboratory tests were performed to estimate the hydraulic and geotechnical properties of the riverbank soils. Actual release rates for the Roanoke Rapids hydropower dam between 2005 and 2009 were analyzed for four basic operational modes of the dam, including both peaking and drawdown events. One extreme case of high flow condition was also analyzed in order to predict riverbank stability for the overbank flow condition. The unsaturated soil properties required for modeling were successfully identified. Seepage and slope stability analyses using these results, taking into account the characteristics of unsaturated soil and time dependent boundary conditions, were primarily performed using the SLIDE software package.

Brief summaries of the research performed for each part of the study, along with the major findings, are provided below.

Comparison of testing techniques and models for establishing the SWCC of riverbank soils

The desorption branch of the SWCCs of the riverbank soils in the lower Roanoke River, NC, were established using six different laboratory methods. Except for silty sand, the differences in SWCCs between the soil samples were not significant as the physical properties of the soils in the study area were broadly similar. Although the results reported here indicate that the six different measuring techniques used in the study provide comparable results, it is recommended that separate techniques be employed for

determining total and matric suction due to the different sensitivity and measurement range of each test method. The experimental data were compared to the mathematical models proposed by van Genuchten (1980), Fredlund and Xing (1994), and Houston et al. (2006), confirming that the Fredlund and Xing, and van Genuchten models yield the best fits with the experimental data. Although the model by Houston et al., which uses parameters based only on particle gradation and soil plasticity, showed good agreement for suction pressures below 1,500 kPa, above this level its use is not recommended as its predictions deviated significantly from the experimental data, where the linear change in the logarithmic value of suction as a function of water saturation.

Laboratory and in-situ determination of hydraulic conductivity and the implications for transient seepage analysis

The hydraulic conductivity was determined using two laboratory tests (the modified constant head permeability test and the consolidation test) and two field tests (the Guelph permeameter test and the auger hole test). The experimental results revealed that the hydraulic conductivity measured for the same soils could vary by as much as 10^4 m/sec. The laboratory measurements of hydraulic conductivity were closer to those typically reported for the soils, whereas the in situ hydraulic conductivity appeared to be towards the upper bound of the expected values. However, transient seepage analyses using the experimental results and applying the actual water surface elevations as a boundary condition indicated that the higher values measured by the auger hole tests produced groundwater table predictions that were closest to those observed in the field. These higher values for the in situ hydraulic conductivity can be attributed to the natural factors that lead to preferential flows such as roots, cracks and structured soils, as well as

the experimental factors that distinguish laboratory and in situ tests such as test methods, anisotropy, sample size and disturbance. Thus, the use of a single evaluation method may not adequately represent the actual permeability characteristics of soils, especially for non-homogeneous cohesive soils, and it is recommended that additional factors be considered, including visual inspection, information on the geological and geomorphological background of the site, and numerical modeling, to increase reliability. In addition, long term monitoring of the ground water table and numerical analysis of seepage are recommended.

Unsaturated shear strength of riverbank soils using multistage direct shear tests

The validity of multistate direct shear tests was studied, and the saturated and unsaturated shear strength parameters were obtained. The multistage direct shear test yielded similar results to those obtained using conventional direct shear tests, with negligible differences for engineering practice. However, some precautions are recommended: it is important to ensure there is no excessive shearing of the soil sample beyond the peak shear stress to the strain softening region, and no shearing occurring before equilibrium has been achieved for every new matric suction. The suction controlled test results confirmed the non-linear relationship between the unsaturated shear strength and matric suction, which fits both an empirical power function and the square-root function proposed by Abramento and Carvalho (1989). The unsaturated shear strength was also compared to estimated values found by applying the saturated shear strength parameters, soil water characteristic curves, and a fitting parameter κ. The estimated shear strength was a good fit for the experimental data over a limited range of suction, while the estimated fitting parameter κ varied with applied suction ranges,

indicating that further clarification is required regarding the applied suction range and the correlation between the fitting parameter κ and the plasticity index.

Effect of reservoir releases on riverbank stability

Riverbank stability was analyzed for both steady state and changing water surface elevation conditions using transient seepage analysis and the limit equilibrium method. Seven constant release rates were applied to represent steady state conditions, and two drawdown events and one continuous peaking event were also considered. The unsaturated soil properties determined in earlier parts of the study were used for the modeling, and bank erosion was estimated using USGS erosion pin data. The modeling results indicated that the riverbanks at the study sites were indeed stable for all their present flow conditions and would remain stable for the next 10 years assuming the same erosion rates although factor of safety decreases at most sites. Higher water surface elevation leads to more stable conditions although it causes loss of matric suction, indicating that the role of water surface elevation seems to be more important than that of unsaturated soil properties. It also may cause more fluvial erosion; only average annual erosion rates were considered in this study. The factor of safety fluctuates depending on the changes in water surface elevation during peaking and drawdown events, although the riverbanks remain stable (FS>1). However, if the presence of low permeability soils is assumed, using the lower hydraulic conductivity obtained from the laboratory tests, the stability of the riverbanks becomes very sensitive to the rate of drawdown of water surface elevation due to the excess pore water pressure. Areas of less permeable soil may exist in the riverbanks and this likely explains the occasional small scale bank failures observed along the study reach.

Interestingly, several numerical issues were identified for cases where the hydraulic conductivity in the models is low. Unrealistic values for the factor of safety were observed, probably as a result of the negative normal stress calculated at the bottom of each slice due to the large excess pore water pressure and relatively high cohesion, even with matric suction. Although the limit equilibrium method is generally regarded as the simplest and most reliable method for slope stability analysis, when combined with transient seepage analysis the results should be treated with caution, especially when low permeability soils are involved.

APPENDICES

Appendix A: Effects of Spatial Variability on the Estimation of Erosion Rates for Cohesive Riverbanks[1]

ABSTRACT

Human activities, such as dam construction, can cause excessive erosion of a riverbank due to alteration of the natural flow regime. This erosion can lead to degradation in water quality and aquatic habitat as well as loss of land and damage to riparian structures. Accurate estimation of erosion rates for cohesive riverbanks is a difficult task owing to the complex nature of cohesive soils and their interaction with the river flow. Past work has attempted to correlate physical and chemical soil properties with erosion rates, however the wide range of soil properties has made it difficult to produce a general model for cohesive soil erosion. The erodibility of riverbank soil on the lower Roanoke River, North Carolina USA, was estimated in situ employing the jet erosion test (JET) apparatus. The JET applies a water jet of uniform velocity directly to the soil and measures the resulting scour depth evolution over time. The measured data are then used to determine two empirical parameters, the erodibility coefficient and critical shear stress. Several JETs were performed on different soil layers at sites with bank materials composed primarily of silts and clays. The physical properties of each soil layer were determined through laboratory analysis. Using boundary shear stress calculations from a simple analytical model, erosion rates are calculated assuming a linear excess shear stress model, and the effects of the spatial variability of soil properties on calculated erosion are investigated. While previous research has shown that the JET

[1] This manuscript was published in River Flow 2010, and is co-authored by **Soonkie Nam**, John

produces consistent results under controlled environments, results here demonstrate the importance of considering spatial variability of soil types when estimating erosion rates.

Keywords: jet erosion test, erodibility, critical shear stress, river bank erosion

A.1 Introduction

Various types of human activities can cause excessive erosion of a riverbank due to alteration of the natural flow regime. Some problems due to erosion include loss of land, damage to riparian structures, transport of pollutants, and degradation in water quality and aquatic habitat. Erosion causes not only financial losses but also environmental problems. Therefore, active controls are beneficial in an effort to reduce erosion.

To quantify the effects of erosion, proper estimation of erosion induced by the activities and controls of human-induced activities are required. However, estimation of soil erodibility and flow characteristics in a river necessarily involve great uncertainty and variability due to the complex nature of soils and their interactions with the river flow.

Riverbank soils can be simply classified as non-cohesive or cohesive. Non-cohesive soils, including sand and gravel, are typically granular and coarser than cohesive soils causing the properties of individual soil particles to dominate the characteristics of the soils. In contrast, cohesive soils, such as silt and clay, are finer and the soil minerals, structure, chemicals and interacting forces are typically more important to the overall soil characteristics than the physical properties of soil particles.

Erodibility of non-cohesive soils is determined by gravitational forces and soil parameters such as particle size, shape, and unit weight of soil (Graf, 1971), whereas that of cohesive soils is much more difficult to estimate. As summarized by Grissinger (1982), correlations of erosion rates with combinations of plasticity, percentage of clay particles, soil mineralogy, cation exchange capacity (CEC), and many other physical and chemical soil properties have been investigated, but the wide range of soil properties and complexity of interactions of different parameters have made it difficult to produce a general model for cohesive soil erosion.

This paper presents a study of the variability of erodibility parameters of cohesive soils in the riverbank of the lower Roanoke River near Roanoke Rapids, North Carolina, USA, estimated by the in situ submerged jet erosion test, and their influences on erosion rate calculations.

Estimation of erosion rate

Due to the complexity of cohesive soil erosion, empirical methods have been widely employed and accepted for cohesive soils for several decades. The linear excess shear stress equation is often used to estimate erosion and is commonly presented with three parameters: the erodibility coefficient (k_d) and applied and critical shear stresses (τ_0 and τ_c), which imply the rate of erosion when a given hydraulic shear stress is applied and the ease of initiating erosion, respectively (Hanson and Cook, 2004, Wan and Fell, 2004).

$$\varepsilon = k_d(\tau_0 - \tau_c)^a \qquad \text{for } (\tau_0 > \tau_c) \tag{1}$$

$$\varepsilon = 0 \qquad \text{for } (\tau_0 \le \tau_c)$$

where, ε = erosion rate (m/s), k_d = erodibility coefficient ($m^3/N \cdot s$), τ_0 = applied shear stress by flow (Pa), τ_c = critical shear stress of soil, and a is a constant commonly assumed to 1.

The applied shear stress (τ_0) is related to the flow conditions, whereas the other two parameters, erodibility coefficient (k_d) and critical shear stress (τ_c), are soil characteristics that typically are determined by experiments. Erosion is considered to occur when the applied shear stress is greater than the critical shear stress of the soil $(\tau_0 > \tau_c)$, and the total erosion is proportional to the erosion rate and time interval over which erosion occurs.

Jet erosion test

There are several available methods for measuring soil erodibility, including flume tests, jet erosion tests, rotating cylinder tests, soil dispersion tests, hole or crack tests, and the erosion function apparatus (Wan and Fell, 2004). In this study, a submerged jet test device was used on riverbanks in the field.

The submerged jet test device was proposed by Hanson (1990a, 1990b, 1991) as an in-situ test technique to determine the erodibility coefficient and critical shear stress of soils (Figure 1). This test evaluates the erodibility of cohesive soils by measuring the depth scoured by a water jet over time. A jet of water is discharged directly to the soil and the depth of the hole produced and duration are measured. Theoretically, the maximum scour depth at equilibrium is required to estimate the erosion parameters. However, it may take hours or even days to reach equilibrium. Hanson & Cook (1997) determined the two empirical erodibility parameters (k_d and τ_c) by adapting analytical

procedures to estimate scour depth and critical shear stress at equilibrium proposed by Stein et al. (1993) and Stein & Nett (1997). The principles and procedures of the test are described in detail in Hanson & Cook (2004). The jet test device has been applied in several studies due to its numerous advantages; it is simple, relatively inexpensive, can be performed in the field even on steep slopes, and the erosion parameters are easily calculated using a spreadsheet developed by Hanson and Cook (1997) (Clark and Wynn, 2007, Wahl et al., 2008, Walowsky Jr. et al., 2008, Wynn and Mostaghimi, 2006).

Figure 1 Jet erosion test device.

A few studies have confirmed the accuracy and consistency of the jet test results under a controlled environment (Hanson and Cook, 1997, Hanson and Cook, 2004, Wahl et al., 2008) while others have reported a wide range of results in nature (Hanson and Simon, 2001, Shugar et al., 2007, Simon and Thomas, 2002, Thoman and Niezgoda,

2008, Wynn and Mostaghimi, 2006). However, in practice, most studies with the jet test have utilized it as a single experimental method to obtain the erodibility parameters due to limitations such as the availability of other tests and field conditions. In addition, the results are typically limited to a small number of tests.

Applied shear stress by flow

The applied shear stress by flow also needs to be determined in addition to the soil-related parameters for erosion rate calculations. Several analytical and numerical methods are available for 2D and 3D, and straight and curved channels. The current study employed a simple analytical equation to estimate the distribution of boundary shear stress. While more advanced techniques exist (e.g. Kean et al., 2009, Shiono & Knight, 1991) the simplified technique presented here allows general trends to be identified even if the magnitudes are not precise.

Boundary shear stress on trapezoidal channels

A simple equation for the boundary shear stress in trapezoidal channel was adapted to estimate maximum shear stress on the slope.

$$\tau_0 = \gamma RS \tag{2}$$

where, τ_0 = average shear stress on the boundary (Pa), γ = unit weight of water (N/m^3), R = hydraulic radius (m), and S = channel slope (m/m).

Equation (2) is based on the assumption of one dimensional flow and that the boundary shear stress is averaged over the wetted perimeter, whereas the actual shear stress distribution on a riverbank will not be uniform due to the channel slope and curvature.

$$\tau_{0\,max} = 1.1 \cdot \gamma RS \tag{3}$$

Thus, Equation (2) can be updated to Equation (3) to calculate the maximum boundary shear stress on the slope (τ_{0max}),estimated using the figures suggested by Anderson et al. (1970) as described in Chang (2002).

A.2 Laboratory and in situ experiments

Soil properties

Soil properties were determined from laboratory tests using disturbed soil samples obtained randomly from the sites, and the sampling locations were recorded to correlate with jet test locations. Grain size distributions and Atterberg test results for the soils are shown in Figure 2 and Figure 3, respectively.

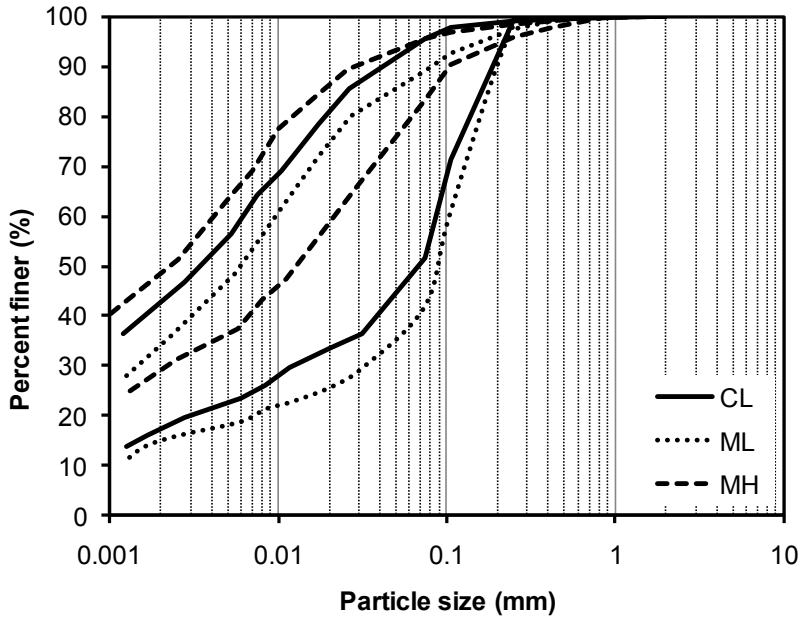

Figure 2 Grain size distribution curves.

As shown in Figure 3, the soils are classified as low and high plasticity silts (ML and MH) and low plasticity clay (CL) by the unified soil classification system (USCS). The overall results are summarized in Table 1 with soil types.

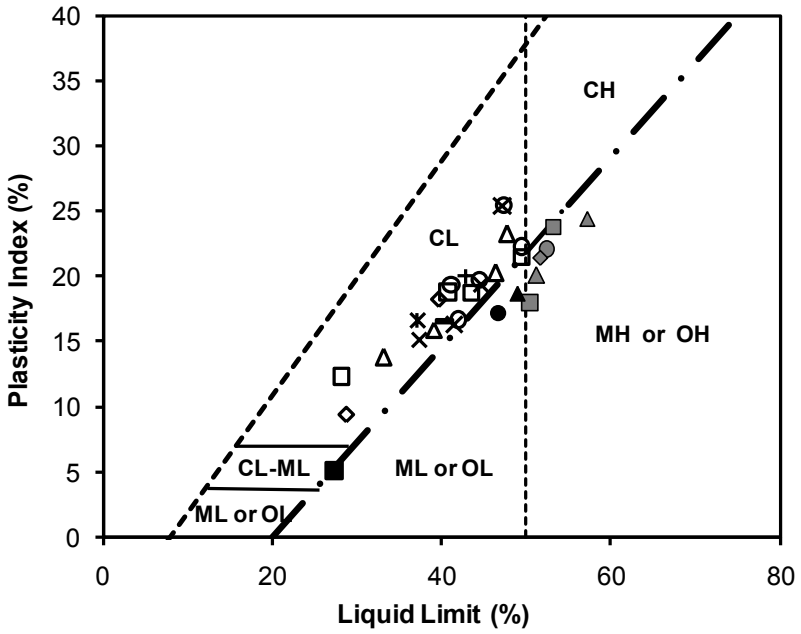

Figure 3 Atterberg test and soil classification.

Table 1 Soil properties.

USCS	Sand %	Silt %	Clay %	LL	PI	No. of Samples
CL	16.6	50.2	33.2	41.8	18.6	26
	10.9	8.1	7.3	5.8	3.9	
ML	25.8	47.9	26.3	41.0	13.8	10 (3)*
	18.4	10.9	9.5	11.9	7.2	
MH	9.2	44.7	46.2	52.7	21.6	7
	3.3	2.9	2.8	2.4	2.4	

* 10 samples for grain size distribution and 3 samples for Atterberg tests.

**Upper rows present average value, lower rows present standard deviation.

***LL=Liquid Limit, PI=Plasticity Index.

Jet erosion test

Eleven in situ jet tests were performed on the riverbank at different locations in different soils: 5 from CL, 2 from ML, and 4 from MH. The test locations were randomly

selected within those soil layers where the properties were known. The detailed procedures for the jet erosion tests are available in Hanson & Cook (2004).

A.3 Results

Erodibility parameters for soils

The results of the jet tests are shown in Figure 4 and Table 2. A wide range of both erodibility coefficients (k_d) and critical shear stress (τ_c) was observed with no clear relationship between the two parameters. The variations of each parameter are also large within the same soil type. Based on the same erosion criteria used by Hanson and Simon (2001), shown with dotted lines in Figure 4, the soils can be classified as moderately resistant to very erodible soils.

Table 2 Jet test results.

USCS	Erodibility coefficient (k_d, $m^3/N \cdot s$)	Critical shear stress (τ_c, Pa)	No. of Samples
CL	2.0×10^{-6}	3.8	5
	2.4×10^{-6}	2.7	
ML	1.2×10^{-6}	5.2	2
	1.5×10^{-6}	5.7	
MH	1.0×10^{-6}	9.6	4
	1.1×10^{-6}	6.3	

*Upper rows present average value, lower rows present standard deviation.

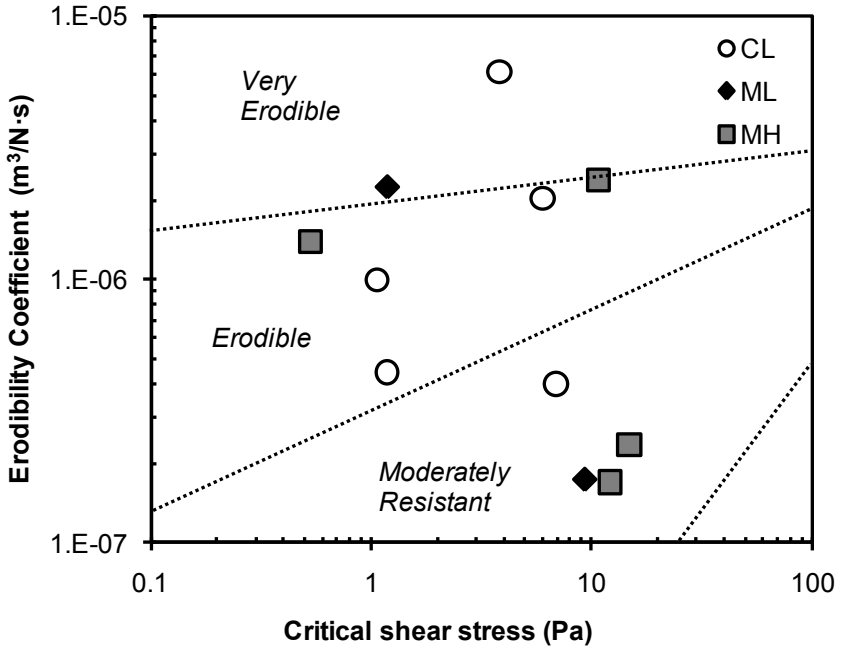

Figure 4 Jet test results from the lower Roanoke River with the classifications of Hanson & Simon (2001).

Although Hanson and Simon (2001) observed a relatively linear relationship between the two parameters after performing 63 jet tests, with increasing critical shear stress corresponding to decreasing erodibility coefficient on a log-log scale, they also observed very erodible to very resistant soils with a wide variation spanning four orders and six orders of magnitude for k_d and τ_c, respectively. Similar relationships and wide variations were also observed by Shugar et al. (2007) and Thoman and Niezgoda (2008).

Estimation of applied shear stress

The boundary shear stress on the bank slope by flow was estimated using a simple analytical method. As a hydropower dam is located about 77 river kilometers upstream from the field, it is assumed that a constant discharge with bankfull flow, which corresponds to 566 m^3/s discharge rate from the dam, could be a critical condition leading

to erosion in the field. Thus, the applied shear stress at this condition was calculated to estimate the maximum erosion on the riverbank.

In the analytical method, the maximum shear stress was assumed to develop at 2/3 of the flow depth and decrease to zero linearly at the top and bottom of the bank. Bed load movement in the river channel was not considered in this study. As shown in Figure 5, the maximum shear stresses were estimated to be 4.1 Pa for the 566 m^3/s discharge condition.

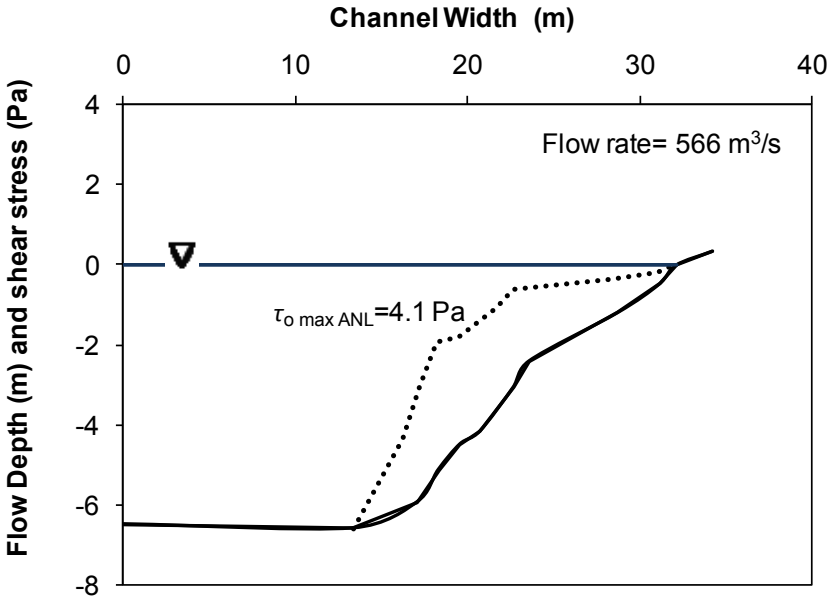

Figure 5 Assumed shear stress distributions by analytical method

Variability of erosion rate

As the erosion rates are determined by three different parameters (k_d, τ_c, and τ_0), soils may have higher predicted erosion rates even though one or two of the parameters are lower. This is due to the fact that the erosion rate is determined as a product of erodibility term and shear stress term, as shown in Equation (1).

Table 3 shows the ratios of the maximum and minimum values of each parameter for the study soils. The ratios indicate how the parameters vary within each soil, and how they change after multiplication. In Table 4, the erosion rates for all combinations of the required parameters under the 566 m^3/s flow condition are compared. Each column in Table 4 includes a series of data under the same applied shear stress. Each calculated erosion rate in the same column has a different erodibility coefficient and critical shear stress but the same applied shear stress. The results in each row are calculated using the same erodibility parameters but different applied shear stresses.

Table 3 Variations of each parameter

Soil Type	$\frac{k_{d\ \max}}{k_{d\ \min}}$	$\frac{\tau_{c\ \max}}{\tau_{c\ \min}}$	$\frac{(k_d \times \tau_c)_{\max}}{(k_d \times \tau_c)_{\min}}$
CL	6.5	15.3	45
ML	7.8	12.9	1.7
MH	27.9	14	35

Case 3 is for the field conditions where the applied shear stress was obtained from calculations. In the other cases, the applied shear stress was increased from 1 to 10, which represent flow conditions other than the bankfull discharge. In Case 3, outlined in bold in Table 4, no erosion was predicted for 6 out of the 11 samples due to the large measured critical shear stress. The other 5 samples (three CL, one ML and one MH soil) were found to be eroded, with the predicted maximum erosion rates of 0.26 m/day, 0.56 m/day, and 0.43 m/day, for the CL, ML and MH soils, respectively. It also shows that the estimated maximum erosion rates in the clayey soils range from 2.3 times (when τ_o=4.1)

to 58 times (when τ_o=8) larger than the minimum erosion rates without considering the no erosion cases.

Table 4 Erosion rates with different applied shear stresses.

Soil Type	Erosion rate (ε , m/day)					
	Case No	1	2	3	4	5
	τ_o (Pa)	1	2	4.1	8	10
CL	k_d=0.40 (m^3/N-s) τ_c=6.90 (Pa)	0.000	0.000	0.000	0.038	0.107
	k_d=0.44 τ_c=1.18	0.000	0.032	0.112	0.261	0.338
	k_d=6.13 τ_c=3.82	0.000	0.000	0.147	2.211	3.270
	k_d=1.00 τ_c=1.07	0.000	0.080	0.261	0.597	0.769
	k_d=2.03 τ_c=6.02	0.000	0.000	0.000	0.350	0.701
ML	k_d=0.17 τ_c=9.26	0.000	0.000	0.000	0.000	0.011
	k_d=2.23 τ_c=1.19	0.000	0.156	0.560	1.311	1.695
MH	k_d=0.17 τ_c=12.13	0.000	0.000	0.000	0.000	0.000
	k_d=0.24 τ_c=14.81	0.000	0.000	0.000	0.000	0.000
	k_d=1.39 τ_c=0.53	0.056	0.176	0.427	0.894	1.134
	k_d=2.39 τ_c=10.79	0.000	0.000	0.000	0.000	0.000

Unit : k_d (m^3/N-s), τ_c (Pa), and τ_o (Pa)

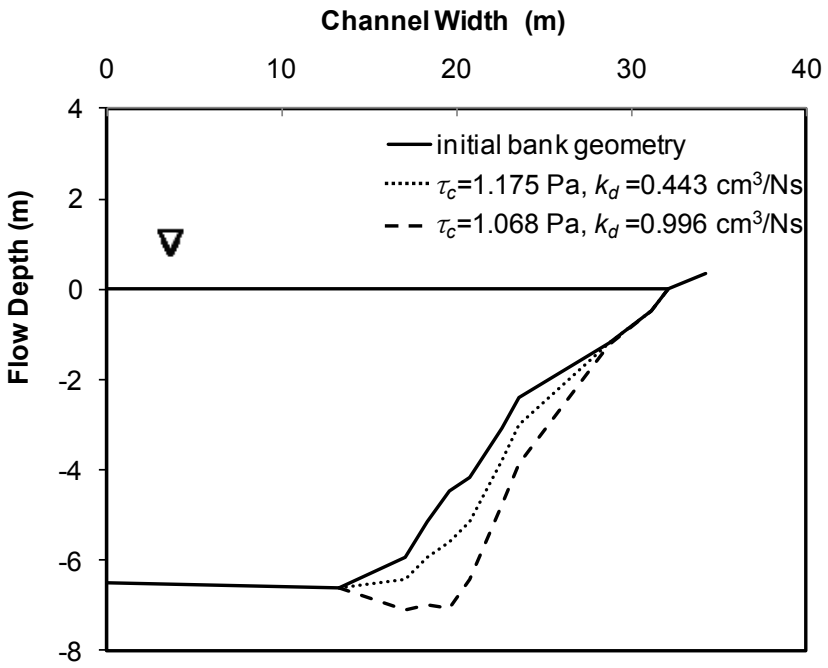

Figure 6 Eroded bank geometry after 10 days

Figure 6 shows an example of the erosion predicted from two different jet test results for the same soil when the applied shear stress was assumed to be 4.1 Pa and the flow continued for 10 days. With different values of the erodibility parameters, the total erosion ranges from zero to 2.57 m.

A.4 Conclusion and discussion

Erosion rates are calculated using a linear excess shear stress equation with erodibility parameters (k_d and τ_c) determined by jet erosion tests, and the applied shear stress obtained from an analytical method. A wide range of erodibility parameters was observed from the jet erosion tests. The standard deviations were larger than the averages, and, thus, larger differences in the calculated erosion rate were observed. Due to the fact that the erosion rate is determined by the product of erodibility coefficient and

shear stress differences, the calculated erosion rates are not proportional to the parameters. The lowest erosion rate was determined to be zero for all three soil types, and the largest erosion rates were 0.27, 0.56, and 0.43 m/day for CL, ML and MH soils, respectively.

Assuming that the jet erosion tests were performed at a representative location for that soil layer and that the other variables are obtained from reliable sources, the erosion rate of clayey soils would be one of the values in the Case 3-CL, namely zero, 0.112, 0.147, and 0.261 m/day. For the overall period when the dam discharge is over 566 m^3/s, the predicted annual erosion from the four different erosion rates will be significantly different.

The estimated erosion in practical cases may involve similar or worse uncertainty in the results due to the fact that the typical number of tests performed in the field for practical cases is also similar or even smaller (Wahl, 2008, Walowsky Jr. et al., 2008). Thus, the variability of the test results should be reviewed before making erosion estimations, using additional information such as statistical analysis with more test results, other references for the erodibility of the similar type of soils, or other empirical correlations using the other frequently available soil properties.

A.5 References

[1] Anderson, A. G., Davenport, J. T., and Paintal, A. S. (1970). *Tentative design procedure for riprap-lined channels*, Highway Research Board.

[2] Chang, H. H. (2002). *Fluvial Processes in River Engineering*, Krieger Publishing Co., Malabar, FL.

[3] Clark, L. A., and Wynn, T. M. (2007). "Methods for determining streambank critical shear stress and soil erodibility: Implications for erosion rate predictions." *Transactions of the ASABE*, 50(1), 95-106.

[4] Graf, W. H. (1971). *Hydraulics of Sediment Transport*, McGraw Hill, New York.

[5] Grissinger, E. H. (1982). "Bank erosion of cohesive materials." *Gravel-bed Rivers*, R. D. Hey, J. C. Bathurst, and C. R. Thorne, eds., John Wiley & Sons, New York, 273-287.

[6] Hanson, G. J. (1990a). "Surface erodibility of earthen channels at high stresses. Part I-Open channel testing." *Transactions of the ASAE*, 33(1), 127-131.

[7] Hanson, G. J. (1990b). "Surface erodibility of earthen channels at high stresses. Part II-Developing an in situ testing device." *Transactions of the ASAE*, 33(1), 132-137.

[8] Hanson, G. J. (1991). "Development of a jet index to characterize erosion resistance of soils in earthen spillways." *Transactions of the ASAE*, 34(5), 2015-2020.

[9] Hanson, G. J., and Cook, K. R. (1997). "Development of excess shear stress parameters for circular jet testing." *Proc., 1997 ASAE Annual International Meeting*, ASAE, 97-2227.

[10] Hanson, G. J., and Cook, K. R. (2004). "Apparatus, test procedures, and analytical methods to measure soil erodibility in situ." *Applied Engineering in Agriculture*, 20(4), 455-462.

[11] Hanson, G. J., and Simon, A. (2001). "Erodibility of cohesive streambeds in the loess area of the midwestern USA." *Hydrological Processes*, 15(1), 23-38.

[12] Kean, J. W., Kuhnle, R. A., Smith, J. D., Alonso, C. V., and Langendoen, E. J. (2009). "Test of a method to calculate near-bank velocity and boundary shear stress." *Journal of Hydraulic Engineering*, 135(7), 588-601.

[13] Shiono, K., and Knight, D. W. (1991). "Turbulent open-channel flows with variable depth across the channel." *Journal of Fluid Mechanics*, 222, 617-646.

[14] Shugar, D., Kostaschuk, R., Ashmore, P., Desloges, J., and Burge, L. (2007). "In situ jet-testing of the erosional resistance of cohesive streambeds." *Canadian Journal of Civil Engineering*, 34(9), 1192-1195.

[15] Simon, A., and Thomas, R. E. (2002). "Processes and forms of an unstable alluvial system with resistant, cohesive streambeds." *Earth Surface Processes and Landforms*, 27(7), 699-718.

[16] Stein, O. R., Alonso, C. V., and Julien, P. Y. (1993). "Mechanics of jet scour downstream of a headcut." *Journal of Hydraulic Research*, 31(6), 723-738.

[17] Stein, O. R., and Nett, D. D. (1997). "Impinging jet calibration of excess shear sediment detachment parameters." *Transactions of the ASAE*, 40(6), 1573-1580.

[18] Thoman, R. W., and Niezgoda, S. L. (2008). "Determining erodibility, critical shear stress, and allowable discharge estimates for cohesive channels: Case study in the Powder River Basin of Wyoming." *Journal of Hydraulic Engineering*, 134(12), 1677-1687.

[19] Wahl, T. L. (2008). "Stability analysis of proposed unlined spillway channel for upper San Joaquin River Basin RM 274 embankment dam alternative." *Hydraulic Laboratory Report*, Bureau of Reclamation.

[20] Wahl, T. L., Regazzoni, P.-L., and Erdogan, Z. (2008). "Determining erosion indices of cohesive soils with the hole erosion test and jet erosion test." Bureau of Reclamation.

[21] Walowsky Jr., D., Wright, P., and Henry, C. (2008). "Jet test to evaluate the head cutting of glacial till in auxiliary spillways in New York state." *Proc., 2008 ASABE Annual International Meeting*, 08-5132.

[22] Wan, C. F., and Fell, R. (2004). "Investigation of rate of erosion of soils in embankment dams." *Journal of Geotechnical and Geoenvironmental Engineering*, 130(4), 373-380.

[23] Wynn, T., and Mostaghimi, S. (2006). "The effects of vegetation and soil type on streambank erosion, Southwestern Virginia, USA." *Journal of the American Water Resources Association*, 42(1), 69-82.

Appendix B: Erodibility of the riverbank soils

B.1 Cumulative and predicted erosion pin data

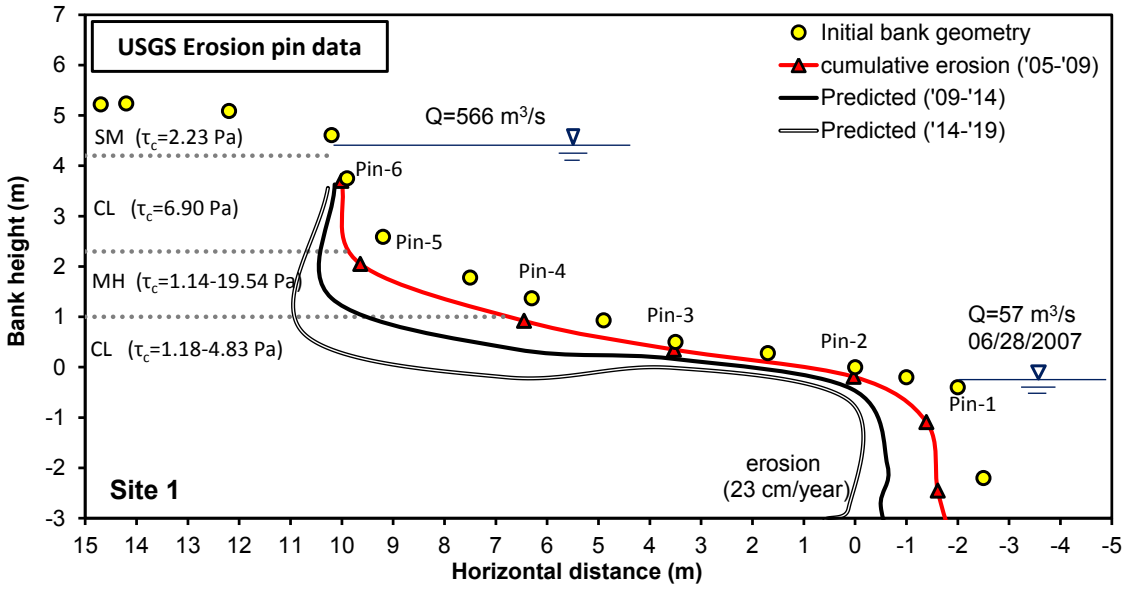

Figure B1 Cumulative and predicted erosion at Site 1 (USGS T61L).

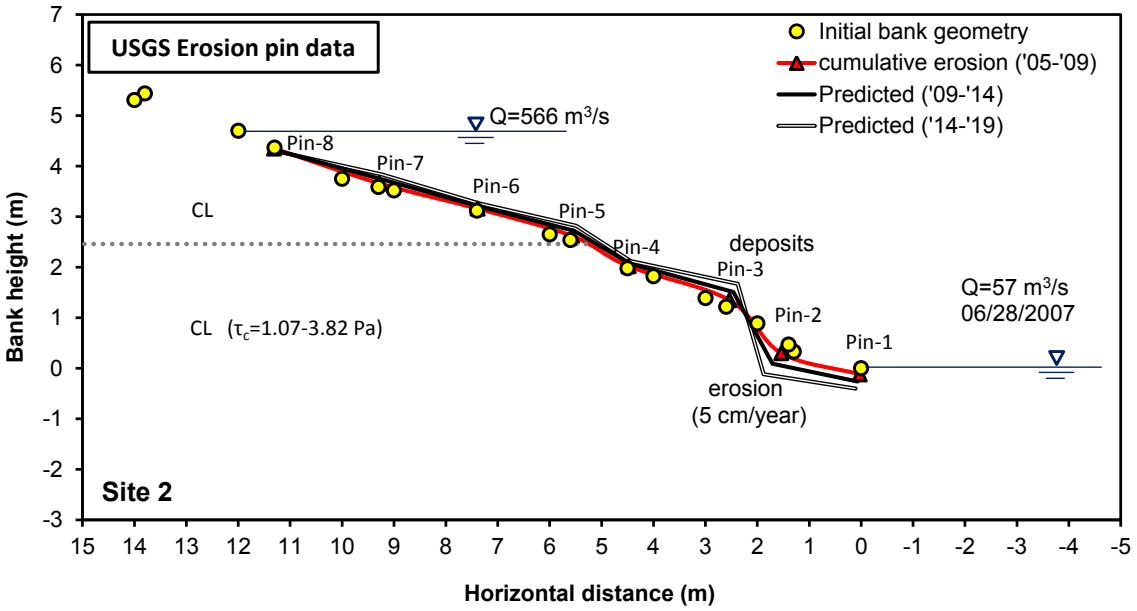

Figure B2 Cumulative and predicted erosion at Site 2 (USGS 11BR).

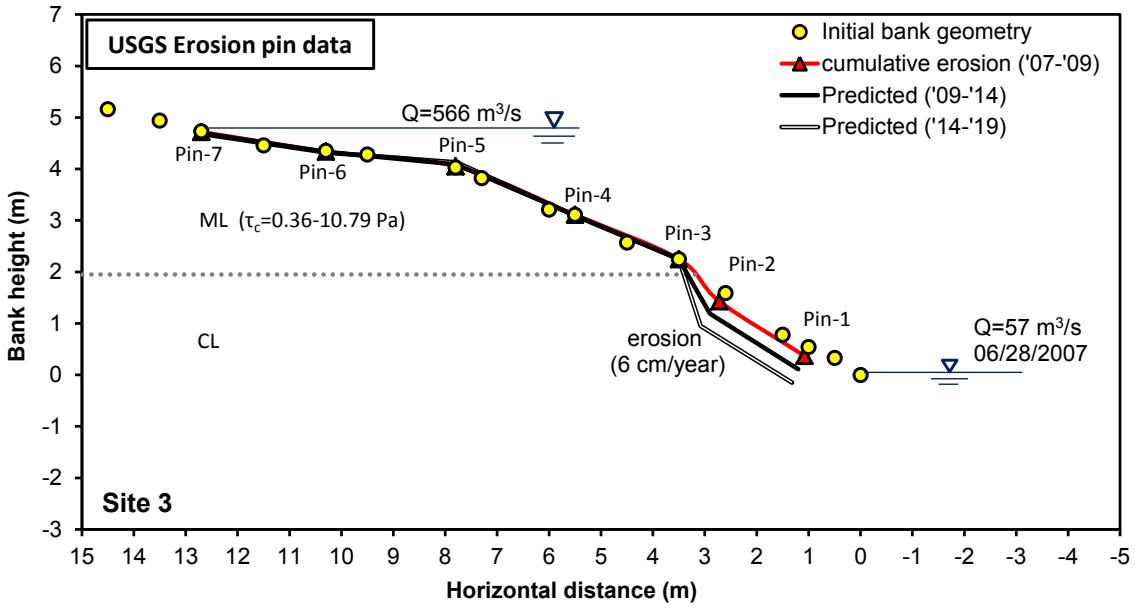

Figure B3 Cumulative and predicted erosion at Site 3 (USGS 9BR).

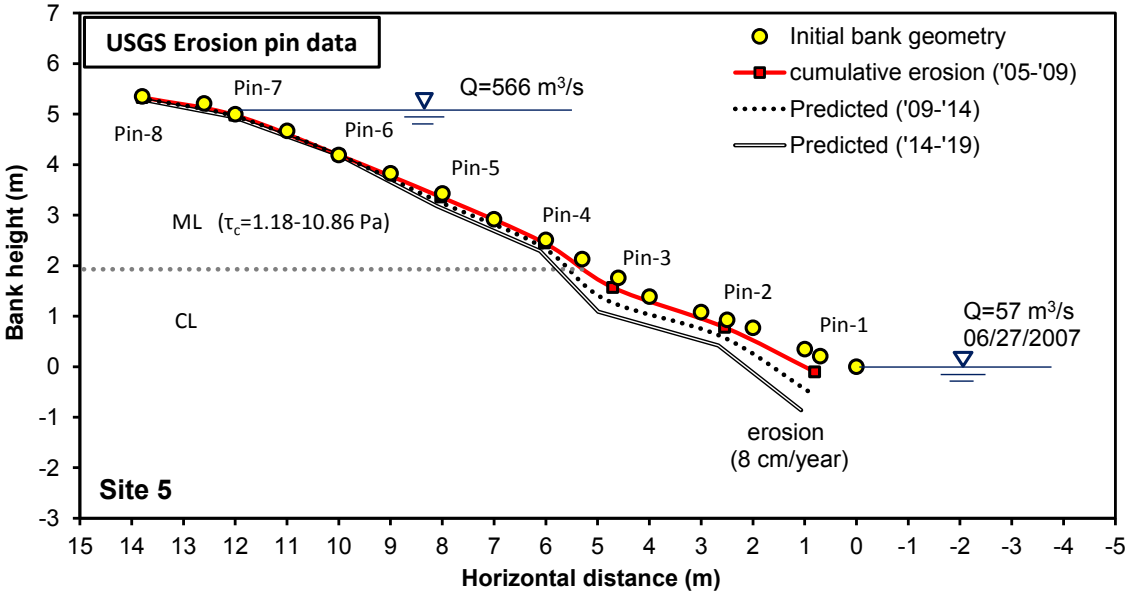

Figure B4 Cumulative and predicted erosion at Site 5 (USGS 8BL).

B.2 Results of the submerged jet erosion test

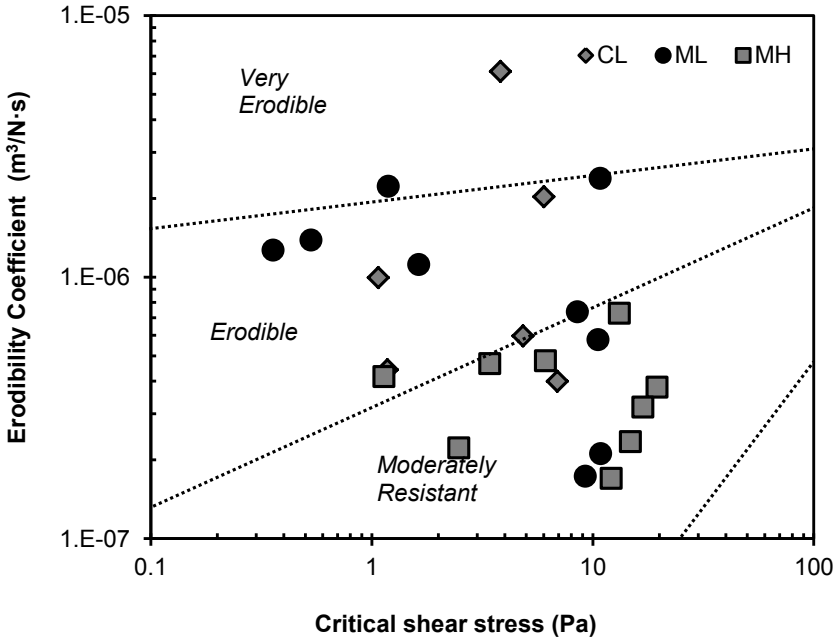

Figure B5 Jet test results by soil type

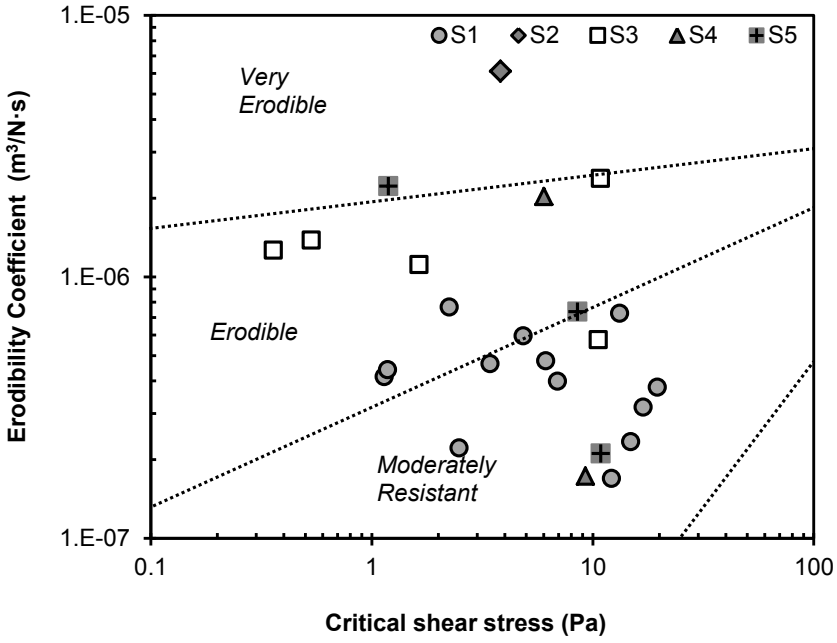

Figure B6 Jet test results by site.

Table B1 Jet erosion test results for CL.

Date	Site & Soil type	Flow rate		k_d (m^3/N-s)	τ_c (Pa)
		m^3/s	ft^3/s		
03/2007	S1-CL1	99	3500*	4.00E-07	6.90
03/2007	S1-CL2	99	3500	4.43E-07	1.18
05/2010	S1-CL2	178	6300	5.96E-07	4.83
05/2008	S2-CL	340	12000	6.13E-06	3.82
05/2008	S2-CL	340	12000	9.96E-07	1.07
05/2008	S4-CL	283	10000	2.03E-06	6.01
Average				1.77E-06	3.97
Standard deviation				2.22E-06	2.44
Maximum				6.13E-06	6.899
Minimum				4.00E-07	1.068

*Previously has been peaking (20000 cfs) twice a day.

Table B2 Jet erosion test results for ML.

Date	Site & Soil type	Flow rate		k_d (m^3/N-s)	τ_c (Pa)
		m^3/s	ft^3/s		
05/2008	S3-ML	272	9600	1.39E-06	0.53
05/2008	S3-ML	283	10000	2.39E-06	10.79
05/2010	S3-ML	178	6300	5.77E-07	10.57
05/2010	S3-ML	178	6300	1.12E-06	1.63
05/2010	S3-ML	178	6300	1.27E-06	0.36
05/2008	S4-ML	283	10000	1.73E-07	9.26
05/2008	S5-ML	283	10000	2.23E-06	1.19
05/2010	S5-ML	178	6300	7.36E-07	8.51
05/2010	S5-ML	178	6300	2.11E-07	10.86
Average				1.12E-06	5.97
Standard deviation				7.98E-07	4.85
Maximum				2.39E-06	10.86
Minimum				1.73E-07	0.36

Table B3 Jet erosion test results for MH

Date	Site & Soil type	Flow rate		k_d (m^3/N-s)	τ_c (Pa)
		m^3/s	ft^3/s		
05/2007	S1-MH	99	3500	1.70E-07	12.13
05/2007	S1-MH	99	3500	2.35E-07	14.81
05/2010	S1-MH	178	6300	3.79E-07	19.54
05/2010	S1-MH	178	6300	3.18E-07	16.88
05/2010	S1-MH	178	6300	2.22E-07	2.48
05/2010	S1-MH	178	6300	4.16E-07	1.14
05/2010	S1-MH	178	6300	4.79E-07	6.11
05/2010	S1-MH	178	6300	7.28E-07	13.19
05/2010	S1-MH	178	6300	4.67E-07	3.42
Average				3.79E-07	9.97
Standard deviation				1.71E-07	6.80
Maximum				7.28E-07	19.54
Minimum				1.70E-07	1.14